

NASA CR-134977  
SKF AL75TO32

(NASA-CR-134977) MICROFOG LUBRICATION FOR  
AIRCRAFT ENGINE BEARINGS Technical Report,  
Sep. 1972 - Jun. 1975 (SKF Industries, Inc.)  
135 p HC \$6.00 CSCL 13I

N76-28553

Unclass

G3/37 46801

## MICROFOG LUBRICATION FOR AIRCRAFT

### ENGINE BEARINGS

By

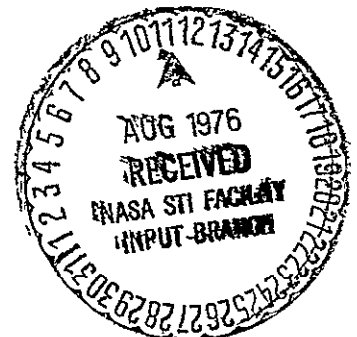
J. W. Rosenlieb

SKF Industries, Incorporated

Prepared for

NATIONAL AERONAUTICS AND SPACE ADMINISTRATION

NASA Lewis Research Center  
Contract NAS3-16826



1. Report No CR-134977		2. Government Accession No.		3. Recipient's Catalog No.	
4. Title and Subtitle MICROFOG LUBRICATION FOR AIRCRAFT ENGINE BEARINGS				5. Report Date April, 1976	
				6. Performing Organization Code LC-120	
7. Author(s) J. W. Rosenlieb				8. Performing Organization Report No. AL75TO32	
9. Performing Organization Name and Address SKF Industries, Inc. 1100 First Avenue King of Prussia, Pennsylvania 19406				10. Work Unit No.	
				11. Contract or Grant No NAS3-16826	
12. Sponsoring Agency Name and Address National Aeronautics and Space Administration Washington, D. C. 20546				13. Type of Report and Period Covered Contractor Report September 72 to June 75	
				14. Sponsoring Agency Code	
15. Supplementary Notes Project Manager, William R. Loomis, Fluid System Components Division, NASA Lewis Research Center, Cleveland, Ohio					
16. Abstract <p>An analysis and system study was performed to provide design information regarding lubricant and coolant flow rates and flow paths for effective utilization of the lubricant and coolant in a once-through bearing oil-mist (microfog) and coolant air system. A system was designed, manufactured, and coupled with an existing test rig simulating an aircraft engine mainshaft design, and evaluation tests were performed using 125-mm bore split-inner-ring angular-contact ball bearings under 14,590 N (3,280 lbs) thrust load.</p> <p>Both static and dynamic tests were performed. Static tests were executed to evaluate and calibrate the mist supply system. A total of thirteen dynamic step-speed bearing tests were performed using four different lubricants and several different mist and air supply configurations. The most effective configuration consisted of supplying the mist and the major portion of the cooling air axially through the bearing.</p> <p>Bearing speeds as high as <math>3 \times 10^6</math> DN were obtained for short periods but the majority of the tests were performed at <math>2.5 \times 10^6</math> DN for extended periods of time, as long as 35 hours in one test run. Cooling air was supplied in a range of 294°K (70°F) to 422°K (300°F) and the mist air at 333°K (140°F) to 366°K (200°F). Successful operation was obtained with an oil flow rate as low as 221 cc (13.5 cubic inches) per hour with the total air supply of 1.63 scmm (57.5 scfm) to a speed of <math>2.5 \times 10^6</math> DN. In another test an air flow of only 1.10 scmm (42 scfm) was successfully used to the same speed.</p> <p>The results of these tests have shown the feasibility of using a once through oil mist and cooling air system to lubricate and cool a high speed, high temperature aircraft engine mainshaft bearing.</p>					
17. Key Words (Suggested by Author(s)) Bearing Mist Lubrication; Bearing Microfog Lubrication; Aircraft Engine Bearing Lubrication; High Speed Bearing Lubrication; Mist Lubrication Microfog Lubrication; Bearing Lubrication			18. Distribution Statement Unclassified - Unlimited		
19. Security Classif (of this report) Unclassified		20. Security Classif. (of this page) Unclassified		21. No. of Pages 127	
				22. Price*	

\* For sale by the National Technical Information Service, Springfield, Virginia 22161

## FOREWORD

The research described herein, conducted by the S K F Industries, Inc. Technology Services Division, was performed under NASA Contract NAS3-16826. The work was completed under the management of the NASA Project Manager, Mr. William R. Loomis, Fluid System Components Division, NASA Lewis Research Center.

TABLE OF CONTENTS

	<u>Page</u>
SUMMARY	1
1.0 INTRODUCTION	3
1.1 Objective	3
1.2 Background	4
2.0 MATERIALS TESTED	7
2.1 Test Bearings	7
2.2 Lubricants	7
3.0 TEST FACILITY	11
3.1 Test Rig	11
3.2 Drive System	16
3.3 Mist and Through Bearing Cooling Air System	18
3.4 Bearing Housing and Shaft Cooling Air System	18
3.5 Rig Bearing Recirculating Lubrication System	21
3.6 Instrumentation	23
4.0 ANALYTICAL STUDY	25
4.1 Evaluation of Cooling Air Flow Rate Requirements	26
4.2 Evaluation of Mist Oil Supply Rate Requirements	28
4.3 Mist and Cooling Air Delivery System	35
5.0 TEST PROCEDURE	43
6.0 TEST RESULTS AND DISCUSSION	45
6.1 Mist System Evaluation Tests	45
6.2 Step-Speed and Extended Period Tests	52
6.2.1 Test No. 1, Step-Speed	52
6.2.2 Test No. 2, Step-Speed	53
6.2.3 Test No. 3, Step-Speed	56
6.2.4 Test No. 4, Step-Speed	60
6.2.5 Test No. 5, Extended Period Test	63
6.2.6 Test No. 6, Recirculating Oil	66
6.2.7 Test No. 7, Extended Period Test	72
6.2.8 Test No. 8, Reduced Mist Oil Flow Rate	76
6.2.9 Test No. 9, Reduced Through Bearing Cooling Air Flow Rate	77
6.2.10 Test No. 10, Standard Bearing	84
6.2.11 Test No. 11, Increased Cooling Air Temperature	91
6.2.12 Test No. 12, Under Race Mist Lubrication	95
6.2.13 Test No. 13, Tangential Cooling Air	101
6.2.14 Test No. 14, Extended Period Test	109



TABLE OF CONTENTS. (CONTD)

	<u>Page</u>
6.3 General Discussion of Results	109
7.0 CONCLUSIONS	118
8.0 RECOMMENDATIONS	120
9.0 LIST OF REFERENCES	121
APPENDIX I - Estimated Bearing Cooling Air Flow Rate Requirement	122
APPENDIX II - Mist and Cooling Air Nozzle Design	125

LIST OF FIGURES

<u>No.</u>	<u>Title</u>	<u>Page</u>
1	Test Bearing	8
2	Test Rig - General Plan View	12
3	Test Rig Layout Drawing	13
4	Isometric View of Mounting Arrangement	14
5	Bearing Inner Race Mounting Sleeve	17
6	Test Rig, Mist and Cooling Air Flow Schematic	20
7	Layout Drawing of Modified Rig	22
8	Estimated Test Bearing Heat Generation Rate	29
9	Inner Race Ball Contact Showing Oil Film Thickness at Various Locations	31
10	Calculated Oil Replenishment Rate	34
11	Manifold and Dual Nozzle Arrangement	38
12	Lubricant Flow Path	39
13	Mist Generator Calibration	46
14	Photographs of Mist Oil Plated Out on Stationary Test Bearing	49
15	Test Bearing Components After 10,000 RPM Evaluation Test	51
16	Test Bearing Components After Test No. 1	55
17	Test Bearing Components After Test No. 2	58
18	Rig Components After Test No. 2	59
19	Test Bearing Components After Test No. 3	62
20	Test Bearing Components After Test No. 4	65
21	Test Bearing Components After Test No. 5	67
22	Bearing and Oil Temperatures Recirculating Oil Test	69

LIST OF FIGURES (CONTD)

<u>No.</u>	<u>Title</u>	<u>Page</u>
23	Test Bearing Components After Test No. 6	73
24	Test Bearing Components After Test No. 7	75
25	Test Bearing Outer Ring Temperature with Various Mist Oil Flow Rates and Cooling Air Flow Rates	81
26	Heat Transferred to Mist and Cooling Air with Changes in Through Bearing Cooling Air and Mist Oil Flow Rate	82
27	Test Bearing Components After Test Nos. 8 and 9	85
28	Test Bearing Components After Test No. 10	87
29	Test Bearing Outer Ring Temperature	89
30	Heat Transfer Rate from Test Bearing	90
31	Test Bearing Outer Ring Temperature	93
32	Heat Transfer Rate from Test Bearing	94
33	Test Bearing Components After Test No. 11	96
34	Test Bearing Outer Ring Temperature	99
35	Heat Transfer Rate to Mist and Cooling Air	100
36	Test Bearing Components After Test No. 12	102
37	Mist and Cooling Air Manifold with Modified Air Nozzles	104
38	Heat Transfer Rate to Mist and Cooling Air	106
39	Test Bearing Outer Ring Temperature	107
40	Test Bearing Components After Test No. 13	108
41	Conducted and Radiated Heat Transfer Rate From Test Bearing	114
42	Bearing Heat Generation Rates with Mist Lubrication and Recirculation Lubrication	117

LIST OF TABLES

<u>No.</u>	<u>Title</u>	<u>Page</u>
1	Physical Properties of Test Fluids	10
2	Calculated Bearing Heat Generation Rate	27
3	Test and Calculated Data - Test No. 1 (Step-Speed), Lubricant - XRL850A, Bearing S/N 13	54
4	Test and Calculated Data - Test No. 2 - (Step-Speed), Lubricant - XRL850A + 5% Kendall Resin, Bearing S/N 15	57
5	Test and Calculated Data - Test No. 3 - (Step-Speed), Lubricant - XRM232A, Bearing S/N 17	61
6	Test and Calculated Data - Test No. 4 - (Step-Speed), Lubricant - XRM205F, Bearing S/N 18	64
7	Test and Calculated Data - Test No. 6 - Lubricant XRM205F, Bearing S/N 13	71
8	Test No. 7 (Extended Period), Lubricant XRL850A + 5% Kendall Resin, Bearing S/N 30	74
9	Test No. 8, Run 1 (Reduced Mist Oil Flow Rate), Lubricant - XRL850A + 5% Kendall Resin, Bearing S/N 18	78
10	Test No. 8, Run 2 (Reduced Mist Oil Flow Rate), Lubricant - XRL850A + 5% Kendall Resin Bearing S/N 18	79
11	Test No. 8, Run 3 (Reduced Mist Oil Flow Rate), Lubricant - XRL850A + 5% Kendall Resin Bearing S/N 18	80
12	Test No. 9 (Decreased Cooling Air), Lubricant XRL850A + 5% Kendall Resin Bearing S/N 18	83
13	Test No. 10 (Standard Bearing), Lubricant XRL850A + 5% Kendall Resin Bearing S/N 22	88
14	Test No. 11 (Increased Cooling Air Temperature), Lubricant XRL850A + 5% Kendall Resin Bearing S/N 15	92
15	Test No. 12, Lubricant XRL850A + 5% Kendall Resin Bearing S/N 15	98
16	Test No. 13 (Tangential Cooling Air), Lubricant - XRM850A + 5% Kendall Resin Bearing S/N 27	105
17	Test Bearing Heat Generation Data (Test 8, Run 1)	116

SUMMARY

The objective of the research performed on this program was to establish the feasibility of lubricating and cooling high-speed mainshaft angular-contact ball bearings of aircraft gas turbine engines by a once-through oil mist and cooling air system.

Analytical and experimental studies were performed to determine the lubricant and coolant flow rates and flow paths needed in an air-cooled, oil-mist lubrication system. A system was designed, manufactured and coupled with an existing SKF owned test rig designed to simulate aircraft engine mainshaft design by avoiding thick sections in the shaft and housing and providing flexibility between the main rig housing and the bearing outer ring. Test bearings were 125-mm bore split-inner-ring angular-contact ball bearings under 14,590N (3,280 lbs) thrust load.

The oil mist system was designed to supply air supported oil particles through ten converging reclassifying nozzles to one side of the test bearing. The oil mist was directed by the nozzles to the opening between the cage bore and inner ring land and to an enlarged chamfer on the inner ring face from which it was centrifugally pumped into the bearing. The cooling air system was designed to supply three flow paths; directly through the bearing in the same direction as the mist, circumferentially around the bearing housing, and through the hollow shaft.

Static bearing tests were performed with the mist system to establish mist oil flow rates and mist air flow rates, uniformity of mist flow from the various mist nozzles, and oil wetting patterns on a static bearing. These tests showed that the mist flow was essentially equal from each nozzle and that the oil was wetting out on the desired bearing elements.

A total of thirteen dynamic step-speed bearing tests were performed with mist lubrication and one with recirculating oil lubrication applied to the test bearing. Three mist tests, one each, were performed with a high viscosity synthesized paraffinic hydrocarbon, a low viscosity synthesized paraffinic hydrocarbon, and an advanced ester (MIL-L-23699) fluid. The remaining mist tests were performed with the low viscosity synthesized paraffinic hydrocarbon plus 5% heavy paraffinic resin. The results of these tests proved the feasibility of using a once-through oil-mist and cooling-air system to lubricate and cool a high-speed, high-temperature aircraft engine mainshaft bearing. The majority of the mist tests were performed with mist and cooling air supplied through the bearing and additional cooling air to the bearing housing. Shaft cooling air was not required.

Bearing speeds as high as  $3 \times 10^6$  DN (D = bearing bore in mm, N = shaft speed in rpm) were obtained but the majority of the tests were performed at  $2.5 \times 10^6$  DN for extended periods of time, as long as 35 hours in one test run. A thrust load of 14,590 N (3,280 lbs.) was applied to the test bearing. Cooling air was supplied at temperatures of 294°K (70°F) to 422°K (300°F) and the mist air at 333°K (140°F) to 366°K (200°F). Successful tests were performed with mist oil flow rates as low as 221 cc (13.5 cubic inches) per hour with the total air supply of 1.63 scmm (57.5 scfm) to speeds of  $2.5 \times 10^6$  DN. Another test with air flow of only 1.19 scmm (42 scfm) was successfully used to speeds of  $2.5 \times 10^6$  DN.

## 1.0 INTRODUCTION

### 1.1 Objective

The high-speed mainshaft ball bearings in aircraft gas-turbine engines are normally lubricated by recirculating oil supplied through pressurized jets impinging on the sides of the bearing or oil pumped through passages between the halves of the split inner ring. Only a minor portion of the oil supplied is required to provide elastohydrodynamic (EHD) lubrication while the major quantity is required to remove the bearing generated heat which represents a power loss in the engine. A large fraction of the bearing generated power loss results from churning of the large quantity of oil required to transfer the heat from the bearing. This interrelated effect between oil rate supplied for cooling and oil churning heat generation can result in a condition where an increase in oil supply will result in a minimal, if any, decrease in the operating temperature of the bearing. This is particularly true at high shaft speeds.

Recent improvements in turbine and compressor component materials, which permit higher operating speeds and thus higher gas-turbine engine efficiencies, result in higher heat generation rates in the bearings and thus higher bearing operating temperatures. At the high bearing temperatures, the oil starts to degrade and in a recirculating system the degrading effect is accumulative due to repeated passes through the bearing and can result in a breakdown in the lubricating ability as well as the formation of varnish and carbon deposits which are detrimental to bearing performance.

One approach to minimize this problem is the use of a once through mist oil system for bearing lubrication and supplemental cooling air to remove the bearing generated heat. Such a system was envisioned to improve higher temperature operating capability, since the small quantity of oil required for lubrication is discarded and the oil degradation is minimized due to the single pass through the bearing. Bearing power loss was also anticipated to be minimized due to greatly decreased oil churning at the high speeds which in turn reduces the overall heat sink capacity requirements. In addition to providing a method of lubrication for high temperature bearings where thermal degradation of the lubricant is of less concern, and the power loss is minimized, mist lubrication can result in a system of less weight and complexity since large capacity supply and scavenge pumps, and heat exchangers are absent. It is noted that these advantages would offset any reductions in engine efficiency from use of bleed-off air from the compressor or

some other source required to supply the mist and cooling air requirements.

The purpose of the research performed on this program was directed at establishing the feasibility of lubricating and cooling high-speed aircraft mainshaft engine bearings by an oil mist (microfog) and cooling air system. The program consisted of two major tasks.

Task I - Perform an analysis and preliminary system study to provide design information for coolant and lubricant flow rate and flow paths with minor test bearing geometry changes to give effective utilization of the cooling gases and lubricating liquids in a once-through oil mist and cooling air system. Design and manufacture a mist and cooling air system for evaluation testing.

Task II - Demonstrate the feasibility and practicability of lubricating and cooling a high speed (DN range of  $2.5 \times 10^6$  and higher)\*, large scale (125 mm bore), aircraft quality engine ball bearing with a once-through mist lubrication and cooling system.

## 1.2 Background

The use of mist-oil lubrication for bearings is not new, the principles were first developed by a European bearing manufacturer in the late 1930's. The problem that nurtured this development was the inability to satisfactorily lubricate high-speed spindle bearings on grinders and similar equipment. Using the principles developed at that time, the generation of microfog oil, its delivery and insertion to lubricate bearings was further developed by various companies and used in a broad range of industrial applications. These applications, however, are less severe (lower DN values, loads and temperatures) than those presently envisioned for aircraft engine bearings of the near future.

Early studies and evaluation testing of mist lubrication of aircraft turbine engine ball bearings was performed by S K F on NASA Contract NAS3-6267 starting in 1966 (1)\*\*. Several different lubricants were evaluated in tests up to  $1.75 \times 10^6$  DN. These tests showed a definite potential; however, these studies were basically conducted with bearings and lubricant supply components which were designed for recirculating oil systems. In particular,

\*The DN value is the product of the bearing bore in mm and the shaft speed in RPM.

\*\*Numbers in parentheses refer to List of References at the end of this report.



the bearings and oil-mist supply configuration, which supplied mist and cooling air to both sides of the test bearing, was inoptimum for supplying mist and cooling air to the bearing areas where the lubricant is required for effective utilization. Thus, initial attempts to operate large mainshaft size angular-contact ball bearings with mist lubrication under advanced turbine powerplant speeds, loads, and temperatures were unsuccessful with most candidate lubricants and only partially successful with one oil, a formulated synthetic paraffinic hydrocarbon, at  $1.75 \times 10^6 \text{ DN}$ .

As the result of these tests, basic oil mist studies were conducted by Mobil Oil Company under Contracts NAS3-9400 and NAS3-13207 (2,3) to determine oil-mist particle size distribution, mist reclassification nozzle operation and wetting efficiencies, heat transfer coefficients through wetted films, and a variety of related basic phenomena underlying oil-mist lubrication technology.

A synopsis of the most important results from the Mobil studies is as follows.

1. Larger mist particle size ( 11 microns and larger) gave greater wetting rates when the oil-mist was impinged on flat rotating disks. Previous reference data had indicated optimum particle size range of 2 to 3 microns for most effective wetting.

2. Centrifugal forces enhance wetting. Wetting rates increased with increasing temperatures and speeds of a rotating disk.

3. Convective heat transfer to the mist is primarily a function of the gas phase. Oil in the mist had little effect on the heat transfer coefficient (e.g., 4 percent increase). Heat transfer coefficients were established to be approximately  $340 \text{ W/m}^2\text{-}^\circ\text{K}$  ( $60 \text{ Btu/hr-ft}^2\text{-}^\circ\text{F}$ ).

4. The use of a 150-mesh screen inserted into the inlet of the mist nozzle increased the wetting rate of the mist by 80 percent.

5. The synthetic paraffinic lubricant was found to have the best wetting characteristic of five fluids studied.

6. Rates of oil output were found to increase with decreasing kinematic viscosity of the oils and with increasing gas flow rate.

AL75T032

Based on these results and the potential advantage of oil-mist lubrication, further studies were performed at S K F on NASA Contract NAS3-16826. The approach used to evaluate mist lubrication and the results of the study are the subject of this report.

## 2.0 MATERIALS TESTED

### 2.1 Test Bearings

The test bearing design selected for this program is a split-inner-ring, angular-contact ball bearing; the type most widely used in aircraft propulsion turbines. This design, S K F 459981-G1, which permits a maximum ball complement by virtue of the separable inner-ring halves, can support high thrust loads in either direction. The high race lands permit the acceptance of large thrust loading without overriding the available groove area. The separable ring feature also permits the use of a precision-machined one-piece cage which is required for high-speed high-temperature operation. These outer land riding cages normally are designed so that the balls are retained both radially inward and outward for ease of assembly in engines. Cages for the test bearings on this program, however, are made so that the balls are retained radially inward only in order to facilitate ball pocket inspection.

The test bearings have a bore diameter of 125 mm and a nominal unmounted design contact angle of  $30^{\circ} 30''$ . The test bearing is illustrated in Figure 1. The ring, balls and cages are manufactured from consumable electrode vacuum melted (CVM) M50 tool steel to provide high temperature hardness. The cages are silver plated AISI 4340 steel according to the latest jet-engine bearing practice to minimize the friction and wear at the ball and ring land contacts.

The basic bearing design was modified by incorporating a 45 degree chamfer (3.8 x 3.8 mm) between the inner-ring face and land surfaces on the side opposite the puller groove. This chamfer surface was provided to permit centrifugal pumping into the bearing of plated out mist oil particles. In addition a taper of 5 degrees was machined on both sides of the cage bore which sloped radially outward toward the center of the bearing to cause the oil plated on the bore surface to be centrifugally pumped into the bearing ball pockets.

### 2.2 Lubricants

The selection of the lubricants for this program were based on the results of tests performed by the Mobil Oil Company in which misting characteristics, wetting characteristics and the deposit forming tendencies of the mist oil impinging on a high temperature surface were evaluated. The results of the tests are reported in (4). The four fluids used in the test program were:

S-1156A R100  
7-27291

1. VENDOR PART NO.	45-541 G-1
2. VENDOR DRAWING NO.	700-13
3. BEARING TOLERANCE	ANAL
4. NO. & SIZE OF BALLS	21-1/16" O.D. DIA.
5. INTERNAL RADIAL LOOSENESS (UNMOUNTED)	.0075"-.0084"
6. MAX. END PLAY (UNMOUNTED)	.030"
7. DESIGN CONTACT ANGLE	28°30'-52°30'
8. OUTER GROOVE RADIUS AS PERCENT OF BALL DIA.	52.00-52.24
9. INNER GROOVE RADIUS AS PERCENT OF BALL DIA.	51.63-51.75
10. SHM WIDTH	.012"
11. PITCH DIA.	6.240"
12. CAGE WIDTH (MAX)	1.024"
13. CAGE SPEC. (FOR OUT OF ROUNDNESS & SQUARENESS)	470939
14. CAGE POCKET CLEARANCE	.019-.032"
15. BALL GRADE (AFBMA)	15
16. INNER RING MATERIAL	M-50
17. OUTER RING MATERIAL	M-50
18. BALL MATERIAL	M-50
19. CAGE MATERIAL	4340
20. CAGE TYPE	ONE PIECE MACHINED OUTER LAND RIDING
21. BEARING DESIGNED TO OPERATE AT (MAX)	650°
22. INNER RING HARDNESS	60 MIN.
23. OUTER RING HARDNESS	60 MIN.
24. BALL HARDNESS	60 MIN.
25. CAGE HARDNESS	53 MIN.
26. CAGE FINISHING CLEARANCE ON DIA.	.001"-.002"
27. CAGE O.D. DIA.	6.671"-6.683"
28. CAGE I.D. DIA.	2.111"-2.121"
29. CAGE PLATING	SILVER AMS 2410 *
30. CAGE PLATING THICKNESS	.001"-.002"

CAGE TO BE 100% FLUORESCENT PENETRANT INSPECTED (470908)

100% VISUAL INSPECTION (470663)

100% MAGNIFYING INSPECTION (471662)

100% FITCH INSPECTION (471637)

MATERIAL IDENTIFICATION CONTROL AS PER SPEC. 471085

INNER RING, OUTER RING &amp; BALLS TO BE BLACK OXIDE TREATED

AS PER AMS 2435

SURFACE FINISH REQUIREMENTS:

	16	RMS	MAX
INNER RING BORE	16		
INNER RING GROOVE	4		
OUTER RING O.D. DIA.	16		
OUTER RING GROOVE	4		
PAINT SUPPORT SURFACE	20		
BALL	1.2		
OUTER RING BORE	4		
INNER RING O.D. DIA.	4		

MAX. CAGE UNBALANCE 35M-CM, BALANCE TO BE CHECKED AT 500RPM (MIN)

INNER &amp; OUTER RING LAND TOLERANCES

A. 3 P. INT. OUT-OF-ROUND WITHIN .0004" F.I.R.

B. ECCENTRICITY TO O.D. DIA. WITHIN .0004" F.I.R.

C. SECTION HEIGHT OF LAND TO O.D. DIA. EQUAL WITHIN .0004" IN SAME AXIAL PLANE

D. 90° CONTACT WHEN ROLLED ON A HARD SUPPORT

CAGE SUPPORT

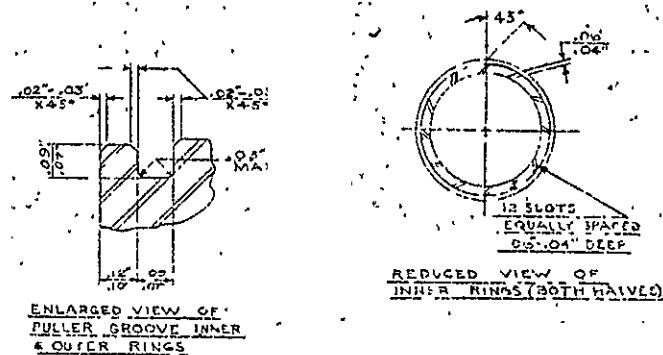
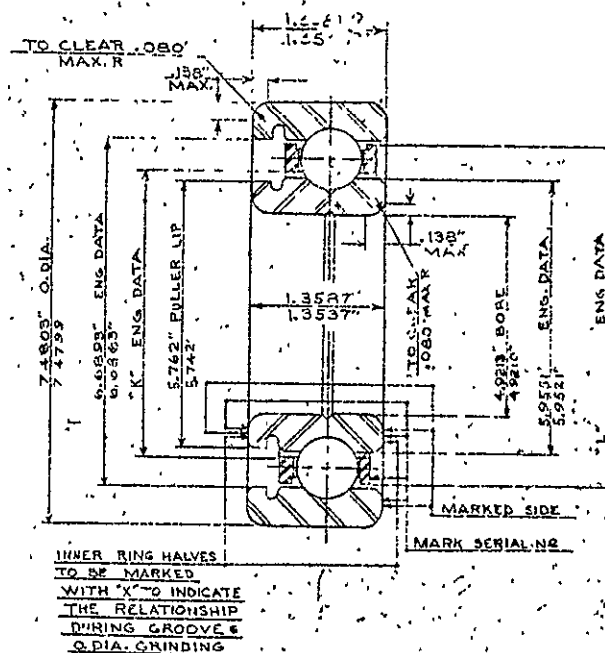
A. 3 P. INT. OUT-OF-ROUND WITHIN .002" F.I.R.

B. 3 P. INT. DIA. EQUAL WITHIN .002" IN SAME AXIAL PLANE

C. 3 P. ARENES TO COMMON MACHINING REF FACE WITHIN .002"

D. 90° CONTACT WHEN ROLLED ON A BLIND FLAT PLATE

\* CAGE TO BE PLATED BY ELECTROLYTIC METHOD

FIGURE 1  
TEST BEARING

AL75T032

1. Mobil XRM205F - Experimental viscous synthetic paraffinic hydrocarbon formulated against oxidation and wear.
2. Mobil XRL850A - Experimental synthetic paraffinic hydrocarbon formulated against oxidation and wear.
3. Mobil XRL850A - Containing five percent by weight of Kendall 0839 Heavy Paraffinic Resin.
4. Mobil XRM232A - Experimental advanced type II ester fluid.

Identification by chemical type, and physical properties for each lubricant, are listed in Table I.

TABLE I - PHYSICAL PROPERTIES OF TEST FLUIDS

Fluid	XRM 205 F	XRL 850 A	XRM 232 A	XRL 850 A + 5% Resin
Chemical Type	Synthetic Paraffinic Hydrocarbon	Synthetic Paraffinic Hydrocarbon	Advanced Type II Ester Fluid	Synthetic Paraffinic Hydrocarbon + 5% (by wt.) Paraffinic Resin type 0839
Formulation	Antioxidant, antiwear	Antioxidant, antiwear	Antioxidant, antiwear	
Flash Point, °F (COC)	515	435	505	455
Fire Point, °F (COC)	635	500	560	515
Autogenous Ignition Point, °F	730	650	740	690
Kinematic Viscosity (cs)				
@ 400°F	5.76	1.50	1.31	1.64
@ 210°F	39.61	6.12	5.14	7.26
@ 100°F	444	35.10	51.3	44.0
@ 0°F	39064	954	783	1343
Density @ 20°C, g/cm <sup>3</sup>	.8473	.8307	.9903	.8334
Surface Tension @ 25°C dynes/cm	32.7	30.4	30.8	30.5
Specific Heat cal/GDC				
@ 200°F	.604	.590	.520	.691
@ 400°F	.693	.676	.588	.803

AL75T032

### 3.0 TEST FACILITY

All tests were performed in an existing S K F owned high speed bearing test facility modified on this program to accommodate the requirements for mist lubrication. The basic test equipment is shown schematically in Figure 2 and consists of the following components:

- Test Rig
- Drive System
- Mist and Through Bearing Cooling Air System
- Bearing Housing and Shaft Cooling Air System
- Rig Bearing Recirculating Lubrication System
- Instrumentation

#### 3.1 Test Rig

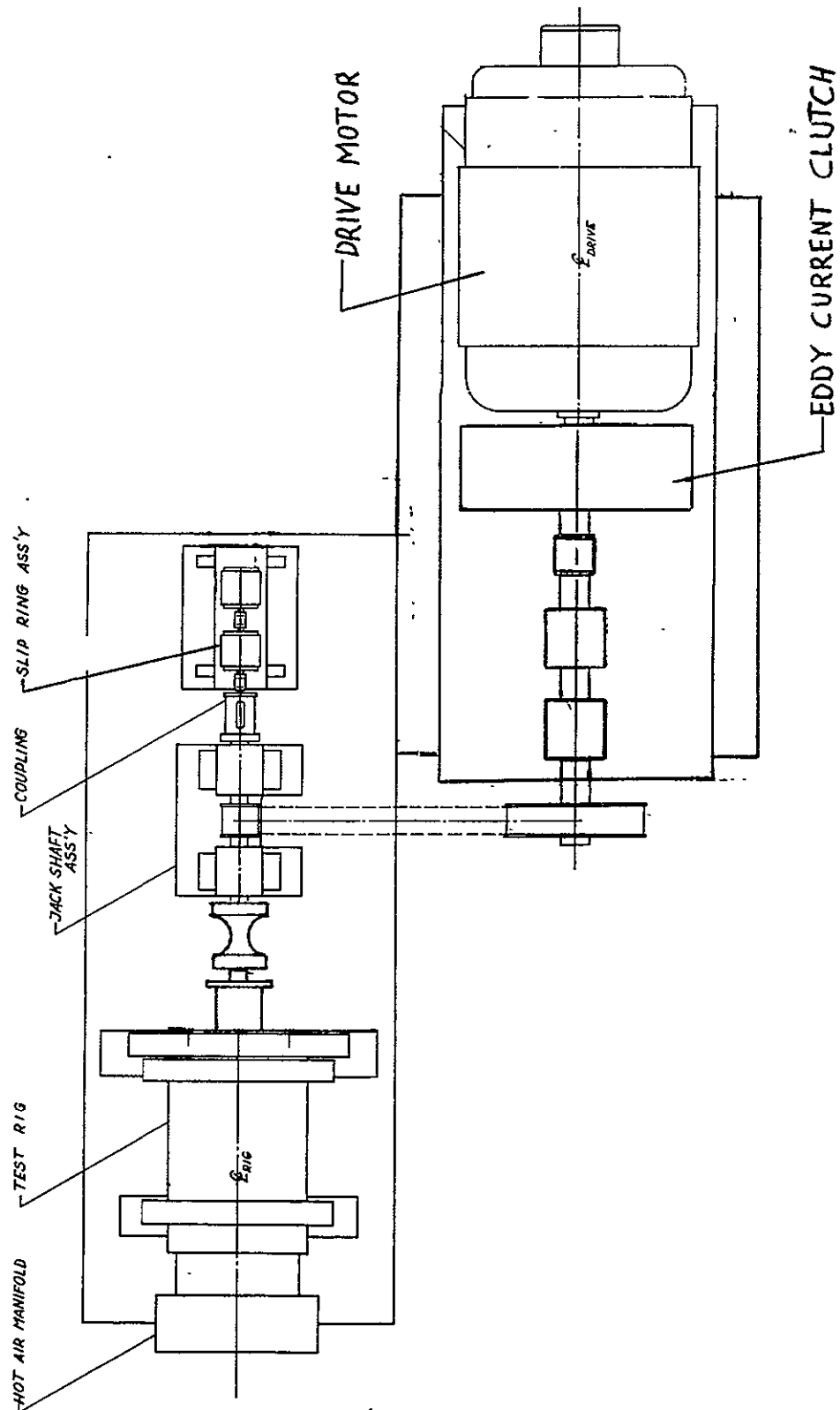
The basic test rig, with a layout drawing shown in Figure 3, is designed to simulate aircraft engine mainshaft designs by avoiding thick sections in the shaft and bearing housings and by introducing flexible sections between the main rig outer housing and the bearing outer rings. This flexibility is intended to simulate to some extent the self-aligning ability of current aircraft engine bearing mounts.

The test rig consists of a 305 mm diameter cylindrical housing in which a hollow shaft of approximately 127 mm maximum diameter is supported by the 125-mm bore angular-contact ball "test" bearing at one end and a 95-mm bore angular-contact ball "rig" bearing at the other. The housing itself is mounted in a horizontal position above a table by means of a special support system which maintains the center line height and parallelism with the table while freely permitting both radial and axial thermal expansion. This arrangement is best shown by the isometric sketch in Figure 4.

The pedestal is positioned in the plane of the test bearing for optimum rigidity and the sliding ring in the plane of the rig bearing. The pedestals are bolted securely to the rig table and also dowelled to maintain alignment.

The test bearing outer ring housing is not attached directly to the rig housing but rather is supported within a "load plug" assembly which itself is supported within the main rig housing by two angular contact bearings (referred to as the "load plug" bearings) mounted in a face-to-face arrangement. A sliding fit is provided between the inner ring mounting sleeve for these angular-contact bearings and the O.D. of the load plug. The axial and rotational movement capability

FIGURE 2

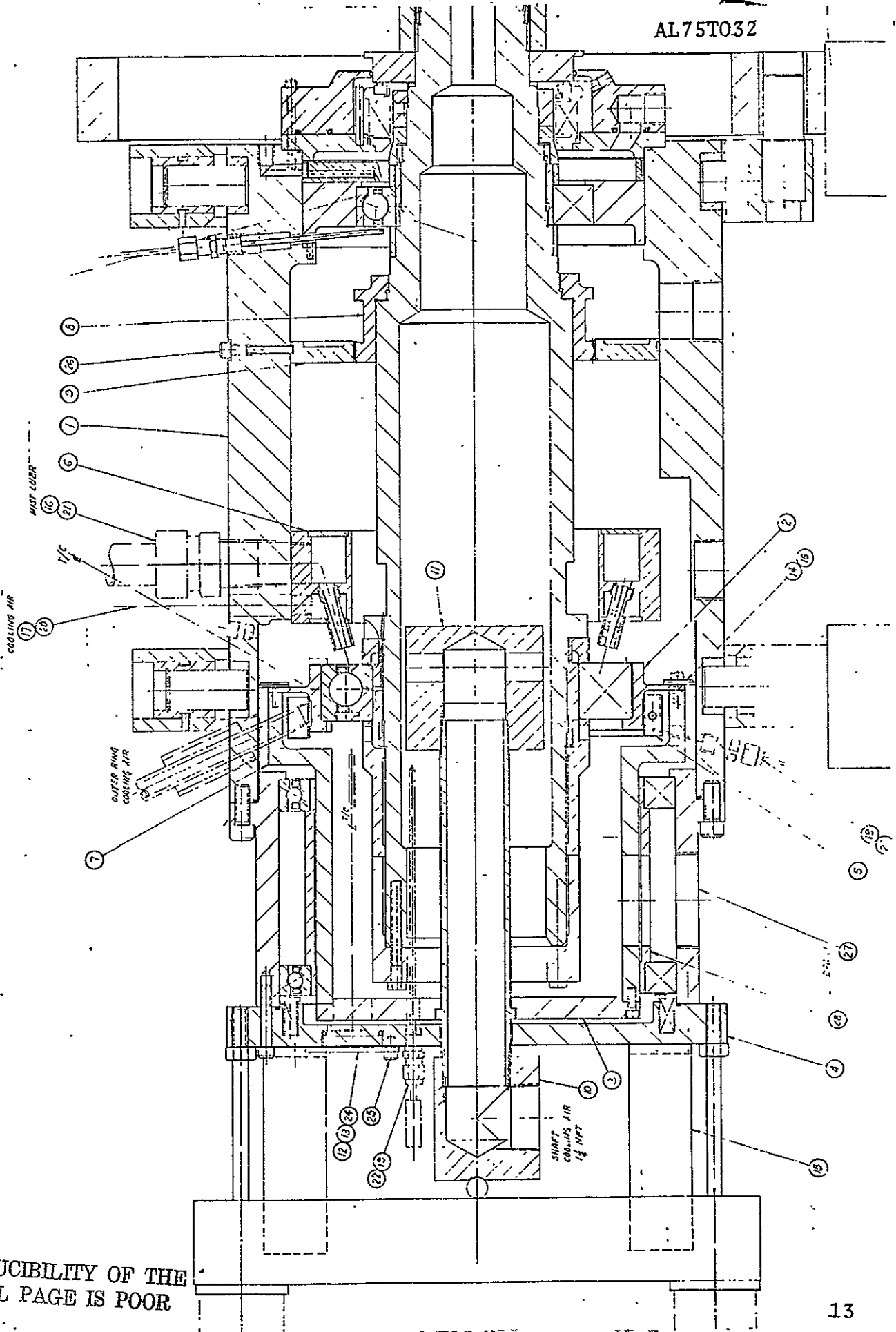
TEST RIG - GENERAL PLAN VIEW



AL75T032

FIGURE 3

TEST RIG LAYOUT DRAWING

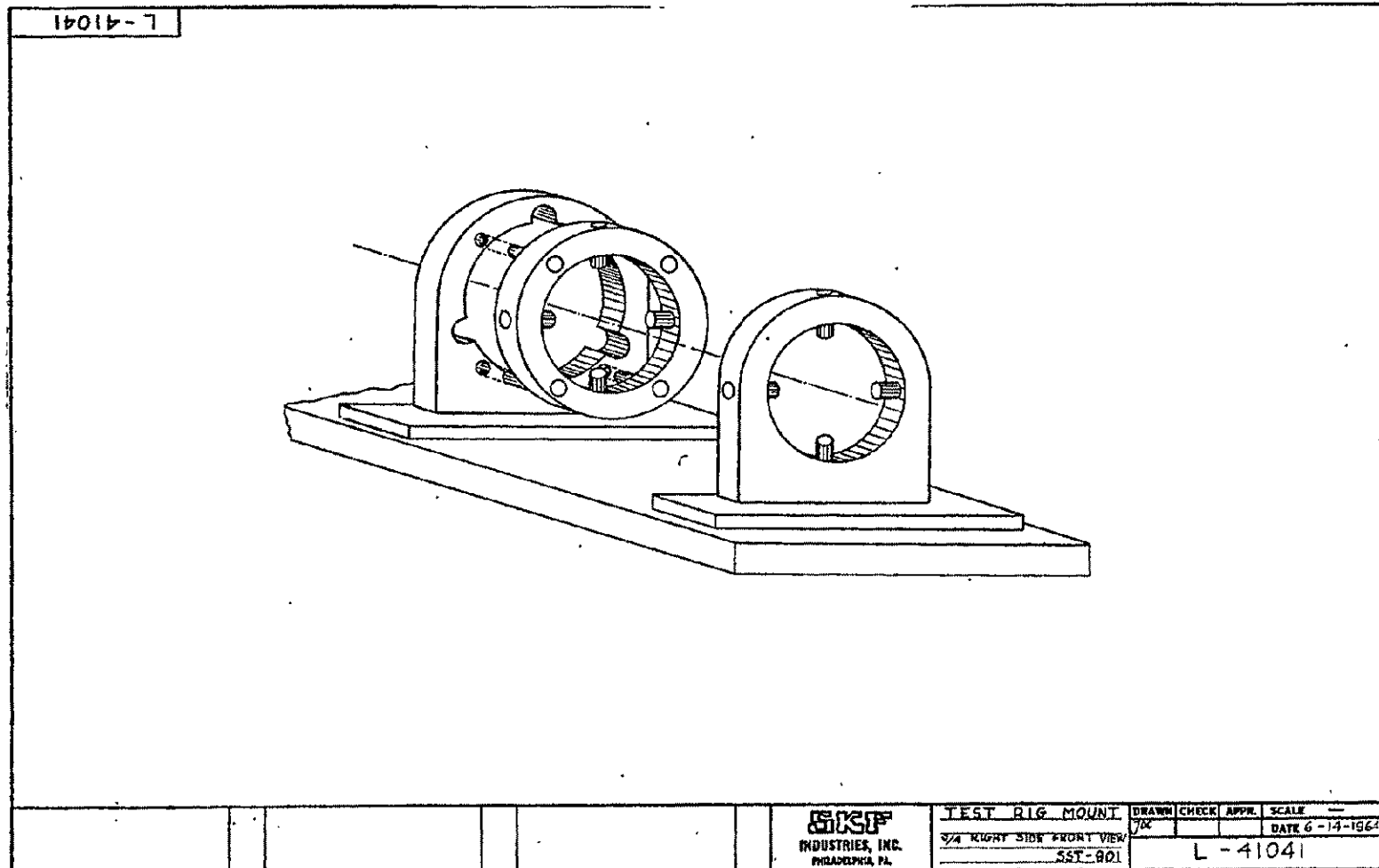


REPRODUCIBILITY OF THE  
ORIGINAL PAGE IS POOR

FIGURE 4

ISOMETRIC VIEW OF MOUNTING ARRANGEMENT

14

RESEARCH LABORATORY **SKF** INDUSTRIES, INC.

AL751032

reduction in internal bearing clearance. M-1 steel sleeves are therefore interposed between the shaft and inner rings of the test and rig bearings. These are of the form shown in Figure 5 and have a gap at room temperature between the shaft and the inside surface of the sleeve under the bearing. Rotation of the sleeve on the shaft is prevented by an interference fit between the shaft and the thinned-down ends of the sleeve. Radial location of the bearings at low temperatures is achieved by the bending stiffness of the sleeves. As the temperature rises during the heat-up period and the shaft expands it progressively closes the gap under the sleeve until contact occurs at a temperature of 533°K. It should be noted that the under-race cooling and lubrication flow holes shown in the sleeve in Figure 5 were not used during the testing. In the through inner race mist lubrication test, radial holes were provided in a modified sleeve which did not contain the axial slots. The rig angular contact bearing on the other end of the shaft utilizes a similar mounting sleeve.

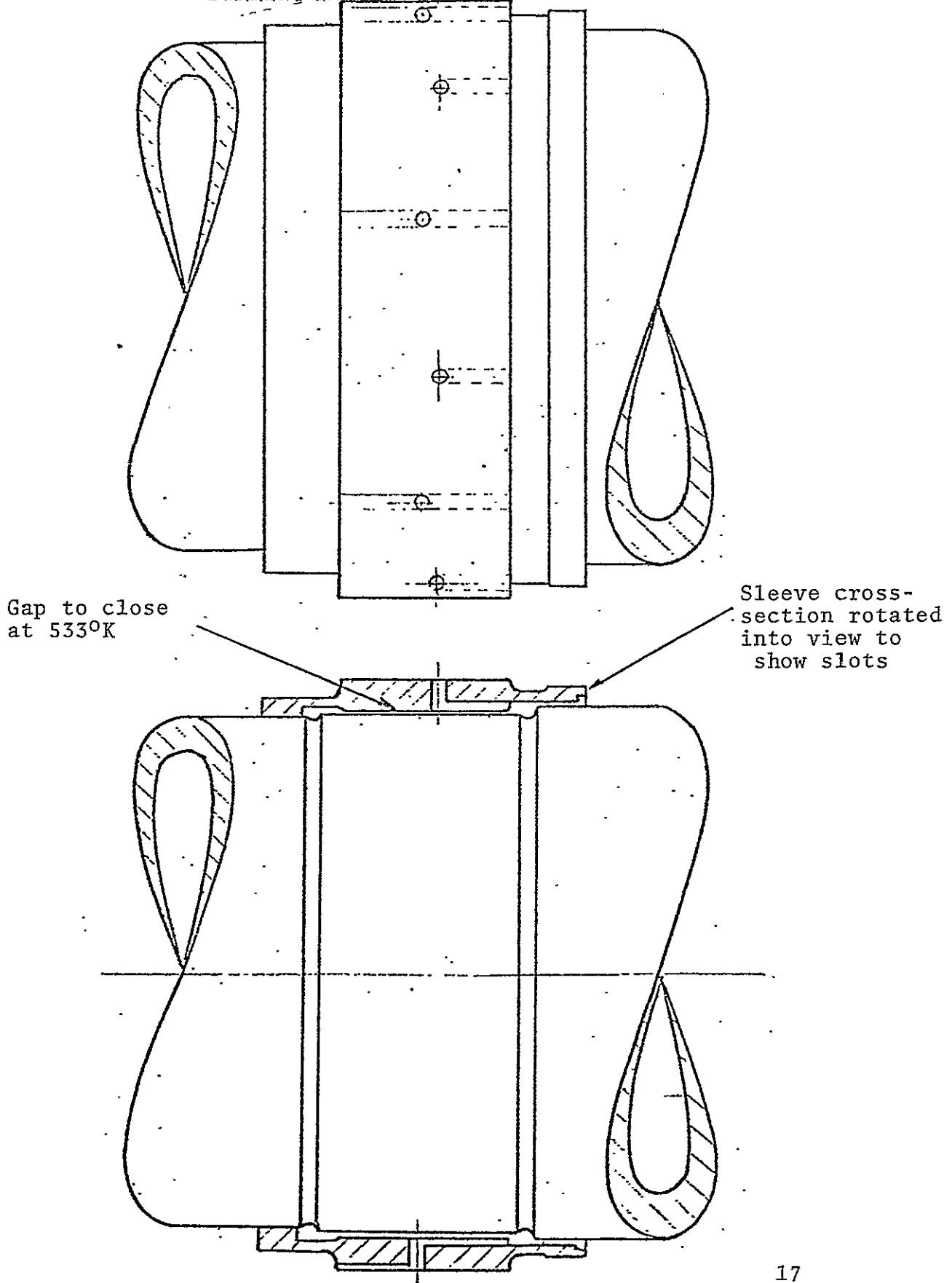
### 3.2 Drive System

The rig drive system consists of a constant speed 75 HP motor which drives the test rig through an eddy-current clutch to provide variable speed. The motor and clutch combination, mounted on an adjustable base bolted to the rig table, drives a jackshaft through a flat belt drive. The jackshaft unit consists of a hollow shaft mounted in matched pairs of preloaded angular-contact bearings with a 76.2 mm diameter removable slightly crowned pulley at its center. The bearings are supported in steel pillow blocks welded to a rigid base and are lubricated by a separate circulating cold mineral oil supply fed to the top cap of each bearing. An oil drain running horizontally across the width of the pillow block returns the oil to the scavenge lines.

The rig shaft is connected to the jackshaft by a Form-Flex coupling. The other end of the jackshaft drives the slip ring and tachometer assemblies through a rotating electrical connector and a small flexible coupling. The jackshaft is hollow to carry the wiring from transducers in the test rig to the slip rings. Shear pins are provided in the base of the motor pulley to permit rapid stoppage of the rig in the event of seizure of a rotating component within the rig. A plain bearing is fitted to the motor shaft to prevent damage to the surfaces in the event of shear pin breakage. Both the rig shaft and jackshaft are dynamically balanced for high speed operation.

FIGURE 5

## BEARING INNER RACE MOUNTING SLEEVE



### 3.3 Mist and Through Bearing Cooling Air System

The mist and through bearing cooling air system is shown schematically in Figure 6. The air flow commences with the air compressor which has a rated output of 2.57 scmm (91 scfm) at 1.38 newtons/meter<sup>2</sup> (200 psig). Air feeds directly to a dryer and filter column which reduces the moisture content to a 227°K (-50°F) dew point and the hydrocarbons to 13 parts per million. This clean, dry air then passes to a 0.57 cubic meter (20 cu. ft.) receiver and hence through a shut-off valve and to a pressure regulator. A pneumatic servo control on this regulator maintains the pressure between  $6.55 \times 10^5$  and  $7.24 \times 10^5$  newtons per square meter (95 and 105 psi). The regulated air then passes through an indicating flowmeter to a 45 kw electrical heater, located in the room containing the test rig, in which the air passes through approximately 6.7 meters of 316 stainless tubing which is radiantly heated by electric heating elements. A pressure gage located just prior to the flowmeter permits pressure correction to be made to the indicated flowmeter.

The flow then divides, one portion going to the mist generator and the remaining portion to the through bearing cooling air manifold located inside the rig and through the ten air nozzles described in Section 4.3. A pressure regulator, used to control the cooling air flow rate, and thermocouple are located in the air line. The heated air flow rate supplied to the mist generator is controlled by a pressure regulator after which it passes through a flowmeter and an auxiliary heater before it enters the mist generator. The mist generator consists of an Alemite 41 cfm mist generating head housed in a cylindrical mist oil container where the mist oil supply is maintained at 366°K (200°F) by thermostat controlled electrical heater located external to the container. Leaving the mist generator the mist air divides and flows through two 20.9 mm (0.824 in.) I.D. stainless steel tubes which enter the mist manifold inside the test rig housing at diametrically opposite positions. Two thermocouples, one in each tube, are located just prior to the rig housing. The description of the manifold and accompanying ten mist nozzles are described in Section 4.3. A thermocouple is positioned approximately 12.7 mm (0.5 in.) downstream of the test bearing to detect the combined mist and cooling air temperature as it leaves the bearing and before it is exhausted through a 50.8 mm (2.0 in.) diameter holes in the load plug and the rig housing face plates.

### 3.4 Bearing Housing and Shaft Cooling Air System

The shaft and bearing housing cooling air is supplied by a different air compressor from which it passes through a filter,

pressure regulator, and flowmeter into a heater similar to that used for the mist and through bearing cooling air. The shaft and cooling air heater and associated equipment is located in a room adjacent to the room housing the test rig. The air flows through a 50.8 mm (2 in.) I.D. tube leading to the test rig. Just prior to entering the rig the air is divided into two flow paths; one carrying housing cooling air and the other carrying the shaft cooling air. The housing cooling air passes through a pressure regulator and a flowmeter before entering the rig through a 9.25 mm (0.364 in.) I.D. tube. The temperature of cooling air supplies are sensed by thermocouples just prior to entering the rig.

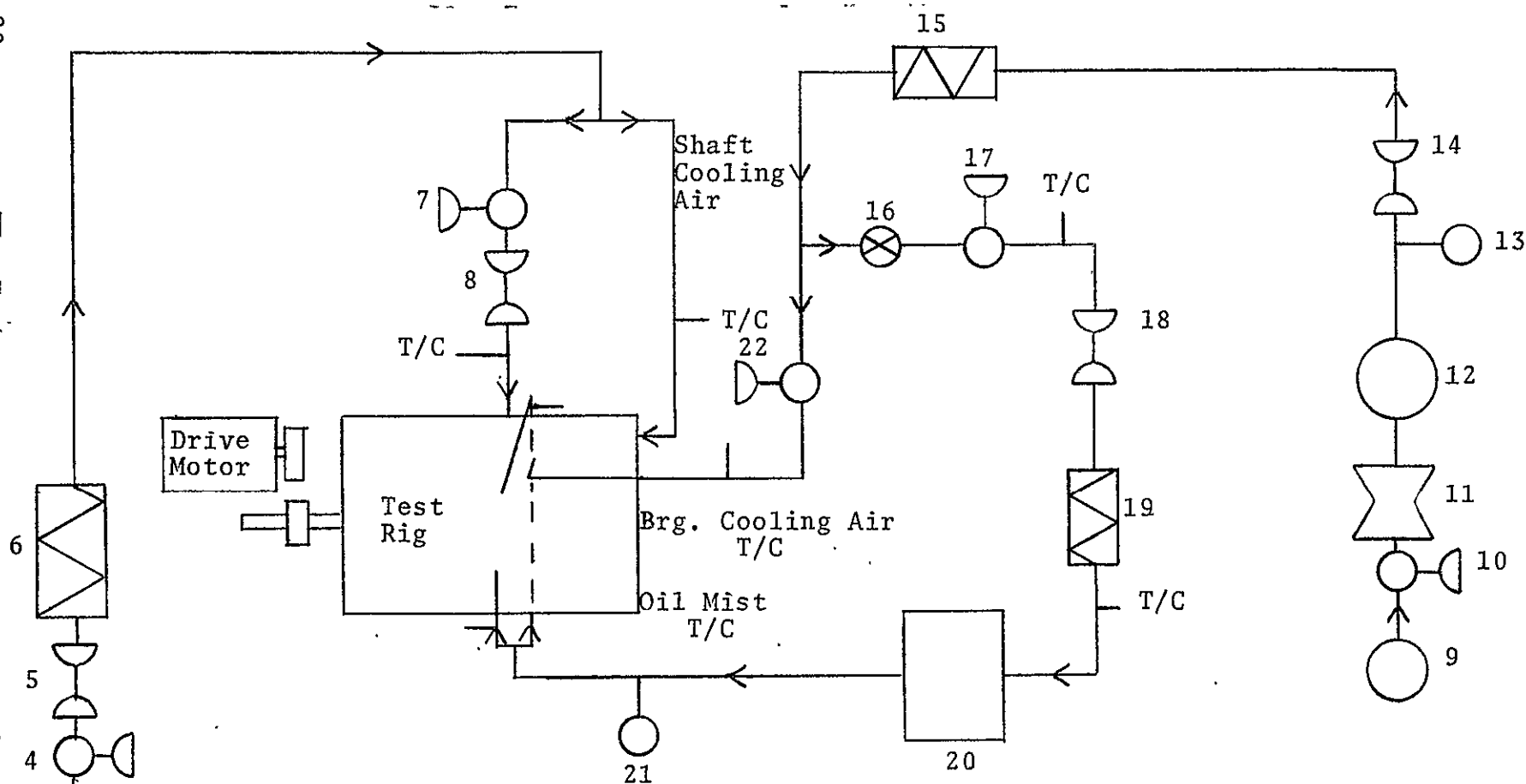
The bearing housing cooling air, entering an angular groove machined in the housing O.D. and enclosed by a housing sleeve, passes around the housing and is exhausted through a hole located 180 degrees from the entrance. It then passes through the opening in the load plug and rig face plates. A thermocouple is located at the exhaust port in the housing sleeve to detect the exhaust air temperature.

The inner race or shaft cooling air enters the hollow shaft through a 35 mm (1.38 in.) I.D. stationary tube attached to the rig housing face plate into a manifold from which is forced radially through four 17.45 mm (0.687 in.) diameter holes located 90 degrees apart. The air then sweeps axially outward between the shaft bore and manifold which was designed to produce a high velocity flow. A thermocouple is located at the end of the annulus formed by the shaft and manifold to measure the exhaust air temperature.

The previously described mist and through bearing cooling air flow paths were used in all test runs except two; the tangential through bearing cooling air test, and the under-race mist oil lubrication test. In the tangential cooling air test, the through bearing cooling air nozzles are plugged and ten additional air nozzles inserted into the air manifold through which the cooling air is supplied. The nozzles are directed to supply the cooling air in a more tangential direction (60° with respect to bearing axes) and in the same sense as the bearing rotation.

For the under-race mist oil lubrication test the mist was supplied into the hollow shaft. To accommodate this arrangement, the shaft cooling air manifold is replaced by a mist manifold which consisted of eight reclassifying nozzles with 2.87 mm (0.113 in.) diameter exit ports. The mist is directed

FIGURE 6  
TEST RIG, MIST AND COOLING AIR FLOW SCHEMATIC



- 1-9 Compressors  
 2 Filter  
 6-15-19 Heaters  
 3-16 Valves  
 4-7-10-17-22 Regulators, Pressure  
 5-8-14-18 Flow Meters  
 11 Dryer  
 12 Receiver Tank  
 20 Mist Generator  
 13-21 Pressure Gages

through the nozzles onto a circumferential groove machined in the bore of the rotating shaft. The nozzles are positioned to direct the mist radially and at a 45 degree angle to a tangent of the shaft bore in the direction of rotation. Twelve holes approximately 2.54 mm (0.10 in.) in diameter are machined through the shaft, bearing mounting sleeve, and inner ring of the bearing to permit centrifugal pumping of the oil plated on the shaft to enter the bearing. A layout drawing of the modifications is presented in Figure 7.

### 3.5 Rig Bearing Recirculating Lubrication System

Oil circulation to the rig bearing proceeds from an internal-gear-type Monel pump, and a Monel filter unit accepting fiberglass elements, to the rig. The fiberglass elements have a specific pore size of 20 microns and deliberately have excess flow capacity, by about two and a half times, in order to secure low pressure drops and long life, even with an oil that is undergoing some thermal degradation.

The combined oil tank and oil heater unit is also designed to act as a defoamer. Oil from the rig drain manifold enters the top of the tank, which is below rig level, in a direction tangential to the cylindrical inside surface of the tank. The swirling motion set up in this way allows time for the entrained air to separate from the oil. The oil then collects in the bottom of the tank where it is drawn out by the pump, either through an oil cooler or through a by-pass line, and the air passes out through the oil condenser mentioned previously.

Both the condenser and the oil cooler are cooled with water from a central recirculating water system. The oil-in temperature to the rig is maintained at its specified limit by controlling the water flow to the oil cooler. The oil tank and defoamer unit has been sized to accommodate up to  $0.0227 \text{ m}^3$  (6 gallons) of lubricant which, together with the capacity of the pipes, pump, filter and inlet manifold, gives a maximum capacity of approximately  $0.0246 \text{ m}^3$  (6.5 gallons).

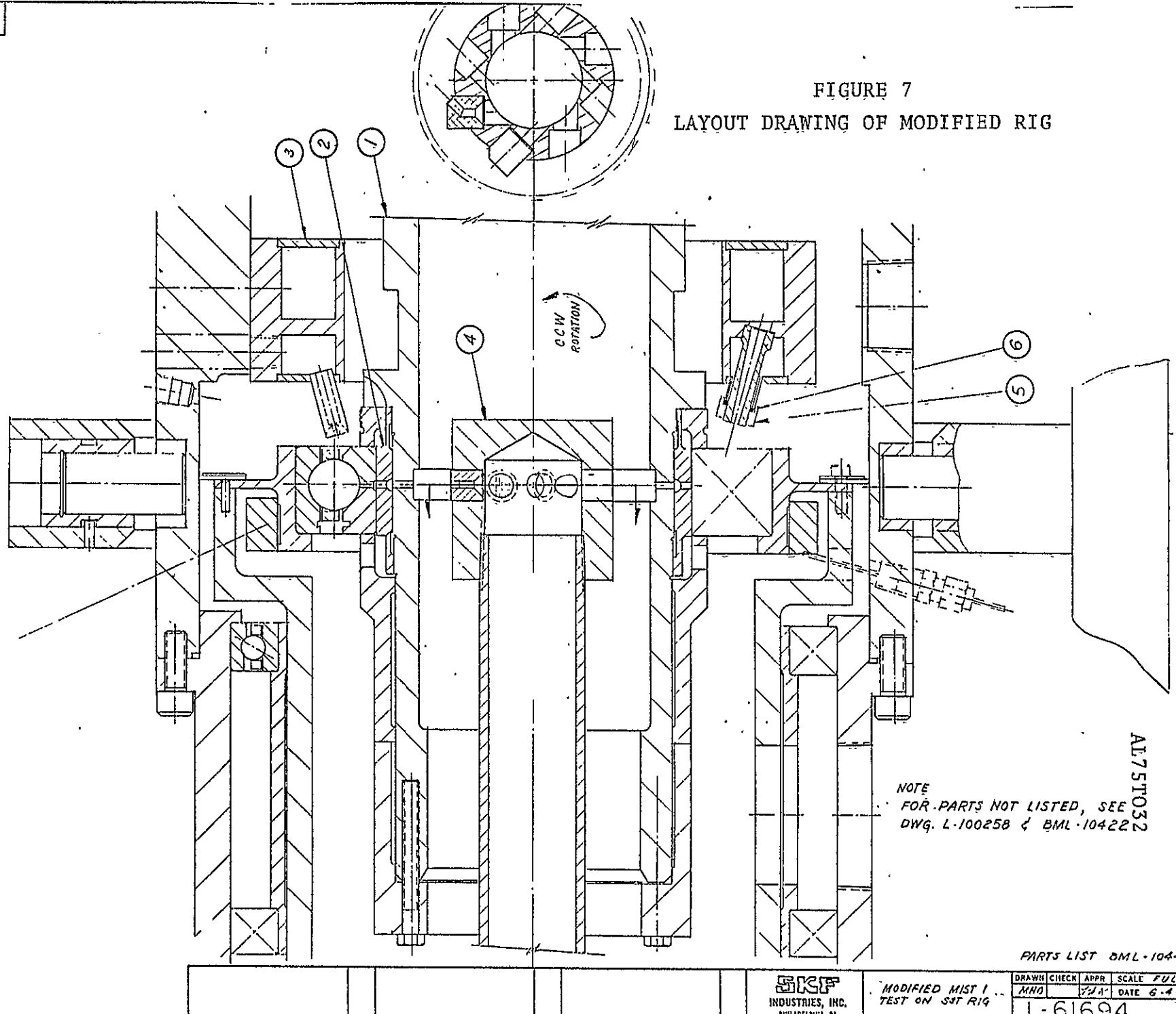
To keep the system oil capacity to a minimum, heat is supplied to the oil through the large cylindrical inside surface of the oil tank by surrounding it with an oil heater. To preclude the possible occurrence of local "hot-spots" in the heater, which could lead to premature coking of the oil on the tank surfaces, liquid metal is used as a heat transfer medium. The metal is a lead-bismuth-tin eutectic which has a melting



L-61694

22

FIGURE 7  
LAYOUT DRAWING OF MODIFIED RIG



NOTE  
FOR PARTS NOT LISTED, SEE  
DWG. L-100258 & BML-10422

AL75T032

PARTS LIST BML-10422

**SKF**  
INDUSTRIES, INC.  
PHILADELPHIA, PA.

MODIFIED MIST 1  
TEST ON SST RIG

DRAWN	CHECK	APPR	SCALE	FUL.
MND			1/4"	DATE 6-4-

1-61694

AL75T032

point of  $343^{\circ}\text{K}$  ( $158^{\circ}\text{F}$ ). This is directly heated by a 230V 12kw electric immersion heater. Corrosion problems with this liquid are minimized by selecting carbon steel for the outer container and heater sheath and by using hard chromium plating on the surfaces of the Monel oil tank which are exposed to the liquid metal.

This system, used to supply oil to jets located on both sides of the rig bearing, was modified to also provide oil to the test bearing during the performance of one test. The modification included a branch line which directs oil through a flowmeter and into two oil manifolds. From the manifolds the oil is inserted into the bearing through jets and returned through the oil drainage system to the oil tank by a scavenge pump. Thermocouples located in the inlet and drain line are used to monitor the oil in and oil out temperatures.

### 3.6 Instrumentation

The desired temperature measurements are detected by shielded iron-constantan thermocouples. The test bearing inner and outer ring temperatures are recorded on a continuous strip chart recorder, Honeywell Electronic 17. All other temperatures are recorded on a Esterline Angus Model E-6704 multipoint recorder. The test bearing drag torque is sensed by a strain gaged beam and recorded on a Hewlett Packard Model 7702B strip chart recorder. The thrust load applied through the load plug to the test bearing is sensed by a Leeds and Northrup Model 8690 millivolt potentiometer. The shaft speed is detected by a magnetic pick-up and presented on a Hewlett Packard Model 531CR electronic counter. All air flow measurements are made by Brooks flowmeters.

The following temperatures are automatically recorded:

- Oil temperature in mist supply tank
- Mist temperature in both lines entering rig
- Mist air temperature entering mist generator
- Mist air temperature at flowmeter
- Through bearing cooling air temperature entering rig
- Shaft cooling air temperature entering rig
- Bearing housing cooling air temperature at flowmeter and entering rig
- Shaft cooling air temperature out
- Bearing housing cooling air temperature out
- Combined mist and through bearing cooling air out
- Rig bearing oil-in temperature
- Rig bearing oil-out temperature
- Test bearing housing
- Rig bearing outer-ring temperature

In addition the following data is recorded manually:

- Shaft speed
- Combined mist and through bearing cooling air flow rate
- Mist air flow rate
- Combined bearing housing and shaft cooling air flow rate
- Bearing housing cooling air flow rate
- Pressure at mist and through bearing cooling air flowmeter
- Pressure at mist air flowmeter
- Pressure at through bearing cooling air flowmeter
- Pressure at bearing housing and shaft cooling air flowmeter
- Pressure at bearing housing flowmeter
- Applied thrust load
- Test bearing drag torque
- Mist generator adjustment screw position
- Recirculating oil pressure
- Recirculating oil flow rate to test bearing

All air flow rate measurements are corrected for the pressure and temperature values at the flow meters.

#### 4.0 ANALYTICAL STUDY

In preparation for designing the mist lubrication and cooling air system for a aircraft gas turbine mainshaft bearing, several different methods of applying the mist oil and cooling air were reviewed. The method considered to provide the best possibility of success was then further evaluated incorporating the theoretically required mist oil and cooling air flow rates. Methods initially considered included:

1. Injection of oil mist and cooling air axially to both sides of the test bearing through oil mist and cooling air nozzles located in a circular pattern similar to that used in many aircraft engine recirculating jet lubrication systems.
2. Injection of mist oil radially through holes in hollow shaft and bearing inner ring with cooling air forced axially through the bearing and through a circumferential path in the outer ring housing.
3. Injection of oil mist and cooling air through nozzles located in a circular pattern on one side of the bearing allowing the momentum and small pressure build up to carry the mist into the bearing and exhaust through a port on the opposite side.
4. Similar to method three plus modification of the bearing inner ring and cage geometry to aid in pumping the lubricant into needed locations within the bearing. In addition cooling air would be forced axially through a hollow shaft to aid in the removal of heat from the inner ring, and circumferentially through the bearing housing to remove heat from the outer ring.

The latter method was selected for more detailed evaluation. Method No. 1 was rejected due to the possibility of the flows from opposite directions bucking each other and thus preventing sufficient penetration into the bearing of adequate cooling air and oil mist. Method No. 2 was considered to have a reasonably good possibility of success and a variation of this method was tested in the latter portion of the test program.

The selected method of application had the advantages of permitting cooling air to be inserted in three different locations which could be independently controlled and the need for each flow path could be established through testing. The housing and shaft cooling air flow paths provided alternatives

to forcing all the cooling air through the bearing where high air velocities could possibly sweep useable oil from the cage, rings and ball surfaces.

#### 4.1 Evaluation of Cooling Air Flow Rate Requirements

One of the major questions with respect to mist lubrication and air cooling of high speed aircraft engine bearings was the feasibility of removing the bearing generated heat by the use of mist and cooling air. To establish the expected quantity of air required, the heat generated by the bearing or the amount of heat which must be transferred from the bearing to obtain a steady-state thermal condition at various shaft speeds and specified loads was first determined. From the established bearing heat generation rate, the quantity of air required was calculated.

The expected heat generation rate of a 125 mm bore angular contact ball bearing with a thrust load of 14,590 Newtons (3280 lbs.) applied and lubricated by mist oil was initially calculated using S K F Computer Program AE69Y004. Additional values were also established from data recorded during tests performed in prior programs since the calculated values were judged to be low because the program considered cage-land viscous shear only and did not consider cage to land contact and ball to cage contacts. The prior tests were conducted with the same test bearing design and applied load as specified for this program. The results of the computer calculations are presented in Table II and shown in graph form in Figure 8.

The curves formed by extrapolating values from the experimental data obtained during prior tests, recorded in References 1 and 5, are also presented in Figure 8. Curve numbered 1 represents the total heat loss as established by the power input to a test rig which incorporated a test bearing, rig bearing, and two seals, when both bearings were lubricated with XRM177F oil mist. Testing was performed by S K F Industries on NASA Contract NAS3-6267. The curve was generated by using a test point at 14,000 rpm, the maximum operating speed, and completing the curve by making it parallel to the computed values.

A comparison of the input power requirement for the mist lubricated bearings was made with that required when the bearings were lubricated with recirculating XRM177F oil. The comparison showed that approximately three times more power was required when recirculating oil was used. Using this information, combined with test bearing heat generation rate

TABLE II - CALCULATED BEARING HEAT GENERATION RATE

Shaft Speed (RPM)	I & O Ring (Btu/hr)	Heat Generated		Cage (Btu/Hr)	Oil Churning (Btu/Hr)
		Inner Ring (Btu/Hr)	Outer Ring (Btu/Hr)		
14,000	3,554	2,472	1,082	39	10,923
16,000	4,413	3,448	965	45	14,709
18,000	6,732	5,390	1,342	53	19,351
20,000	10,649	9,128	1,520	61	24,473
22,000	16,650	14,863	1,787	71	29,264
24,000	24,976	22,869	2,110	82	33,460

data obtained on NASA Contract NAS3-14320 (5) in which recirculating oil was used at higher shaft speeds. Curve numbered 2 was obtained. This curve was generated by taking one third of the measured test bearing heat generation rate as that which would be representative of a mist lubricated bearing. This curve is essentially parallel to the curve formed from the computed values and thus justified the extrapolated used in Curve 1.

The average of Curves 1 and 2 was selected as a logical level of values to the use for design purposes and is presented as a dashed line in Figure 8.

This projected curve of the heat which would be generated in the mist lubricated bearing was utilized to determine the quantity of cooling air required to maintain a steady state thermal condition in the bearing at an operating temperature of 533°K (500°F) at the maximum anticipated speed, i.e., 24,000 rpm ( $3 \times 10^6$  DN). The calculations are presented in Appendix I which indicate that a total air flow of approximately 5.66 scmm (200 scfm) would be required when the air inlet temperature was 366°K (200°). Based on the conceived method of supplying the mist and cooling air as presented earlier, it was considered logical that 50 percent of the air should be passed through the bearing to contact the inner surfaces. The remaining air would be applied on external surfaces by forcing it through the housing and the hollow shaft. On this basis, it was established that the maximum flow rate through and external to the bearing should be between 2.55 and 2.83 scmm (90 and 100 scfm) each.

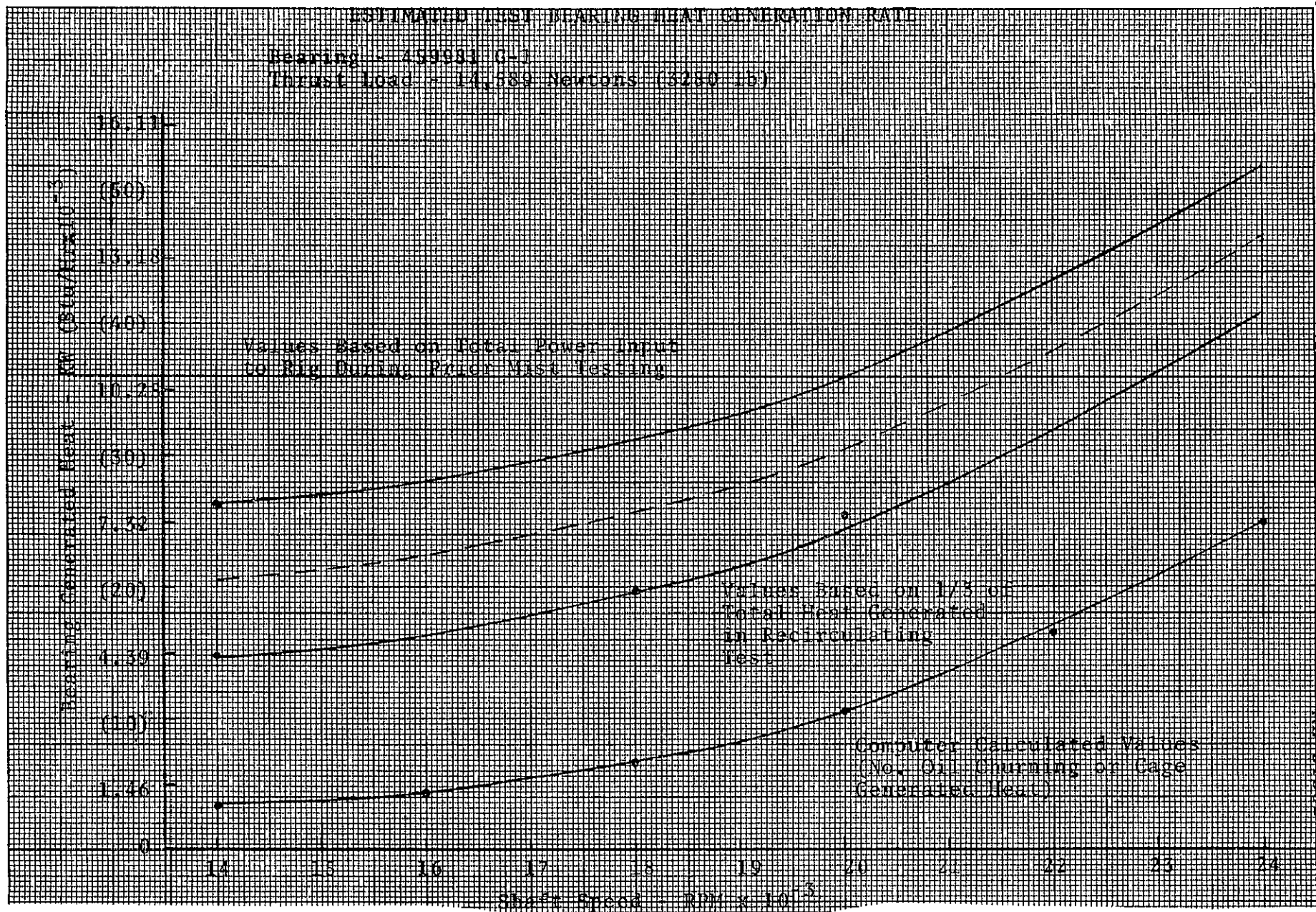
#### 4.2 Evaluation of Mist Oil Supply Rate Requirements

Elastohydrodynamic lubrication theory was applied to establish the quantity of oil necessary to lubricate the bearing inner-ring contacts. These contacts are considered to be the most critical with respect to oil replenishment as the oil displaced from the inner ring will have a tendency to flow to the cage pockets and outer ring due to centrifugal forces. The maintenance of an elastohydrodynamic oil film relies on a sufficient supply of lubricant in the inlet of the contact between the contacting surfaces. Insufficient lubricant supply in the inlet results in a phenomenon called "EHD film starvation" characterized by the reduction in EHD film thickness and in the distance from the front edge of the contact to the miniscus line at which the fluid pressure begins to rise.

The calculations of required oil replenishment rate are based on the assumption that all of the oil displaced out of the inner-ring track as a ball passes must be replaced by the

FIGURE 8

REPRODUCIBILITY OF THE  
ORIGINAL PAGE IS POOR



41751032



mist supply, a very conservative assumption. It is known that some of the oil displaced from the track does flow directly back into the depleted track by the action of surface tension forces after the rolling element has passed. Some of the oil which is lost is also recirculated in the bearing by centrifugal, gyroscopic, and windage forces and finds its way back to the contact area thus decreasing the amount of replenishment oil required. It has been shown that, at high speeds, values of starvation can be relatively high and still provide sufficient lubrication.

In performing the oil flow rate calculations the following assumptions were made:

(1) The contact is only slightly starved, i.e. the film thickness ( $h_o$ ) is 90% of the unstarved film thickness ( $h_f$ ) calculated from classical theory.

(2) The half-films clinging to the ball and race ahead of the contact, see Figure 9, are to be increased in thickness by oil mist directed onto the track or ball. (This is based on the assumption that at high speed, the contact will be severely starved without a mist spray or other supply onto the rolling track, as is indicated under certain operating conditions by recent developments in EHD starvation theory.)

(3) At each ball passage, the oil on the track is displaced out of the track except for a thin layer of film thickness  $h_o/2$ .

Starvation theory developed in Reference 6 shows that in order to maintain a ratio  $h_o/h_f = 0.90$ , the half film height ( $h_1$ )/2 at the contact inlet must satisfy the following conditions:

$$h_o/h_1 = 0.70 \quad (1)$$

$$\frac{u\alpha\eta R_x^{1/2}}{h_1^{3/2}(3+2K)} = 0.10 \quad (2)$$

where  $u$  = rolling velocity at the contact (in/sec)

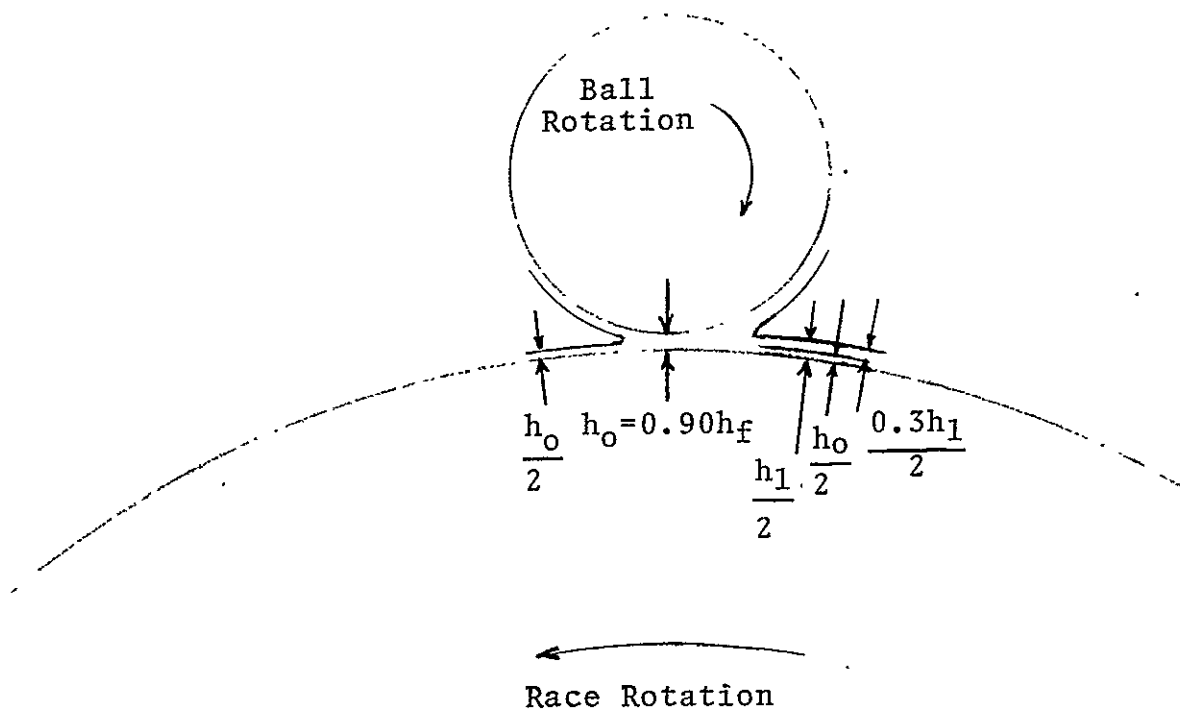
$\eta$  = viscosity of oil at the inlet of contact (lb-sec/in<sup>2</sup>)

$\alpha$  = pressure-viscosity coefficient (in<sup>2</sup>/lb)

$R_x$  = equivalent radius of curvature in the rolling direction (in)

FIGURE 9

INNER RACE BALL CONTACT SHOWING  
OIL FILM THICKNESS AT VARIOUS LOCATIONS.



$R_y$  = equivalent radius of curvature transverse to rolling direction

$k = R_x/R_y = 0.027$  for a typical ball-raceway contact with contact ellipse axis ratio equal to 10.

$h_o$  = plateau film thickness in the contact (in).

The amount of increase of inlet film thickness between two successive contacts due to spray is

$$h = h_1 - h_o = 0.3h_1 \quad (3)$$

The time interval between two contacts is  $t = s/u$  where  $s$  is the rolling element spacing. The contact frequency is

$$f = \frac{1}{t} = \frac{u}{s} \quad (4)$$

The rate of oil supply to the rolling track is given by

$$q = \ell \Delta h w \frac{f}{2} \quad (5)$$

where  $w$  is the effective width of the rolling track and  $\ell$  is the length of rolling track.

For  $z$  rolling elements,

$$\ell = sZ$$

From the S K F Computer Program AE69Y004 the inner race major axis contact is approximately 0.16 inch for all speeds from 14,000 to 24,000 rpm with a thrust load of 14,589 Newtons (3280 lbs.).

The factor  $1/2$  in the above equation for  $q$  denotes that the layer thickness varies linearly with distance from  $h_o/2$  to  $h_1/2$  at the inlet. Thus, after substituting for  $\Delta h$  from (3), one has

$$q = 0.15 h_1 w u z \quad (6)$$

Substituting for  $h_1$  from (2) into (6) and using  $k = 0.027$  gives,

$$q = 0.15 w u z \{3.28 u \alpha R_x^{1/2}\}^{2/3} \quad (7)$$

For the test bearing, S K F No. 459981-G1, one has

$$\begin{aligned} Z &= 21 \\ u &= 0.156 \text{ N (ips)} \\ N &= \text{shaft speed (rpm)} \\ R_x &= 0.356 \text{ in.} \end{aligned}$$

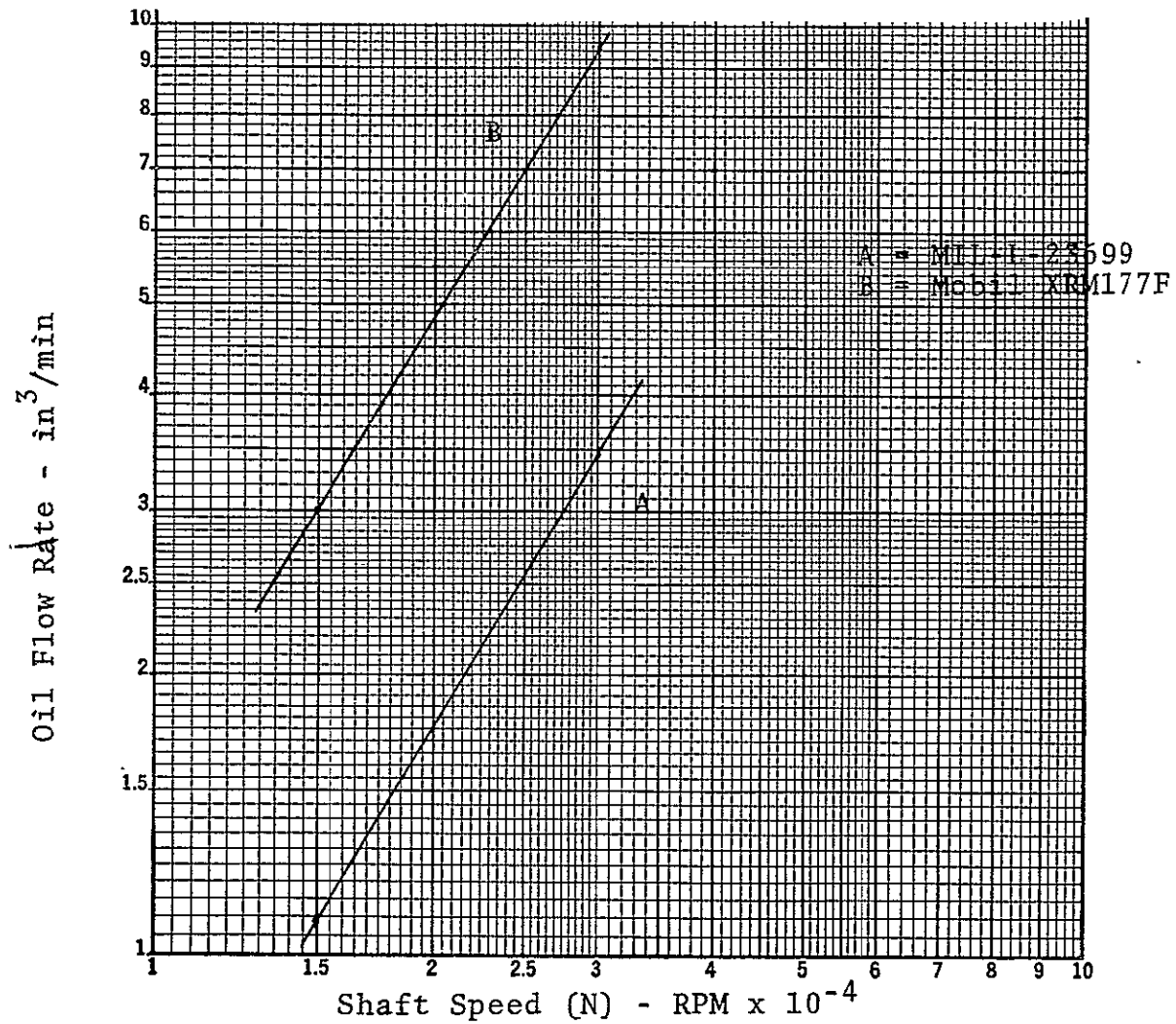
Two test lubricants whose properties are representative of the candidate lubricants were considered. Their properties and the calculated  $q$  values at  $N = 14,000$  rpm are tabulated as follows:

	Type II Ester MIL-L-23699 (Jet No. II)	Synthetic Paraffinic Hydrocarbon (XRM-177)
Density @ 20°C	0.99 gm/cm <sup>3</sup>	0.84 gm/cm <sup>3</sup>
$\alpha$	$1.1 \times 10^{-4} \text{ in}^2/\text{lb}$	$1.5 \times 10^{-4} \text{ in}^2/\text{lb}$
Kinematic Vis. @ 500°F	0.88 c.s.	3.3 c.s.
Absolute Vis. @ 500°F	0.87 c.p.	2.77 c.p.
" " " "	$1.26 \times 10^{-7} \text{ lb-sec/in}^2$	$4 \times 10^{-7} \text{ lb-sec/in}^2$
Kinematic Vis. x $\alpha$	$1.39 \times 10^{-11} \text{ sec}$	$6 \times 10^{-11} \text{ sec}$
$q$	$0.97 \text{ in}^3/\text{min}$	$2.84 \text{ in}^3/\text{min}$

Figure 10 is a plot of the variation of the calculated required oil supply rate for  $h_o/f_f = 0.90$  with the shaft speed for the two oils.

The calculations show that oil replacement rates of 0.034 lb/min for Mobil Jet II and 0.086 lb/min for Mobil XRM-177F are required when operating at 14,000 rpm. These values appear quite large in comparison to experimental data. In a previous mist lubrication test performed on NASA Contract NAS3-6267 a test bearing was run successfully for approximately 4 hours with Mobil XRM-177F lubricant at 14,000 rpm at a mist flow rate of something less than 0.015 lb/min. In this instance the eventual bearing failure appeared to be the result of thermal imbalance rather than being precipitated by a lack of lubricant. This however is difficult to ascertain since in some circumstances the breakdown of surface lubricating films could precipitate a thermal imbalance failure. However, on the basis of the successful operation achieved in that test, the assumption that the oil forced from the track is completely

FIGURE 10  
CALCULATED OIL REPLENISHMENT RATE



lost seemed indeed excessively conservative and that a value of approximately 20 percent of the calculated values was reasonable.

Therefore, in selecting the mist generator and the mist oil flow rate for testing, values equal to 20 percent of the calculated values were used.

#### 4.3 Mist and Cooling Air Delivery System

In establishing the oil mist and cooling air delivery system several design parameters were considered. These included the selection of the ratio of air passed through the bearing to the externally applied air; quantity of mist air, mist generator size selection; sizing of mist transfer piping and manifold; number, design and location of mist nozzles; point of application of the mist, and modifications to the bearing to assist in distributing the oil to the desired locations within the bearing.

Due to the apparently large quantity of mist and cooling air flow required to cool the test bearing, as established in Section 4.1, the selection of a system to supply mist and cooling air through the bearing and cooling air around the bearing was considered essential even though the complexity may be difficult to apply in all gas turbine mainshaft bearing mounting configurations. To take full advantage of the heat transfer surfaces, both internal and external of the bearing it was concluded that an equal split between the total required flow would be reasonable. Thus, considering the maximum desired operating speed of 24,000 rpm, as the design speed, an air flow rate of 2.55 to 2.83 scmm (90 to 100 scfm) would need to be passed through the bearing and the same amount external to the bearing. It also is considered reasonable to divide the external cooling air proportionally, based on the ratio of the calculated heat generated at the inner ring and outer ring, and direct the flows along the surfaces of a hollow shaft and through a circumferential groove machined in the bearing housing.

The air passing through the bearing would consist of a combination of mist air and auxiliary cooling air with the additional cooling air applied externally.

Based on the estimated mist oil flow requirement determined in Section 4.2 an Alemite high volume oil-mist generator was selected. The mist generator rated as a 41 cfm unit had been used in prior mist lubrication tests at S K F and a calibration of the unit using Esso Turbo Oil 4040 at 294°K (70°F) and room temperature air resulted in an oil flow rate of

574 cm<sup>3</sup>/hr (35 in<sup>3</sup>/hr) when 1.275 scmm (45 scfm) of air was passed through the mist generating nozzle. Thus the maximum estimated oil flow rate requirement, assuming the use of XRM-177F oil, of 357 cm<sup>3</sup>/hr (34 in<sup>3</sup>/hr) could be obtained with a mist air flow rate of 1.27 scmm. The remaining through bearing air would be supplied as auxiliary cooling air which would contain no oil.

The oil-mist research, conducted by the Mobil Oil Company, reported in References 2 and 3, established that the best oil wetting occurred on a rotating disk when the application nozzle was of a reclassifying design. The reclassifying nozzle increases the mist oil partial size thus increasing the momentum of the oil particles which decrease the effect of air currents from dispersing the particles away from the desired surfaces. Commercial mist generators produce oil particles in the 4 micron range which minimize the premature plating out of the oil in the transfer lines. The reclassifying nozzle design found most effective by Mobil consisted of a screen located in the entrance of the application nozzle on which oil is collected and larger particles emitted.

Mobil also established that maximum wetting of the desired surface occurred when the nozzle was located 4 to 8 nozzle diameters from the surface and optimum efficiency of the oil supplied is obtained when a secondary air nozzle, concentric and outside the mist nozzle, is provided to blow any oil dripping from the primary nozzle into the bearing.

Based on this information the basic nozzle configuration was established as a dual mist and air nozzle. The mist nozzle being a converging configuration with a screen at the entrance to increase the mist particle size. The air nozzle would be a straight nozzle concentric and external to the mist nozzle. A total of ten dual nozzles was selected to be positioned in a circular pattern to provide a well distributed flow pattern to the bearing; thus, attempting to eliminate hot spots. The design of the dual nozzles is presented in Appendix II. A 150 mesh screen using 0.066 mm (0.0026 in.) diameter stainless steel were selected for the nozzle inlet which provides a 37 percent open area.

To accommodate the mist and cooling air nozzles, a manifold was designed which consisted of two circumferential open sections. The larger mist manifold section was located behind the cooling air manifold section to accommodate the longer mist nozzles and to simplify the assembly. The cross section opening the mist manifold was intentionally made large 30 x 20.3 mm (1.185 x

0.80 in.) to accommodate the inlet pipes and keep the mist flow velocity low. It is recommended by the Alemite Company that the mist flow velocity should be below 7.62 meters/sec (25 ft/sec) to minimize the plating out of the oil in transfer. A drawing of the manifold and the dual nozzle arrangement is presented in Figure 11. Two 20.9 mm (0.824 in.) I.D. tubes were selected to carry the mist to the manifold. The tubes enter the manifold diametrically opposite to each other.

In the lubrication of a ball bearing, there are four major types of contact areas which must be plated with oil: 1) the contact area between the ball and inner ring (inner ring ball track), 2) the contact between the ball and the outer ring (outer ring ball track), 3) area between the cage and the land on which it rides and 4) the contact area between the ball and cage pocket. The ball tracks can be lubricated by applying oil to either the ball or the races.

Since the oil entering a bearing migrates toward the outer ring, the most difficult area to lubricate is the inner ring ball track. It is also noted from the calculated bearing heat generation rate values presented in Table II that proportionally more heat is generated at the ball inner-ring contacts than at the ball outer-ring contacts as speed increases. This condition results from differences in the contact angle at the inner and outer rings. At high speeds the outer-race contact angle decreases and the inner-ring contact angle increases thus producing less sliding at the outer ring. In addition to being more difficult to lubricate more heat must be conducted from the inner ring to obtain a thermally stable operating bearing.

Thus it was decided that the dual mist and cooling air nozzles should be directed from the inboard side of the bearing toward the space between the inner ring and cage and against a chamfer machined on the ring side face. In this manner the air, at its lowest temperature, impinges on the inner ring on the loaded half to obtain maximum cooling of this area. A portion of the oil or mist enters the bearing inner cavity where it is available to be picked up by the ball (collision between the mist particles and ball) as it traverses around the shaft. An additional portion of the oil is plated out on a chamfered surface, see Figure 12, provided for this purpose. The chamfer is configured to insure that the inner corner (that corner closest to the ball) is well within the outer edge of the cage. The oil on the chamfer migrates along the surface to the inner corner due to centrifugal force where it is thrown off and impinges on the cage bore or carried further

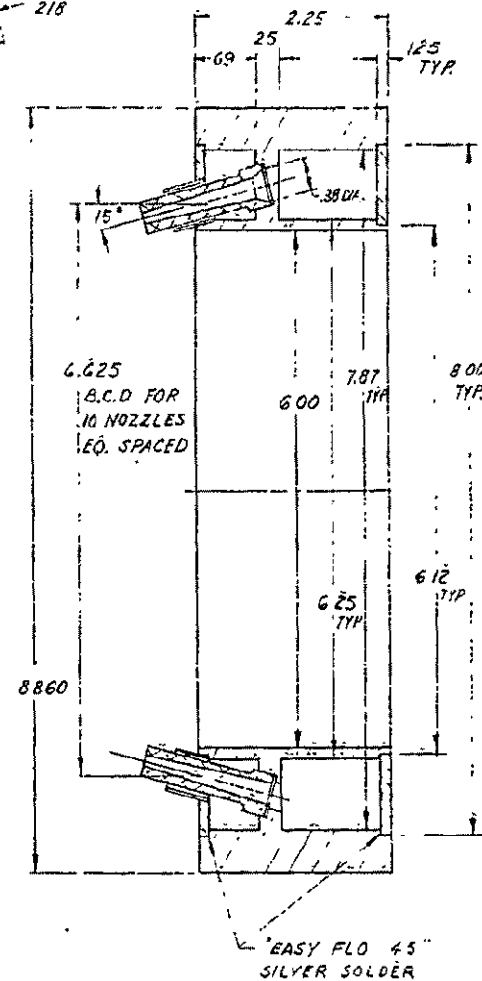
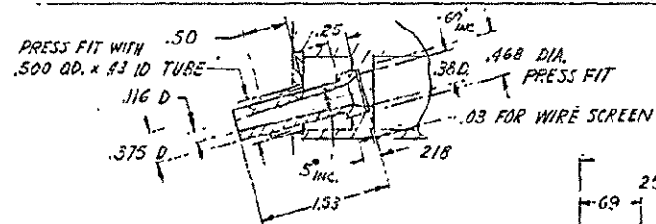
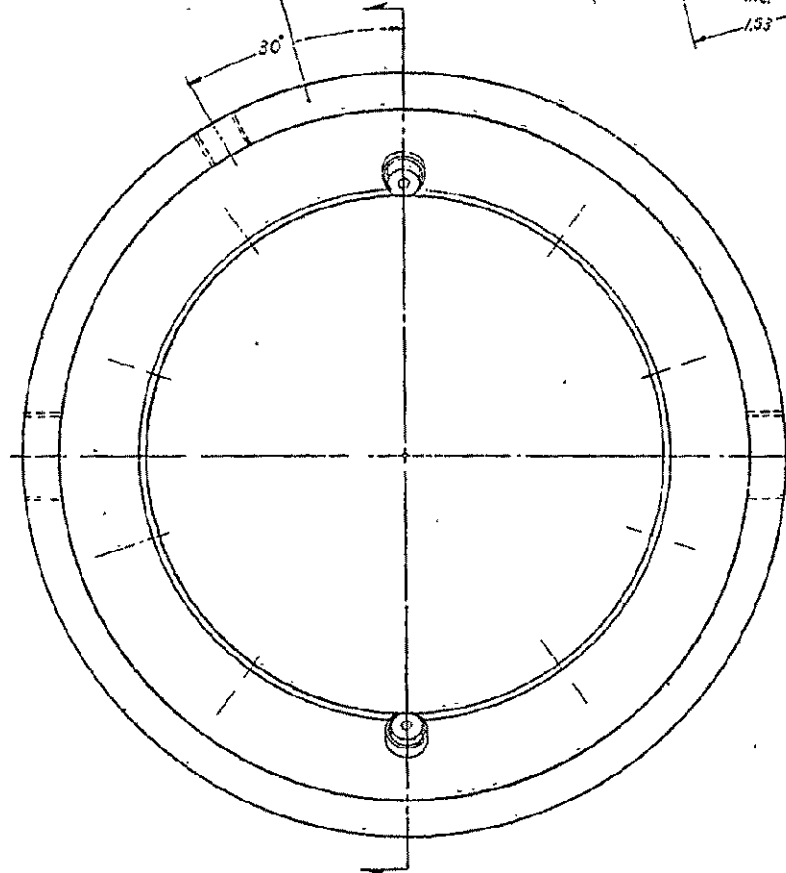
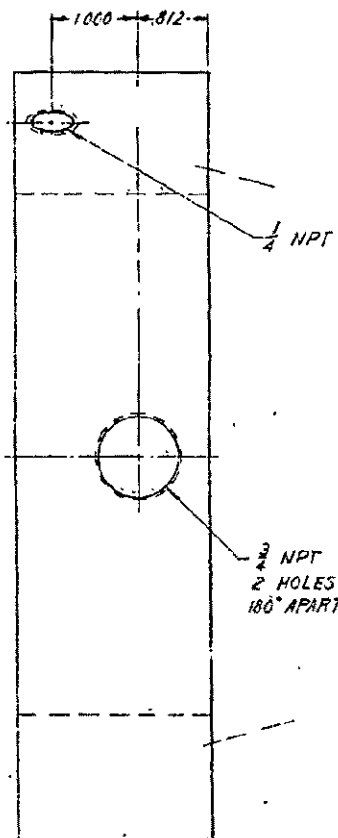


999197

DIMENSIONAL LIMITS

FIGURE 11

## MANIFOLD AND DUAL NOZZLE ARRANGEMENT



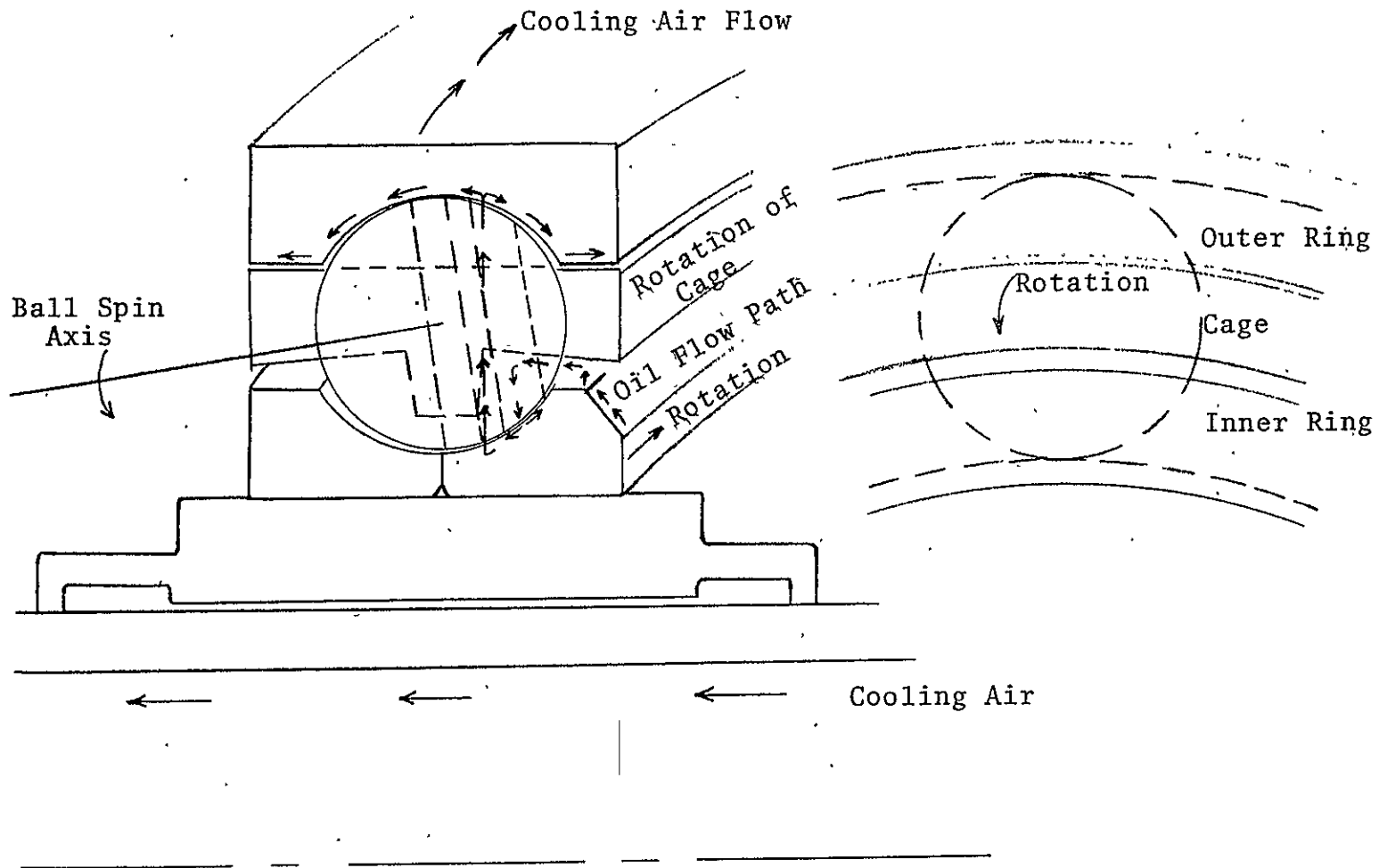
MAT'L  
304 ST ST'L & COVER PLUG,  
ALUMINUM FOR NOZZLES  
AND TUBING

SKF  
INDUSTRIES, INC.  
PHILADELPHIA, PA.

MIST HOUSING  
SST LOAD PLUG  
WITH MIST LUBR.

DRAWN	CHECK	APPR	SCALE	FULL
JAN				
DATE			3-23-73	
L-61655				

FIGURE 12  
LUBRICANT FLOW PATH



AL75T032

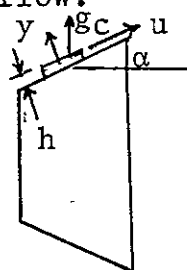
into the bearing by the air. The cage is modified to form a radially inward slope on its inner diameter surface along which the oil flows, again due to centrifugal forces, to the ball pocket where it lubricates the contact area between the ball and cage and wet the inner ring contact path on the ball. Mist oil particles are also plated out on the inner race due to direct contact and windage forces generated by the rotating bearing.

The lubricant on the ball provides lubrication to the inner ring and ball contact area. As the ball rotates into the inner race that portion of the oil which does not form the EHD film is forced to both sides of the major ellipse. Some of the extruded oil remains on the ball and some on the race where it has a tendency to migrate toward the outer race due to the centrifugal force generated by the rotation of the ball and inner ring. In so doing, part of the oil flows back into the inner ring ball track where it is again available to form the EHD film. Surface tension and cohesion forces also tend to draw the extruded oil back into the ball track area. In addition, according to EHD lubrication theory, that oil which forms the EHD film is equally divided on the ball and race and aids in forming the next contact EHD film. That oil which migrates to the outer stationary ring is available to lubricate the outer ring contact area and the outer ring land and cage contacts.

The following calculations were performed to determine if the centrifugal pumping along the surface of the chamfer on the inner ring and the taper on the cage bore is adequate to transmit the required oil into the bearing.

The formula given below describes the relation between the oil flow along a conical surface and the parameters, speed (N) film thickness (h), viscosity ( $\mu$ ), and half cone angle ( $\alpha$ ).

Letting  $u$  denote the fluid velocity parallel to the conical surface, and  $y$  a coordinate perpendicular to the direction of flow.



$$\mu \frac{\partial^2 u}{\partial y^2} + \frac{\rho g c}{g} \sin \alpha = 0 \quad (8)$$

AL75T032

where  $\rho$  = density of oil  
       $g_c$  = angular acceleration  
       $g$  = acceleration constant

The boundary condition is

AL75T032

Assuming oil layer thicknesses  $h = 0.001$  in. and  $0.005$  in. the oil flow rates are  $37.8 \text{ in}^3/\text{min}$  and  $4728 \text{ in}^3/\text{min}$  respectively.

The parametric values for the flow along the cage bore taper are the same as above except for  $\alpha$  which equals  $5^\circ$  and  $g_c$  which equals  $2.58 \times 10^6 \text{ in}/\text{sec}^2$ . Then assuming oil layer thicknesses  $h = 0.001$  in. and  $0.005$  in. the oil flow rates are  $1.8 \text{ in}^3/\text{min}$  and  $225 \text{ in}^3/\text{sec}$ .

A comparison of these values with the mist flow rate requirements established in Section 2.2 of  $0.54 \text{ in}^3/\text{min}$  for Mobil XRM-177F oil shows that adequate centrifugal pumping exists to transmit the oil into the bearing.

### 5.0 TEST PROCEDURE

Three basic types of tests were performed using the test rig during the program. The basic test types were:

1. Mist system evaluation tests
2. Step-speed tests
3. Extended-period tests

The mist system evaluation tests were performed to provide an initial operational and performance check of the mist system. Items evaluated include mist flow rate with each of the lubricant test fluids, oil wetting pattern on a stationary bearing, uniformity of mist flow from each nozzle, and wetting pattern on the test bearing operating at a relatively low speed. The procedure used in these tests are described in Section 6.1.

The step speed tests were performed to provide relative information between the effectiveness of the various lubricants and variations in the mist and cooling air system. Essentially the same test procedure was followed in all step-speed tests.

Prior to each test a thrust load of 14,589 newtons (3280 lbs.) was applied to the test bearing. The load was applied through the load plug to the outer ring of the test bearing where it was transmitted through the balls to the inner ring and into the shaft. The load was reacted through the rig bearing to the rig housing. The load was selected to provide a minimum contact stress of approximately  $1.28 \times 10^9$  newtons per square meter (200,000 psi) at a speed between 14,000 rpm and 24,000 rpm. The theoretical contact stress and contact angle, calculated using S K F Computer Program AE69Y004, at the inner and outer ring at various test speeds are presented below:

<u>Shaft Speed</u> <u>(rpm)</u>	<u>Contact Stress/Contact Angle</u> <u>(ksi)/(degrees)</u>	
	Inner Ring	Outer Ring
14,000	182/35.5	219/15.5
16,000	179/37.6	229/11.7
18,000	179/37.9	240/12.5
20,000	177/38.8	249/10.7
22,000	177/39.4	256/9.9
24,000	176/39.8	263/9.2

With the thrust load applied, the cooling air and mist air were turned on and allowed to pass through the rig while the oil in the mist supply tank was heated to the desired 266°K (200°F).

The rig housing recirculating system was also activated and the recirculating oil heated to approximately 353°K (175°F). The same test oil was used in both the mist and recirculating systems. During this period adjustments were made in the various air heaters and pressure valves to obtain the operating temperature and the desired flow rates.

Having reached the operating conditions in the lubrication systems and cooling air systems, the shaft was accelerated to 10,000 rpm at a fairly uniform rate in approximately one half hour. The test bearing temperature was allowed to stabilize and test data recorded. The shaft speed was then accelerated in incremental steps allowing the bearing temperature to stabilize after each increase and data recorded. This procedure was continued until the maximum desired speed was obtained or a bearing failed. Following the testing, the rig was disassembled and the bearing visually inspected using a light microscope with magnification up to 30X. The rig housing was also inspected for oil decomposition products. The heat transferred to the mist and cooling air was calculated by using the equation  $q = \Delta t c_p \dot{w}$  where:

$q$  = heat transfer rate  
 $\Delta t$  = inlet and outlet temperature difference  
 $c_p$  = specific heat of air at constant pressure  
 $\dot{w}$  = air flow rate

The extended period tests were performed to evaluate long period operation. The test procedure used was similar to that used in the step speed tests with the exception that the shaft was accelerated directly to 20,000 rpm at a fairly uniform rate in approximately one half hour. The rig was then run for a period up to 10 hours, shut off and allowed to cool to room temperature and the cycle repeated until 50 hours of operation at 20,000 rpm was obtained or the test bearing failed.

## 6.0 TEST RESULTS AND DISCUSSION

### 6.1 Mist System Evaluation Tests

Prior to initiating the bearing mist lubrication tests, several evaluation tests were performed on the mist system. The system consisted of the air compressor, air heaters, mist generators, mist supply lines, mist manifold and application nozzles and associated instrumentation.

The initial tests were calibration runs to determine the mist oil flow rate versus mist air flow rate with each of the four test fluids. The calibration runs were performed by heating the mist oil supply located in the mist generator to 366°K (200°F). The air at a temperature, approximately 477°K (400°F), sufficient to provide a mist temperature between 355 and 366°K (180 and 200°F) was supplied to the generator at three different flow rates: 0.28, 0.42 and 0.84 scmm (10, 15 and 20 scfm). After an operating period of two hours at a specific air flow rate the run was terminated. The quantity of oil used was measured by refilling the supply tank to its original level following cool down to room temperature. A calibration curve for each test fluid is presented in Figure 13.

At the lower air flow rates, the oil flow rates of the test fluids were approximately the same; however, at the highest flow rate appreciable differences in the oil flow rate resulted, especially with the more viscous XRM205F fluid which was considerably less than the other three fluids. The measured oil flow rates were approximately three times the values received from the generator vendor for 366°K (200°F) oil and 295°K (72°F) air. This difference is attributed to the increased air velocities through the mist generator nozzles due to the high air inlet temperature. Based on these results, it was concluded that a lower mist air flow rate would be required to supply the desired oil replenishment rate previously calculated.

To evaluate the uniformity of the mist flow rate through each nozzle, visual observations were performed by directing a high intensity light on each stream. This test showed that all nozzles were operating and the flow was essentially the same. To provide a more accurate test, a mist receptacle packed with cotton was devised which would filter the oil from the mist air as it was passed through. The mist air entered the filter through a plastic hose which was placed over an individual nozzle. By weighing the receptacle and transfer hose before and after a test, the quantity of oil emitted from a particular



FIGURE 13  
MIST GENERATOR CALIBRATION

MIST OIL FLOW RATE -  $\text{IN}^3/\text{MIN}$

150

125

100

75

50

25

5

10

15

20

25

30

35

40

MIST AIR FLOW RATE - SCFM

Mist Oil Supply Temperature -  $200^{\circ}\text{F}$   
Mist Temperature -  $180-200^{\circ}\text{F}$

YRM252A

XRI850A  
and  
XRI850A  
Plus 5% Xoncel 0859  
Resin

XRM2053

nozzle was established.

Two nozzles were selected for the evaluation testing, one nearest to a manifold entrance tube and one furthest from an entrance tube. The oil flow from each nozzle was captured for a period of two hours with a mist inlet temperature of approximately 180°F. The captured oil from the nearest and furthest nozzles weighed 67 and 70 grams respectively, thus indicating that the flow from each nozzle was essentially the same. It was noted in these checks that an appreciable quantity of the mist oil plated out in the transfer line at the nozzle exit where a sharp bend was located.

The first mist evaluation test using a test bearing was performed on a static bearing to determine the points of mist impingement and the surface areas wetted. The test bearing was mounted in a dummy housing with a double plate sealing the bore and placed into the rig in its standard location. All oil was removed from the bearing prior to its assembly into the rig.

The test oil (Mobil XRL850A) was heated in the mist generator reservoir to 366°K (200°F). The mist air was heated to obtain a mist temperature of 355°K (180°F) at the exit of the mist generator. With a mist air flow rate of 10 scfm, the mist was passed through the ten nozzles of the mist manifold and impinged on the bearing for one minute.

Immediately after shutoff, the bearing was removed and the oil deposited on the bearing observed in a dark room using an ultra violet lamp. Due to the florescent property of the oil, those surfaces of the bearing covered with oil appeared white. The heavier the oil coat the brighter the appearance. The whitest surfaces, those with the thickest oil layer, were the modified chamfer on the inner ring and the ball surfaces adjacent to the nozzles but not shielded by the cage. A lighter layer of oil was also present on the cage and races. Very little oil was plated on the exposed side surface of the outer ring. An inspection of the bearing side opposite the mist nozzles showed that the balls were well coated but little oil was present on the side of the rings and cage. The results of the test thus indicates that the mist was impinging on the bearing in the desired location and wetting the desired surfaces. By weighing the bearing and housing before and after testing it was shown that approximately 40% of the oil leaving the mist generator was plated on the test bearing. The remaining oil was assumed to have plated out in the supply lines, the bearing compartment or passed through the bearing. Considerable mist was observed passing through the bearing.

Photographs taken of the bearing housing assembly following the test are presented in Figure 14. These photographs were taken using minimal room lighting and the ultra violet light for illumination. However, in taking the photographs two problems were encountered: 1) Ultra violet reflections not observed by the eye over exposed certain sections of the film and required repositioning the light in a less favorable location thus producing distortions with respect to intensity of florescence. 2) Oil migration during the period required to take the photographs. The pictures, therefore, do not accurately represent the true wetted pattern. However, they show the contrast between some of the lubricated and unlubricated areas thus depicting the effectiveness of the investigative approach.

The final mist system evaluation test was a dynamic test with the shaft operating at a maximum speed of 10,000 rpm ( $1.25 \times 10^6$  DN). In addition to determining the oil wetting pattern on a dynamic bearing, the test was performed to check out the operation of the rig and evaluate the effectiveness of each of the cooling air flow paths. Test fluid XRL850A was used in conjunction with test bearing S/N 13.

Mist and cooling air were passed through the rig for approximately one hour before starting the shaft. Since the test speed was to be limited to 10,000 rpm, considerably below the speed for which the design flow speeds were calculated, the initial flow rates were set at the following values.

	Flow Rate (scmm-scfm)	Temperature (°K-°F)
Mist	0.28-10	353-175
Through bearing cooling air	1.13-40	366-200
Shaft cooling air	0.99-35	366-200
Bearing housing cooling air	0.42-15	344-160
Mist oil flow rate	490/cm <sup>3</sup> /hr (30 in <sup>3</sup> /hr)	

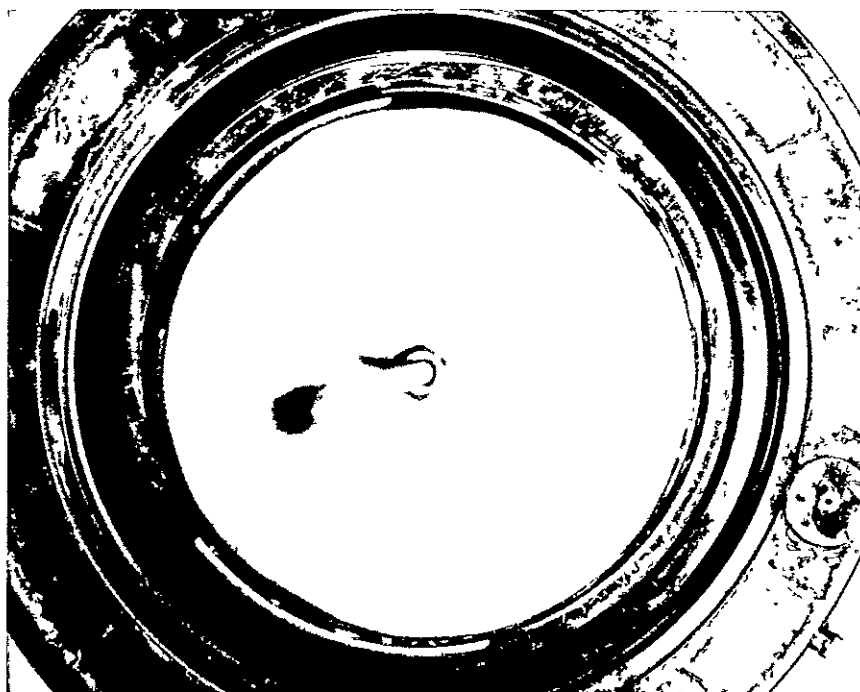
The shaft was accelerated in 2500 rpm increments to the maximum velocity of 10,000 rpm in approximately 30 minutes. At 10,000 rpm the inner and outer races stabilized at 394°K (250°F) and 411°K (280°F) respectively. The shaft cooling air was turned off and the outer ring cooling air increased to 0.56 scmm (20 scfm). In approximately 6 minutes the inner ring temperature increased to 400°K (260°F) and the outer ring decreased to 405°K (270°F). The through bearing cooling air was then decreased to 0.65 scmm (23 scfm). After a period of 4 minutes the inner and outer ring temperatures stabilize after increasing to 405°K and 412°K (270 and 280°F) respectively.

FIGURE 14-PHOTOGRAPHS OF MIST OIL PLATED OUT  
ON STATIONARY TEST BEARING

REPRODUCIBILITY OF THE  
ORIGINAL PAGE IS POOR



Side adjacent to mist nozzles



Side Opposite to Mist Nozzles

The bearing cooling air was then turned off and the bearing temperature started increasing immediately and within 0.5 minutes both ring temperatures had increased  $5.5^{\circ}\text{K}$  ( $10^{\circ}\text{F}$ ). With 0.65 scmm (23 scfm) of through bearing cooling air reinstated the ring temperatures returned to  $405^{\circ}$  and  $412^{\circ}\text{K}$  ( $270^{\circ}$  and  $280^{\circ}\text{F}$ ). The test was then terminated to permit disassembly and inspection of the bearing.

The results of the test indicated that the shaft cooling air may not be necessary, especially at the relatively low speeds. The through bearing cooling air appeared to be the most effective. Observation of the bearing, using an ultra violet light showed that all surfaces of the bearing (ball, cages and races) were evenly coated with a heavy coat of oil. The period of time required for the disassembly did allow time for the oil to migrate toward the bottom of the housing but the quantity of the oil still on the parts indicated that the bearing was being well lubricated during operation.

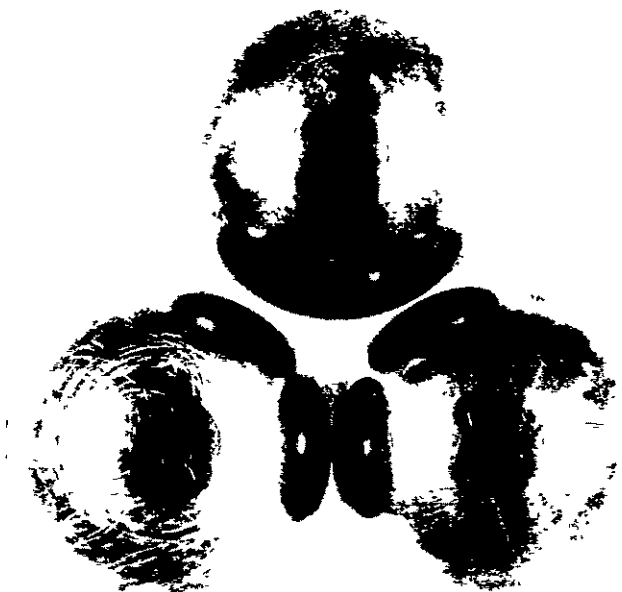
A visual inspection of the test bearing showed extensive scratches on several but not all balls. This condition could have resulted from dirt particles being blown through the bearing with the cooling or mist air, however, the scratches were not present on the rings or cage pockets. The positive cause of the scratches on the ball could not be determined. On both the inner and outer races evidence of several ball tracks were present and the Dulite (black oxide coating) had been removed. The wear in the race was considered to be somewhat greater than would be expected at the operating speeds and short period of operation (approximately 1.5 hours) which would indicate an insufficient quantity of lubrication or poor quality lubricant. However, the cage was in excellent condition with normal polishing of the silver plated pockets and minor polishing of the land riding cage rails. Photographs of the bearing components taken after the test are presented in Figure 15.

In general the mist system evaluation tests indicated that the mist oil was being supplied in a sufficient quantity, based on the established design requirement, at a considerably less mist air flow rate than had been calculated. The tests also indicated that the mist was being supplied uniformly with respect to the nozzles and impinging on the designed points of application. The bearing condition following the 10,000 rpm check indicated that insufficient lubrication may be present; however, it was extremely difficult to make any firm decision with respect to this evaluation parameter since conflicting evidence was present. The bearings ran at a reasonable tempera-

FIGURE 15  
TEST BEARING COMPONENTS AFTER 10,000 RPM  
EVALUATION TEST

Mist System Test - Slow Speed Operation  
Low Viscosity Synthetic Paraffinic Hydrocarbon Fluid

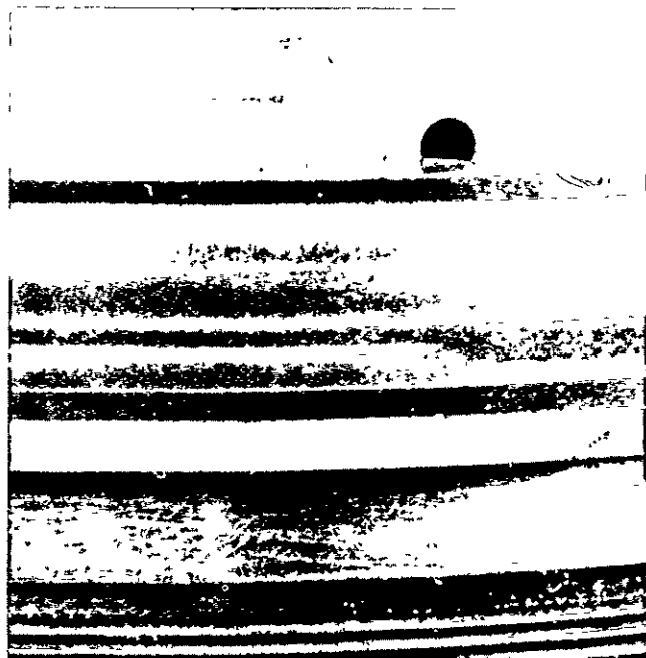
Bearing S/N 13



BALLS



CAGE



INNER RING LOADED HALF ON SHAFT



OUTER RING

ture which would not be expected if poor lubrication conditions were present.

## 6.2 Step-Speed and Extended Period Tests

The initial four step-speed tests were performed to determine any major performance characteristic differences resulting from the use of the four selected lubrication test fluids. From the evaluation of the test data, one fluid was selected for use in the extended period tests and additional step-speed tests. Six additional step-speed tests were performed to evaluate variations in cooling air flow rates, mist oil flow rates, cooling air temperature, and mist and cooling air delivery system changes. Three extended period tests were performed and one step-speed test using recirculating oil to lubricate the test bearing to obtain data for comparison with the mist lubrication test data.

### 6.2.1 Test No. 1, Step-Speed

The first test was performed using XRL850A lubricating fluid in the form of mist to lubricate the test bearing and the same oil supplied through jets to the rig bearing. The use of the same oil in the mist and recirculating systems was used throughout the test program. The same test bearing (S/N 13) as used in the 10,000 rpm mist system evaluation tests was used. A thrust load of 14,589 newtons (3280 lbs.) was applied to the bearing as was done in all dynamic testing.

The test was initiated by passing cooling air, including shaft cooling air, and mist through the rig until the desired mist oil, mist and cooling air temperatures were obtained. The shaft was accelerated to 10,200 rpm and data recorded. The shaft was further accelerated to 16,000 rpm. The total time taken to reach 16,000 rpm was approximately 2 hours. During this time period numerous adjustments were made to the various cooling air flow rates. As initially observed in the 10,000 rpm test, the shaft cooling air was found unnecessary since the outer ring temperature was generally higher than the inner ring even with the shaft cooling air turned off. Shaft cooling air was not used in any other step-speed tests or extended period tests.

The shaft speed was then increased in discrete steps to a maximum speed of 24,000 rpm ( $3 \times 10^6$  DN) for a brief period. Due to either instability in the drive motor servo speed control loop or drive belt slippage the highest stable speed obtained was 21,400 rpm. A total of 2.15 hours at speeds above 21,000

rpm was realized of which 1.6 hours were run at a stabilized outer ring temperature of 527°K (490°F). The test data are presented in Table III which shows that the heat transferred to the mist and cooling air at 21,400 rpm was 7638 watts (36,085 Btu/hr). The mist oil flow rate was 858 cc/hr (53 cubic inches per hour) with a total air flow of 2.9 scmm (102.5 scfm).

The test bearing was in good condition after testing with only minor changes noted. More debris dents were present in both the inner and outer races and some micropitting was present. The debris denting results from solid foreign material passing through the bearing and the micropitting, which has been observed on other bearings made of M50 steel, is considered to be the result of stress concentrations around near-surface inclusions and carbide stringers and probably some effect of the black oxide coating process. The cage was in excellent condition with only minor polishing of the silver plating in the ball pockets and land riding rails. The balls appeared to be similar to pretest condition with no observable increase in the scratch mark. Photographs of the bearing components are presented in Figure 16. No oil decomposition products were observed on the bearing or rig components. In general the post test bearing condition appeared the same as bearings which were tested using recirculating lubrication in previous test programs conducted at S K F under similar conditions.

The results of this test indicated that mist lubrication was a viable means of lubricating a high speed, high temperature aircraft gas turbine mainshaft bearing. It showed that the bearing heat generation rate established prior to testing was a conservative value and less cooling air than anticipated was required to maintain a stable bearing temperature. Twenty percent of the calculated required oil replenishment rate appeared to be adequate to lubricate the bearing.

#### 6.2.2 Test No. 2, Step-Speed

The second step-speed test was performed with XRL850A plus 5% by weight of Kendall 0839 resin as the lubricating fluid and a new test bearing, S/N 15. A thrust load of 14,589 newtons was applied to the test bearing and mist and cooling air passed through the rig during the pretest heating period. The shaft was accelerated to 10,000 rpm and data recorded following stabilization of the bearing temperature. The shaft was further accelerated in discrete steps to 16,000 rpm, 20,000 rpm and to a maximum of 23,000 rpm for a short period. The speed could not be maintained at 23,000 rpm due to instability and was lowered to 21,200 rpm until termination of the test. A failure of the slip ring assembly prevented measurement of the inner ring temperature at the 21,200 rpm speed. A total of 2.1 hours was



TABLE III

## TEST AND CALCULATED DATA

Test No. - 1 (Step-Speed), Lubricant - XRL850A, Bearing S/N 13

Shaft Speed (rpm)	Brg. O.R. Temp. (°K-°F)	Brg. I.R. Temp. (°K-°F)	Mist Oil Flow Rate (cm <sup>3</sup> /hr-in <sup>3</sup> /hr)	Through Brg. Flow Rate (scmm-scfm)	Cooling Air In/Exhaust Temp. (°K-°F)
10,200	405-270	400-206	819-50	1.70-60.2	349/383-170/230
16,000	450-350	413-285	1966-120	2.19-77.2	344/405-160/270
21,400	527-490	533-500	858-53	2.04-72.0	339/411-150/380

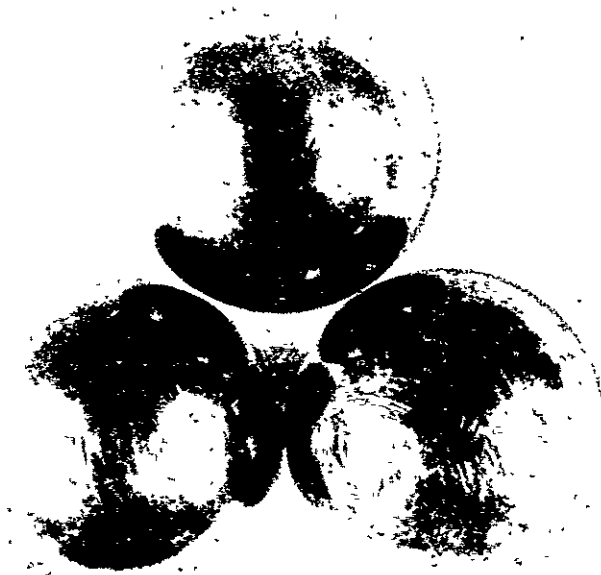
Shaft Speed (rpm)	Housing Cooling Air-Flow Rate (scmm-scfm)	In/Exhaust Temp. (°K-°F)	Mist Air Flow Rate (scmm-scfm)	In/Exhaust Temp. (°K-°F)	Total Air Flow Rate (scmm-scfm)
10,200	0.43-15.3	333/389-140/240	0.39-13.9	339/382-150/230	2.52-89.2
16,000	0.45-15.8	308/405-95/270	0.83-29.4	339/405-150/270	3.47-122.4
21,400	0.45-16	312/428-100/375	0.41-14.5	344/466-160/380	2.90-102.5

Shaft Speed (rpm)	HEAT TRANSFER RATE			
	TBCA (Watts-Btu/hr)	HCA (Watts-Btu/hr)	Mist (Watts-Btu/hr)	Total (Watts-Btu/hr)
10,200	1142-3902	482-1646	351-1198	1975-6746
16,000	2682-9160	875-2990	1024-3498	4582-15,647
21,400	5237-17,885	1391-4752	1010-3448	7638-26,085

FIGURE 16

TEST BEARING COMPONENTS AFTER TEST NO. 1

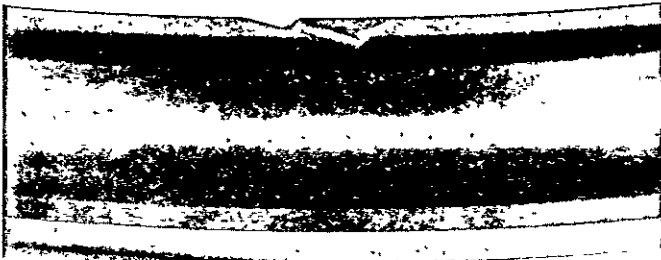
Step-Speed Mist Test  
Low Viscosity Synthetic Paraffinic Hydrocarbon Fluid  
Maximum Speed 24,000 rpm, Bearing S/N 13



BALLS



CAGE



INNER RING LOADED HALF



OUTER RING

REPRODUCIBILITY OF THE  
ORIGINAL PAGE IS POOR

accumulated at speeds above 21,000 rpm of which 1.64 hours were at an outer ring temperature of approximately 527°K (490°F).

The test data are presented in Table IV. A mist oil flow rate of 787 cc/hr (48 cubic in/hr) was supplied at the highest shaft speed. The data shows that only approximately half as much mist and cooling air was required as in Test 1 to maintain the test bearing at the desired temperature of 533°K (500°F) at the maximum speed. It is also noted that the heat transfer rate to the air was 3864 watts (13,195 Btu/hr) which is also approximately half that calculated in Test 1. This difference, at the time of the test, was attributed to a decrease in the traction forces due to the resin added to the oil even though the magnitude of the change did not seem plausible. As the test program continued it became obvious that the discrepancy was due to a loss of mist and through bearing cooling air through the labyrinth seal between the test and rig bearing and past the Teflon seal between the test bearing housing and rig housing. It was assumed in all calculations that the total air supplied passed through the bearing. A measure of the loss rate could not be established but was observed to increase with the supply rate as would be expected. Therefore, the calculated heat transfer rate is considered to be conservative on the high side in all tests, especially those with high mist and through bearing cooling air flow rates.

The post test bearing inspection showed that the bearing was in good condition and very similar to the bearing used in Test 1 with the exception that tracking was present on the balls but only minor scratches. Photographs of the bearing components are presented in Figure 17. No oil decomposition products were present on the bearing or adjacent parts in the rig, see Figure 18.

### 6.2.3 Test No. 3, Step-Speed

The third step-speed test was performed with XRM232A lubricating fluid and a new test bearing, S/N 17. The test was performed in the same manner as the two previous step-speed tests with the same applied thrust load of 14,589 newtons. The shaft was accelerated to 10,000 rpm, data recorded, and then to 16,000 rpm within approximately 2 hours. The shaft was then accelerated to 22,000 rpm in incremental steps of 2,000 rpm. After a few minutes at 22,000 rpm before thermal stability was obtained, there was a sudden test bearing failure and the drive motor was shut off immediately. The failure was essentially instantaneous with no prior indication that it would occur. The bearing ran for approximately 50 minutes at 20,000 rpm before the speed was increased to 22,000 rpm.

TABLE IV

## TEST AND CALCULATED DATA

Test No. - 2 (Step-Speed), Lubricant - XRL850A + 5% Kendall Resin, Bearing S/N 15

Shaft Speed (rpm)	Brg. O.R. Temp. (°K-°F)	Brg. I.R. Temp. (°K-°F)	Mist Oil Flow Rate (cm <sup>3</sup> /hr-in <sup>3</sup> /hr)	Through Brg. Cooling Air (scmm-scfm)	Cooling Air In/Exhaust Temp. (°K-°F)
10,000	405-270	400-260	1245-76	2.01-71.1	366/377-145/220
16,000	450-350	422-300	787-48	1.39-49.2	341/407-155/275
20,000	489-420	436-325	787-48	1.39-49.2	348/433-165/320
21,200	527-490	---	787-48	0.88-31.0	344/458-160/365

Shaft Speed (rpm)	Housing Cooling Air-Flow Rate (scmm-scfm)	In/Exhaust Temp. (°K-°F)	Mist Air Flow Rate (scmm-scfm)	In/Exhaust Temp. (°K-°F)	Total Air Flow Rate (scmm-scfm)
10,000	0.42-15.0	308/389-95/240	0.56-19.9	346/377-163/220	3.0-106.0
16,000	0.42-14.9	305/416-90/290	0.37-13.2	349/407-168/275	2.19-77.3
20,000	0.42-14.9	305/447-90/345	0.37-13.2	351/433-173/320	2.19-77.3
21,200	0.31-11.1	341/458-170/365	0.37-13.2	341/458-170/365	1.56-55.3

## HEAT TRANSFER RATE

Shaft Speed (rpm)	TBCA (Watts-Btu/hr)	HCA (Watts-Btu/hr)	Mist (Watts-Btu/hr)	Total (Watts-Btu/hr)
10,000	1684-5750	688-2349	358-1224	2730-9323
16,000	1862-6360	943-3221	446-1525	3252-11,106
20,000	2401-8200	1202-4106	613-2095	4217-14,401
21,200	2020-6900	1029-3515	814-2780	3864-13,195

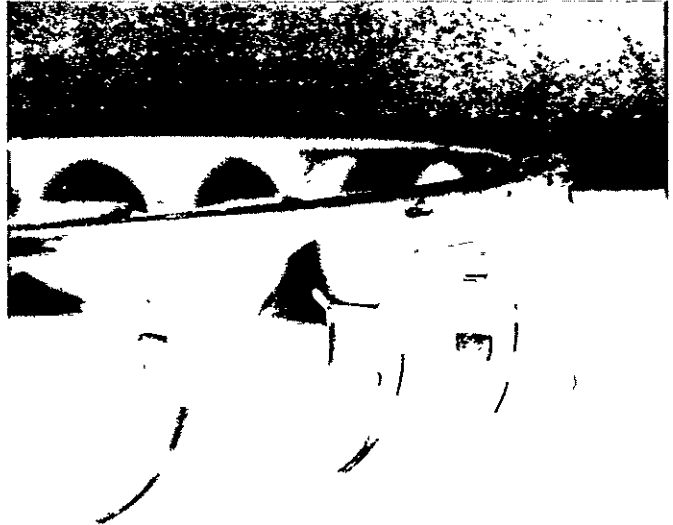
FIGURE 17

TEST BEARING COMPONENTS AFTER TEST NO. 2

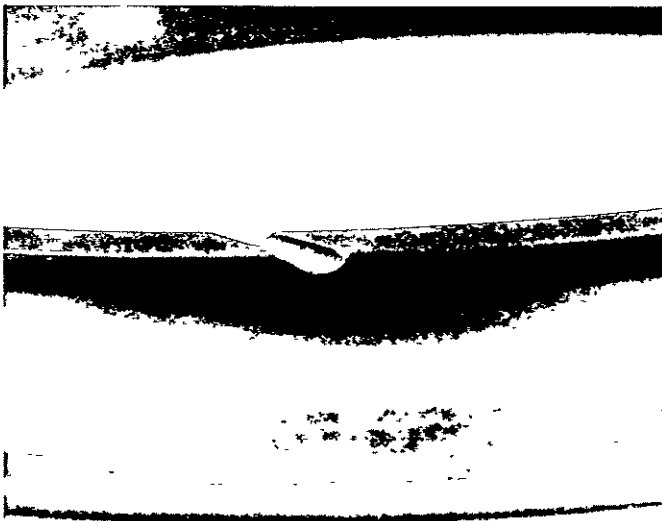
Step-Speed Mist Test  
Low Viscosity Synthetic Paraffinic Hydrocarbon  
Fluid Plus 5% Heavy Paraffinic Resin  
Maximum Speed 23,000 RPM - Bearing S/N 15



BALLS



CAGE



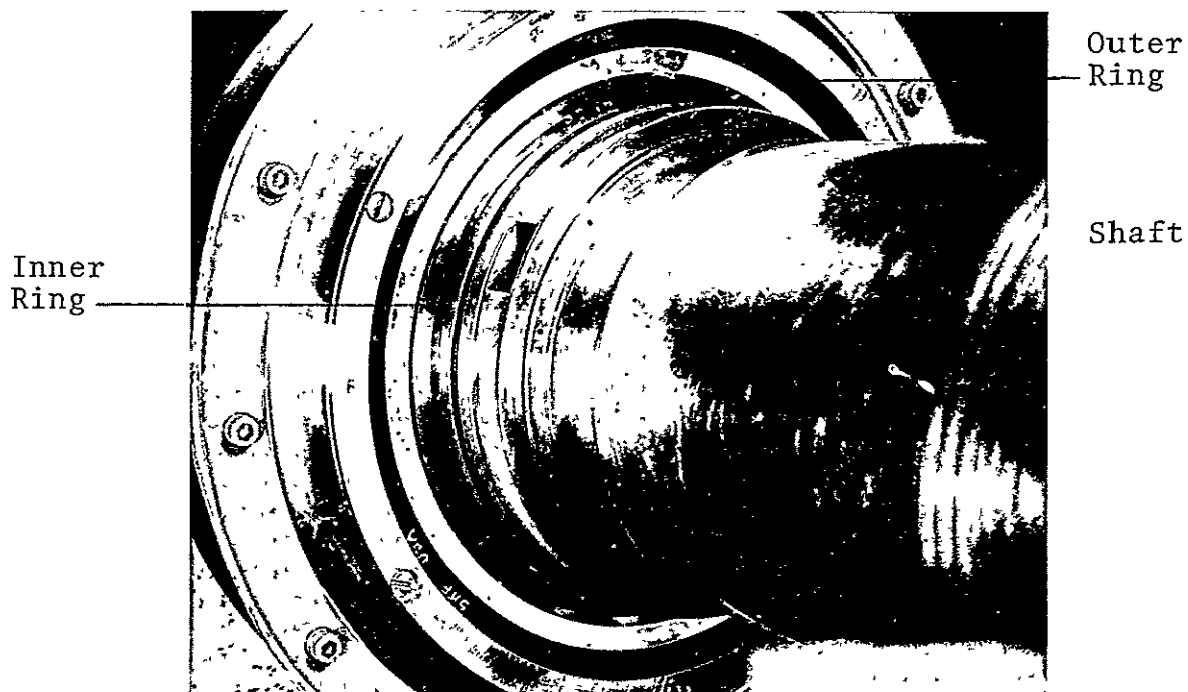
INNER RING LOADED HALF



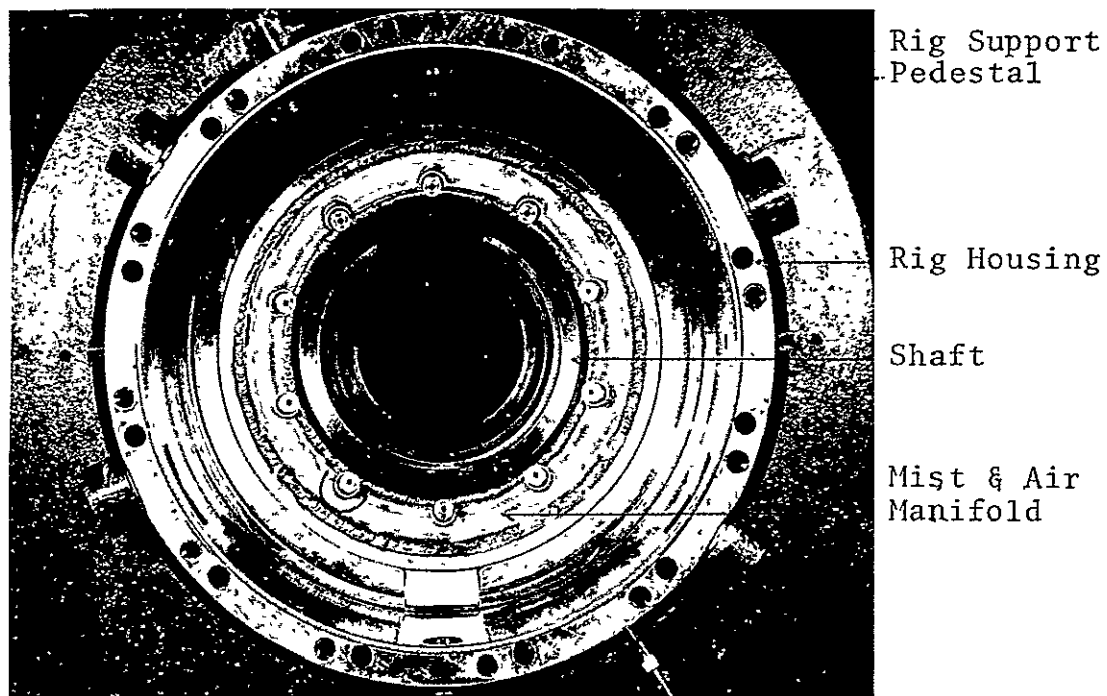
OUTER RING

FIGURE 18

RIG COMPONENTS AFTER TEST NO. 2



INBOARD VIEW OF TEST BEARING, BEARING HOUSING AND SHAFT



VIEW OF RIG HOUSING, MIST AND AIR MANIFOLD AND END OF SHAFT

The data recorded prior to the bearing failure are presented in Table V. The mist oil flow rate was 639 cc/hr (39 cubic inches per hour) with a total air flow of 1.85 scmm (65.5 scfm) at the maximum speed (20,000 rpm) where bearing temperature stability was obtained. The heat transferred to the air at 20,000 rpm was 2102 watts (10,594 Btu/hr).

Inspection of the test bearing showed that a thermal imbalance failure had occurred. Damage to the bearing was extensive with considerable material removed from both halves of the inner race and smeared on the outer race, balls, and cage pockets, see Figure 19. Smearing of a much lesser degree had also occurred between the down stream (opposite side to mist and through bearing cooling air entrance) cage rail and the outer ring land surface. This was the first test in which wear, except for minor polishing, had been observed between the cage and the guide land.

Based on the results of this test, even though the absolute cause of the failure could not be established, the first two synthetic hydrocarbon test fluids were considered preferable to the XRM232A as a mist lubricant for high speed high temperature jet engine bearing application.

#### 6.2.4 Test No. 4, Step-Speed

The fourth step-speed test was performed with XRM205F lubricating fluid and a new test bearing, S/N 18. The test was performed in the same manner as the previous tests and the same applied thrust load of 14,589 newtons. The shaft was accelerated in incremental steps and data recorded at speeds of 8,000, 13,000, 16,000 and 18,000 rpm after the bearing temperature had stabilized.

With the shaft operating at 18,000 rpm and essentially the same mist and cooling air flow rates and temperatures as applied in Test 3 at the same speed, the test bearing temperature was operating at approximately 55°K (100°F) higher temperature. The heat transfer rate to the air was also higher by 1138 watts (3886 Btu/hr). This condition was considered to be the result of the higher fluid viscosity (39 centistokes at 372°K {210°F}) compared to 5 centistokes for the other oils. To prevent the bearing temperature from increasing above 533°K (500°F) the through bearing cooling air flow rate was increased from 0.93 scmm (33 scfm) to 1.73 scmm (61 scfm). The bearing outer ring temperature decreased 8.3°K (15°F) and the shaft speed was increased to 20,000 rpm. Almost immediately the shaft seized terminating the test. Inspection of the rig showed that the rig bearing had failed.

TABLE V

## TEST AND CALCULATED DATA

Test No. - 3 (Step-Speed), Lubricant - XRM232A, Bearing S/N 17

Shaft Speed (rpm)	Brg. O.R. Temp. (°K-°F)	Brg. I.R. Temp. (°K-°F)	Mist Oil Flow Rate (cm <sup>3</sup> /hr-in <sup>3</sup> /hr)	Through Brg. Flow Rate (scmm-scfm)	Cooling Air In/Exhaust Temp. (°K-°F)
10,000	391-245	389-240	754-46	0.95-33.6	336/365-145/200
16,000	452-355	427-310	639-39	0.92-32.6	351/416-175/290
18,000	477-400	---	639-39	0.89-31.6	391/439-245/330
20,000	501-440	---	639-39	0.85-29.9	389/455-240/360

Shaft Speed (rpm)	Housing Cooling Flow Rate (scmm-scfm)	In/Exhaust Temp. (°K-°F)	Mist Air Flow Rate (scmm-scfm)	In/Exhaust Temp. (°K-°F)	Total Air Flow Rate (scmm-scfm)
10,000	0.40-14.1	297/358-75/185	0.37/13.2	337/337-148/200	1.72-60.9
16,000	0.40-14.1	297/413-75/285	0.33-11.6	334/416-143/290	1.65-58.3
18,000	0.40-14.1	297/433-75/320	0.33-11.7	339/439-150/330	1.58-56.0
20,000	0.39-13.9	303/455-85/360	0.33-11.7	342/455-156/360	1.85-65.5

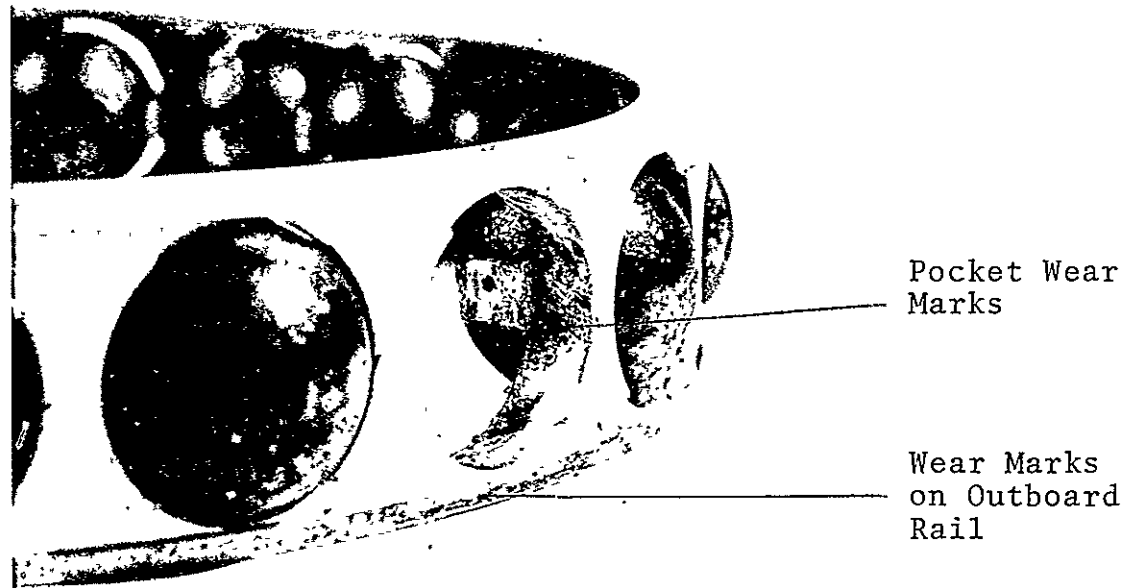
Shaft Speed (rpm)	TBCA (Watts-Btu/hr)	HCA (Watts-Btu/hr)	Mist (Watts-Btu/hr)	Total (Watts-Btu/hr)
10,000	584-1993	491-1679	217-741	1292-4413
16,000	1185-4049	938-3205	540-1845	2664-9099
18,000	838-2864	1124-3839	665-2272	2599-8875
20,000	1134-3874	1214-4145	754-2575	3102-10,594



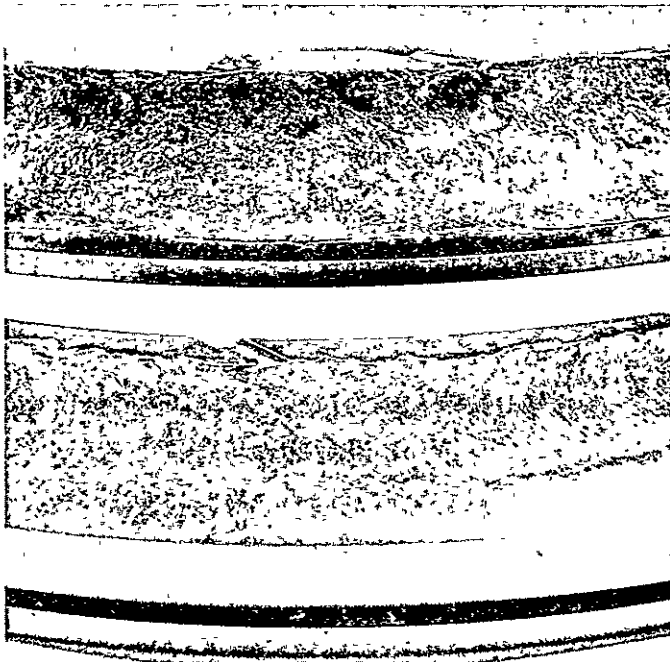
FIGURE 19

TEST BEARING COMPONENTS AFTER TEST NO. 3

Step-Speed Mist Test  
Advanced Type II Ester Fluid  
Failure Occurred at 22,000 rpm - Bearing S/N 17



BALLS AND CAGE



INNER RINGS



OUTER RING

The data recorded prior to the rig bearing failure are presented in Table VI. The mist oil flow rate was 901 cc/hr (55 cubic inches per hour) with a total air flow of 1.72 scmm (60.7 scfm) at 18,000 rpm shaft speed. The heat transferred to the air was 4240 watts (14,480 Btu/hr).

The test bearing was in good condition as established by the post test inspection. Polishing of the silver plating in the ball pockets had occurred and some minor smearing of silver on the downstream outer ring cage guiding land, see Figure.20.

#### 6.2.5 Test No. 5, Extended Period Test

It was not plausible to select the best or rank the performance of the various lubrication test fluids based on a single evaluation test of each, especially when a basic method of lubrication and cooling is being extended to more severe conditions than it is normally applied. However, for the purpose of this program, the lubricating fluid XRL850A plus 5% Kendall resin was selected for use in the remaining tests in the program.

The XRM232A fluid was not considered due to the test bearing failure that occurred during its use even though the failure may not have been the direct result of the fluid. The XRM205F fluid was eliminated because of the higher bearing temperatures and heat generation rates in Test 4 relative to Tests 2 and 3. This condition is attributed to the higher viscosity of XRM205F than the other test fluids. The XRL850A plus the resin was selected over the base fluid because of the much higher bearing heat generation rate calculated for Test 1. The high calculated rate may be in error however as mentioned earlier due to air leakage at the high flow rate.

The extended period test was performed in the same manner as the step-speed tests with the exception that the shaft speed was accelerated directly to 20,000 rpm at a relative constant rate after the pretest heating of the mist oil and cooling air. The goal of the test was to run at 20,000 rpm ( $2.5 \times 10^6$  DN) for 50 hours. The test was to be performed in no less than five separate runs with the bearing allowed to cool to room temperature between each run.

Test bearing S/N 13, used previously in Test 1, was used in the test. The bearing operated successfully for 35.5 hours at the desired speed and outer ring temperature between 505°K and 533°K (450°F-500°F) before a failure occurred while bringing the shaft up to speed during run 9. The accumulated hours of

TABLE VI

## TEST AND CALCULATED DATA

Test No. - 4 (Step-Speed), Lubricant-XRM205F, Bearing S/N - 18

Shaft Speed (rpm)	Brg. O.R. Temp. (°K-°F)	Brg. I.R. Temp. (°K-°F)	Mist Oil Flow Rate (cm3/hr-in3/hr)	Through Brg. (scmm-scfm)	Cooling Air In/Exhaust Temp. (°K-°F)
8,000	377-220	366-200	819-50	0.91 32.2	369/394-205/250
13,000	477-400	460-365	819-50	0.93 32.8	372/433-210/320
16,000	511-460	477-400	819-50	0.89 31.5	374/455-215/360
18,000	530-495	489-420	901-55	0.93 32.8	374/469-215/385

Shaft Speed (rpm)	Housing Cooling Air - Flow Rate (scmm-scfm)	In/Exhaust Temp. (°K-°F)	Mist Air Flow Rate (scmm-scfm)	In/Exhaust Temp. (°K-°F)	Total Air Flow Rate (scmm-scfm)
8,000	0.38 13.3	302/405-85/270	0.40 14.1	344/394-160/250	1.69-59.6
13,000	0.36 12.7	297/424-75/305	0.40 14.1	340/433-153/320	1.66-58.6
16,000	0.36 12.7	297/466-75/380	0.40 14.1	344/455-160/360	1.65-58.3
18,000	0.36 12.7	300/483-80/410	0.43 15.2	345/469-163/385	1.72-60.7

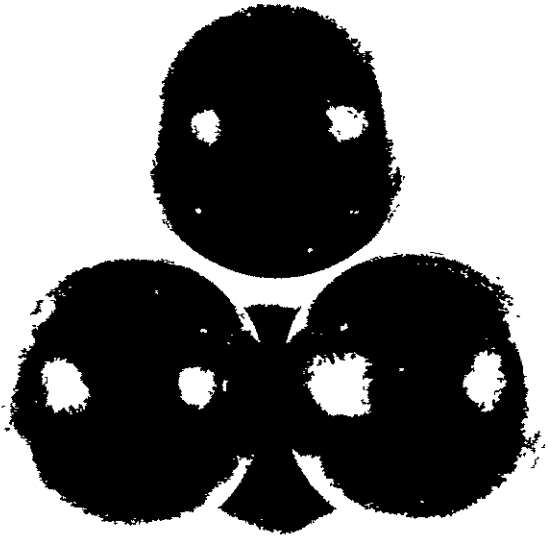
## Heat Transfer Rate

Shaft Speed (rpm)	TBCA (Watts-Btu/hr)	HCA (Watts-Btu/hr)	Mist (Watts-Btu/hr)	Total (Watts/Btu/hr)
8,000	561-1915	381-1300	827-2823	1768-6038
13,000	1136-3880	671-2290	1028-3510	2834-9680
16,000	1546-5280	802-2740	1365-4660	3713-12,680
18,000	1757-6000	893-3050	1590-5430	4240-14,480

FIGURE 20

TEST BEARING COMPONENTS AFTER TEST NO. 4

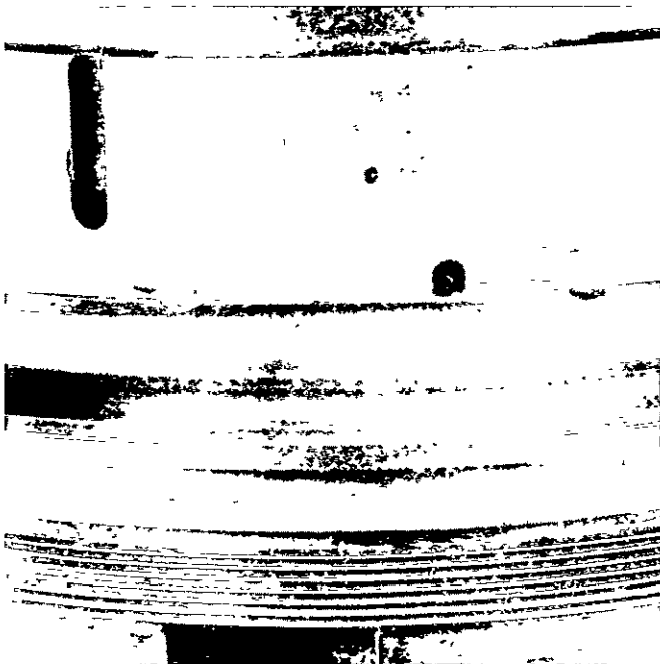
Step-Speed Mist Test  
High Viscosity Synthetic Paraffinic Hydrocarbon Fluid  
Maximum Speed 20,000 RPM - Bearing S/N 18



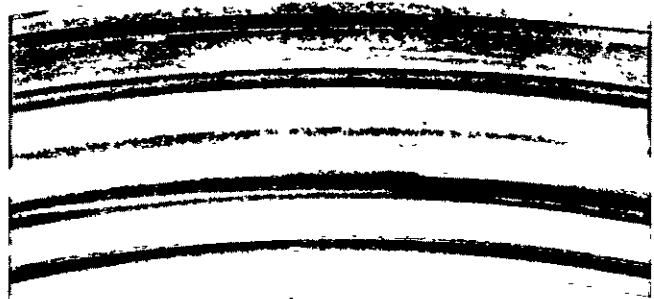
BALLS



CAGE



INNER RING LOADED HALF ON  
SHAFT



OUTER RING

testing were accomplished during 8 different runs of 5.2, 8.0, 7.8, 2.0, 1.6, 8.2, 2.5 and 0.2 hours respectively. The mist and cooling air flow rates and temperatures were similar to those applied in Test 4.

Inspection of the test bearings after failure indicated that a thermal imbalance failure had occurred as gross smearing had resulted between the balls, cage and rings. The greatest smearing had occurred between the downstream cage rail (that furthest from the mist and cooling air nozzles) and the outer ring land and between the balls and races. Only minor wear had occurred on the upstream cage rail, see Figure 21. In addition, a heavy accumulation of coked oil was present on the bore of the downstream cage rail as would be expected due to the high temperatures resulting from the failure. A visual inspection

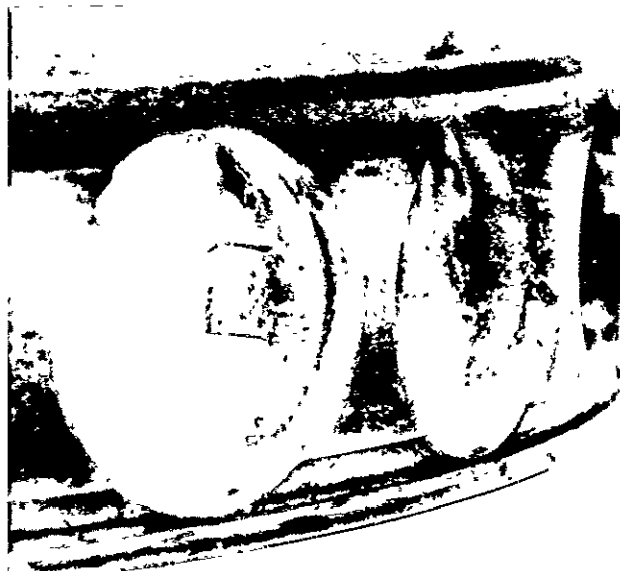
FIGURE 21

TEST BEARING COMPONENTS AFTER TEST NO. 5

Extended Period Mist Test - 20,000 RPM  
Low Viscosity Synthetic Paraffinic Hydrocarbon  
Fluid Plus 5% Heavy Paraffinic Resin  
Successfully Operated for 35.5 Hours Prior to Failure  
Bearing S/N 13



BALLS



CAGE



INNER RING LOAD HALF



OUTER RING

REPRODUCIBILITY OF THE  
ORIGINAL PAGE IS POOR

with test bearing S/N 18, used previously in Test 4 with the same fluid, and the 14,589 newtons thrust load applied.

It was initially intended that data would be obtained at each desired speed with oil flow rates of 0.0038, 0.0076 and 0.0114 m<sup>3</sup>/min (1, 2, and 3 gpm). However, this was not possible as the minimum flow rate was insufficient to produce stabilized thermal conditions at the higher speeds.

Stabilized thermal conditions were obtained at shaft speeds of 8,000, 13,000, 16,000, 18,000 and 21,000 rpm and data recorded. These speeds except for 21,000 rpm are identical to those where data was recorded in the mist lubrication test (Test 4) with the same fluid.

After increasing the speed from 8,000 to 13,000 rpm the minimum oil flow rate had to be increased from 0.0038 to 0.0057 m<sup>3</sup>/min (1 to 1.5 gpm) to obtain thermal stability. The 0.0057 m<sup>3</sup>/min (1.5 gpm) rate was also sufficient to obtain stability at a speed of 18,000 rpm; however, at 21,000 rpm the flow rate had to be increased to a minimum of 0.0076 m<sup>3</sup>/min (2 gpm). It is possible that the jetted oil stream did not impinge on the bearing at the low oil flow rates and high shaft velocities due to the air velocities generated around the bearing. This condition has been observed in other tests.

During the test, the oil inlet temperature was measured approximately 76 mm (3 inches) before entered the rig and the oil-out temperature was measured in the downstream drain line (oil that passed through the bearing) approximately 76 mm (3 inches) from the rig. Due to the upstream drain size it was not possible to measure the temperature of the oil which was jetted against the bearing but did not pass through (the large diameter vertical drain prevented assurance that a thermocouple located in the line was submerged in the draining oil).

A graph of the oil-in, oil-out and inner and outer ring temperatures versus shaft speed for an oil flow rate of 0.0076 m<sup>3</sup>/min (2 gpm) is presented in Figure 22. It is noted from this graph that the oil-out temperature is lower than the oil-in temperature at speeds below approximately 10,000 rpm. This condition results from heat being transferred from the oil to the rig before entering the drain line. A correction factor of 5036 watts (17,200 Btu/hr) established from the measured bearing drag torque at 8,000 rpm was thus applied to the bearing heat generation rates calculated from the inlet and outlet oil temperature values over the total speed range.

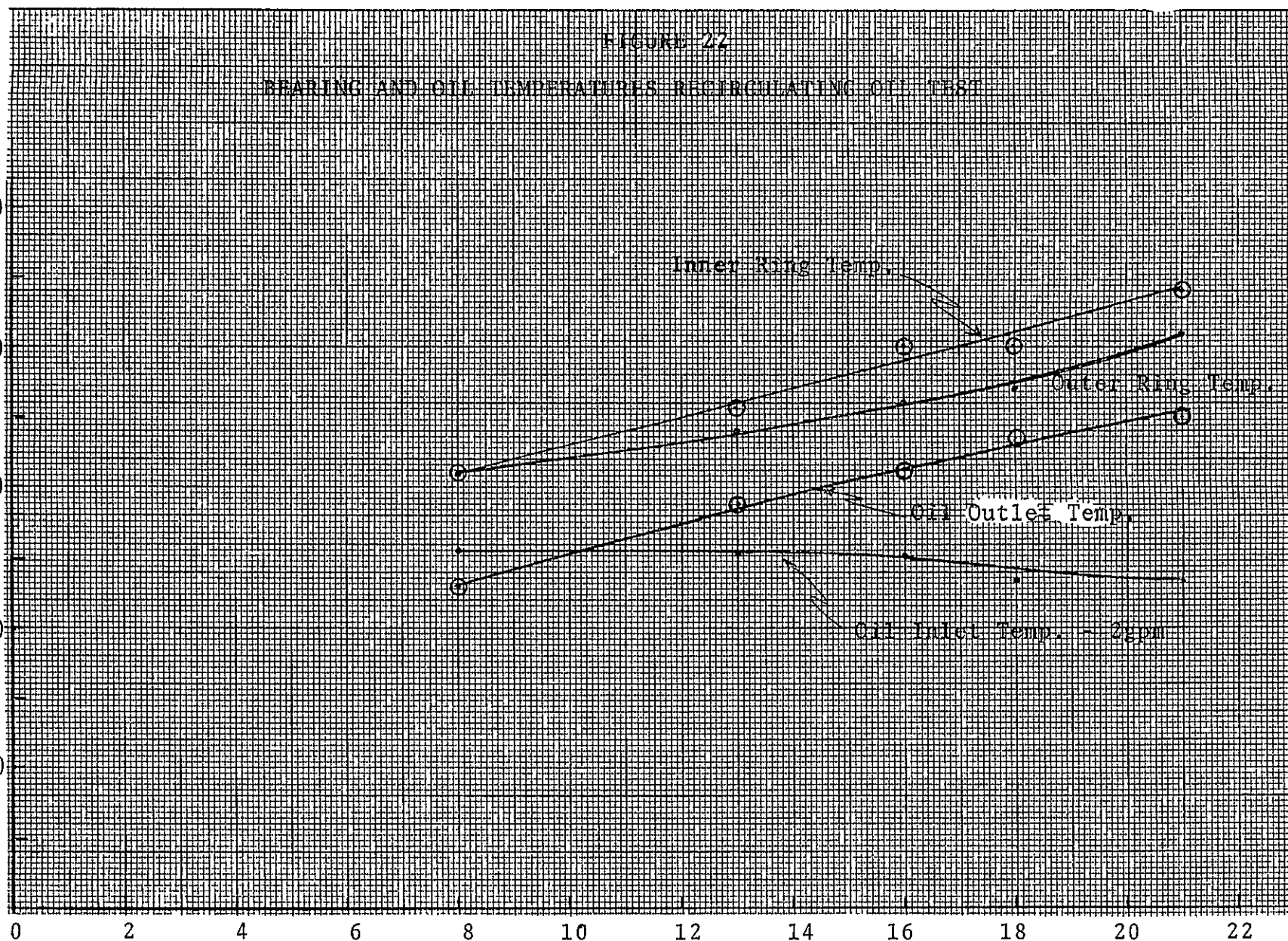
TEST BEARING OUTER RING TEMP. - °K (°F)

69

(500)  
505  
(400)  
450  
(300)  
394  
(200)  
339  
(100)  
283  
(0)

SHAFT SPEED-RPM  $\times 10^{-3}$

FIGURE 22  
BEARING AND OIL TEMPERATURES RECIRCULATING OIL TEST



AL75T032



At the lower speeds, there was generally good agreement between the bearing heat generation rates measured by the two different methods. At the higher speeds, however, the values calculated from the oil At values appreciably exceeded those established from the drag torque values. This condition could result from less oil passing through the bearing and thus the measured oil outlet temperature used in the calculations being larger than the average value from both drains. It is also reasonable that the measured drag torque was less than the true value. At the higher speeds and higher bearing temperatures, the drag in the torque measuring device increased with load produced by thermal differentials between the rig housing and load plug. Therefore, the average value of the two methods used is presented in Table VII and are considered to be representative of the true value.

Through the full speed range, the general trend shows an increase in bearing heat generation rate with increased oil flow rate which is expected as the result of increased oil churning. The data also shows, that with the oil flow rates applied, there is a decrease in bearing temperature with increased oil supply up to a shaft speed of 18,000 rpm. At 18,000 rpm the bearing temperature increased slightly when increasing the flow from 0.0083 to 0.00114 m<sup>3</sup>/min (2.2 to 3 gpm). At 21,000 rpm essentially no effect was noted with an increase of 0.0038 m<sup>3</sup>/min (1 gpm) oil flow rate. The test thus indicates that there is an upper limit on cooling capacity obtained by increased oil flow rate. This limit, however, is a function of method of oil application, bearing cavity and drain configuration. Thus, each system configuration would have its own specific characteristics.

Comparing the bearing heat generation rates of the mist and recirculating lubrication tests, it is seen that considerably less heat is generated when mist is used. This results from the decreased oil churning with mist lubrication. The ratios of heat generated, recirculating to mist, at the test speeds were:

Shaft Speed (rpm)	Heat Generation Ratio (recirculating/mist)
8,000	2.8
13,000	3.7
16,000	3.6
18,000	4.2

TABLE VII  
TEST AND CALCULATED DATA

Test No. - 6, Recirculating Oil Test Run, Lubricant XRM205F, Bearing S/N 13

Shaft Speed (rpm)	Lube Flow Rate (gpm)	Calculated Brg. Power Loss (Btu/hr)	Oil-Out Temp. (°F)	Oil-In Temp. (°F)	Brg. Temp. (°F) O.R.	I.R.
8,000	1	---	190	240	335	340
8,000	2	---	230	250	310	310
8,000	3	---	248	265	315	310
13,000	1.5	32,796	280	238	425	360
13,000	2.0	36,008	290	248	340	355
13,000	2.5	46,142	292	250	325	350
16,000	1.5	46,991	345	250	390	-
16,000	2.0	45,102	312	252	360	400
16,000	2.6	46,961	308	262	360	380
18,000	1.5	54,871	350	225	435	445
18,000	2.2	61,212	335	235	370	400
18,000	3.0	58,703	345	282	390	410
21,000	2.0	64,947	350	235	410	440
21,000	2.2	62,515	345	235	410	430
21,000	3.0	76,424	360	262	410	440

The test bearing was in good condition following the test. The only obvious change was the presence of oil decomposition products on the cage, see Figure 23.

#### 6.2.7 Test No. 7, Extended Period Test

A second extended period test was performed using the same oil, XRL850A plus 5% Kendall resin, as used in the first extended period test (Test 5) to determine if a longer period of operation could be obtained. The test was performed with the standard 14,589 newtons thrust load applied and test bearing S/N 30. The test was terminated after 29.2 hours operation at 20,000 rpm due to a test bearing failure. The test time at the desired operating speed was obtained in four runs of 7.8, 10.6, 10.6 and 0.2 hours, allowing the rig to return to room temperature between runs.

Following the bearing failure, operating conditions were reviewed to determine if any changes had taken place which may have contributed to the failure. During this investigation it was noted that it was possible that the through bearing cooling air flow rate was 0.337 scmm (11.9 scfm) which is considerably lower than the desired flow rate of 0.85 scmm (30 scfm) as established during the prior step-speed tests and used in the first extended period test.

Although there was conflicting evidence as to the exact through bearing cooling air flow rate, Test 9 performed specifically to determine the feasibility of running with reduced cooling air added credence to the lesser flow rate being supplied. Representative test data for the test, based on the low air flow, are presented in Table VIII.

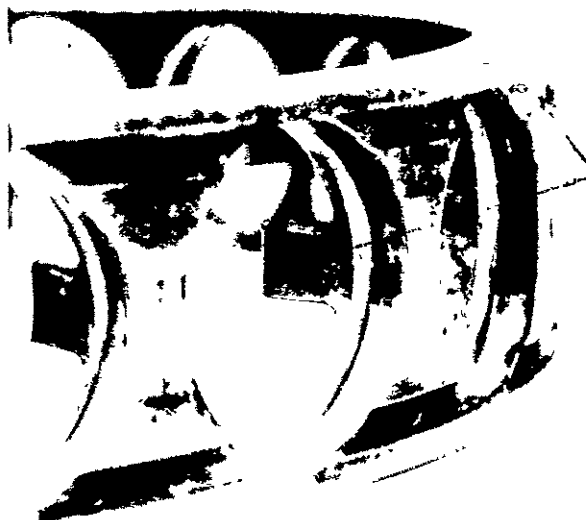
Inspection of the test bearing revealed a condition very similar to that of the bearing failed in the first extended period test. Gross smearing had occurred between the downstream cage rail and the outer ring land and between the balls and races. The leading face of the ball pockets was greatly worn and the trailing face was plated with smeared material. Essentially no wear had occurred on the upstream cage rail, see Figure 24.

FIGURE 23

TEST BEARING COMPONENTS AFTER TEST NO. 6  
Step-Speed Recirculation Oil Test  
High Viscosity Synthetic Paraffinic Fluid  
Maximum Speed 21,000 RPM-Test Bearing S/N 18



BALLS

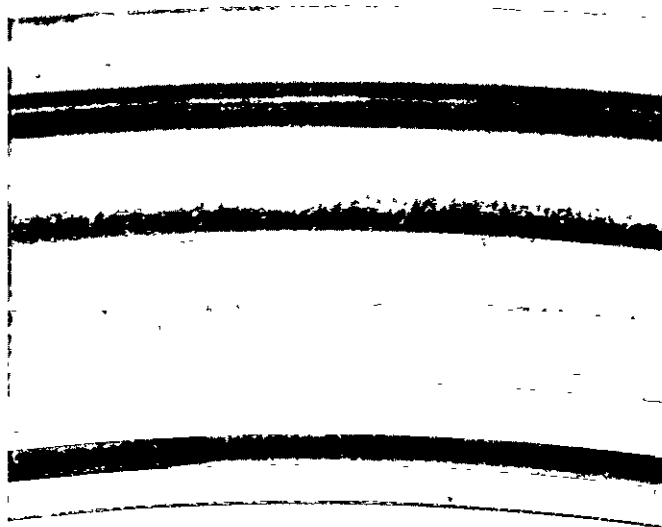


Oil De-  
composi-  
tion  
Products

CAGE



INNER RING LOADED HALF



OUTER RING

TABLE VIII

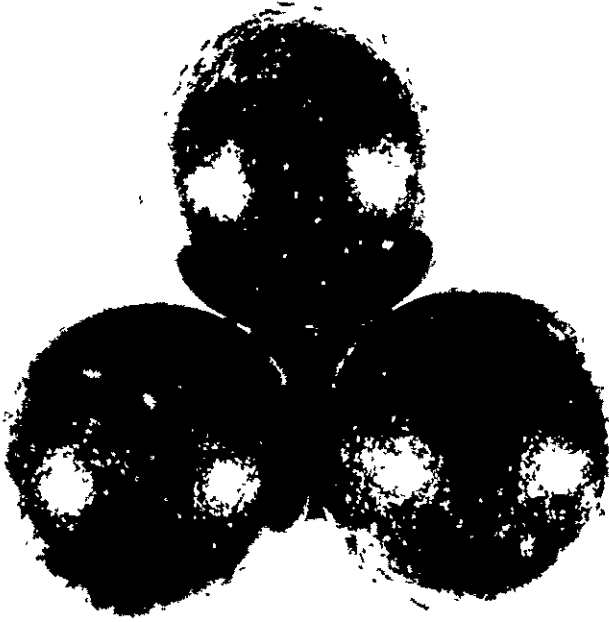
Test No. - 7 (Extended Period), Lubricant XRL850A + 5% Kendall Resin, Bearing S/N 30

Shaft Speed (rpm)	Brg. O.R. Temp. (°K-°F)	Brg. I.R. Temp. (°K-°F)	Mist Oil Flow Rate (cm <sup>3</sup> /hr-in <sup>3</sup> /hr)	Through Brg. Flow Rate (scmm-scfm)	Cooling Air In/Exhaust Temp. (°K-°F)
20,000	489-420	475-395	737-45	0.34-11.9	369/463-205/375
Shaft Speed (rpm)	Housing Cooling Air Flow Rate (scmm-scfm)	In/Exhaust Temp. (°K-°F)	Mist Air Flow Rate (scmm-scfm)	In/Exhaust Temp. (°K-°F)	Total Air Flow Rate (scmm-scfm)
20,000	0.41-14.5	315/366-108-200	0.35-12.5	339/463-150/375	1.1-38.9
Shaft Speed (rpm)	TBCA (Watts-Btu/hr)	HEAT TRANSFER RATE HCA (Watts-Btu/hr)	Mist (Watts-Btu/hr)	Total (Watts-Btu/hr)	
20,000	640-2186	560-1914	958-3271	2160-7376	

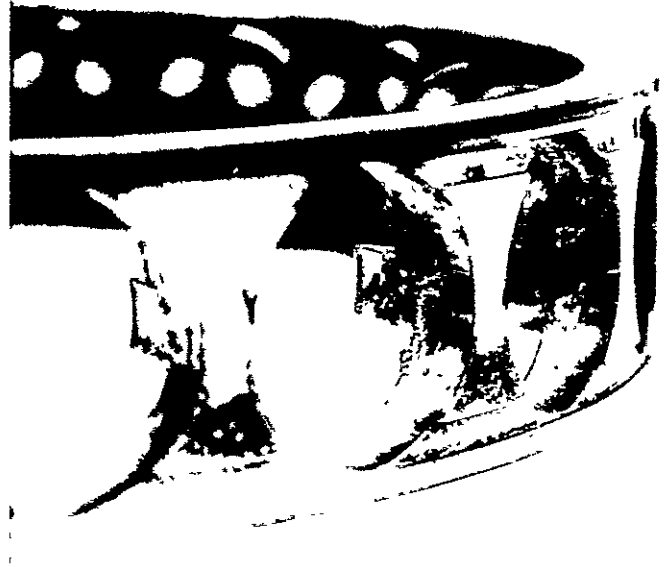
FIGURE 24

TEST BEARING COMPONENTS AFTER TEST NO. 7

Extended Period Mist Test-20,000 RPM  
Low Viscosity Synthetic Paraffinic Hydrocarbon  
Fluid Plus 5% Heavy Paraffinic Resin  
Successfully Operated for 29.2 Hours Prior to Failure  
Bearing S/N 30



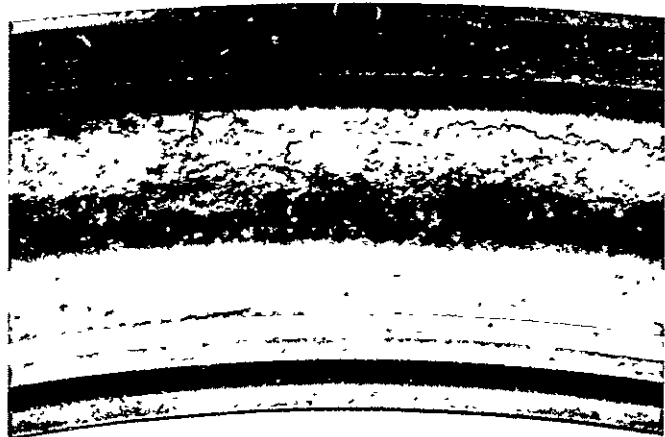
BALLS



CAGE



INNER RING, BOTH HALVES



OUTER RING

#### 6.2.8 Test No. 8, Reduced Mist Oil Flow Rate

The purpose of this test was to determine the possibility of operating with appreciable less mist oil than that which had been supplied in prior tests (639 to 819 cc/hr, 39 to 50 cubic inches/hr).

Prior to performing the test, the mist generator was calibrated to establish the mist oil flow rates for various settings of the oil-flow adjustment screws. Calibrations were performed with one of the adjustment screws closed while varying the position of the other. During all previous tests both adjustment screws were positioned wide open. The calibrations were made with conditions similar to those in prior tests, an air inlet temperature and flow rate to the generator of 438°K (330°F) and .36 scmm(12.75 scfm) respectively and an oil reservoir temperature of 372°K (210°F). The average mist temperature entering the rig was 341°K (155°F). Mist flow rates were obtained at adjustment screw settings of 2½ turns, 2 turns, and 1 turn open which resulted in flow rates of 442, 387, and 221 cc/hr (27, 23.6 and 13.5 cubic inches/hr) respectively.

The test was performed in three separate runs, each with a different oil flow rate. All three runs were performed with approximately the same cooling air and mist air flow rates and temperatures using the same mist lubricant (XRL850A + 5% Kendall resin) and the same bearing thrust load of 14,589 newtons. The mist air inlet temperature and flow rate was maintained as nearly as possible to the values used during the calibration of the mist generator. Test bearing S/N 18 was used in the test. This bearing had been used previously in Tests 4 and 6.

The first test run was performed with the maximum mist oil flow rate, 803 cc/hr (49 cubic in. per hour) as limited by the generator design and mist air flow rate. This flow rate was obtained with both adjustment screws open and is approximately equal to that applied in several prior tests using the same oil. Test data was recorded at each 2,000 rpm shaft speed increments from 10,000 to 20,000 rpm ( $1.25 \times 10^6$  DN to  $2.5 \times 10^6$  DN) after temperature stabilization occurred. The purpose of this run was to establish a baseline of conditions for comparison with later runs and to provide assurance that the rig was operating properly and thus minimizing the possibility of failures resulting from causes other than insufficient lubrication of the test bearing. The second and third runs were made with

mist oil flow rates of 442 and 221 cc/hr (27 and 13.5 in<sup>3</sup>/hr). respectively. No problems were encountered in either run which showed that for the particular rig and bearing configuration tested appreciably less mist oil (approximately 25%) will provide adequate lubrication than was originally shown to be satisfactory. The test data are presented in Tables IX-XI.

From the graphs of the test data presented in Figures 25 and 26 no indications of major differences resulted from changing the quantity of oil flow. Although at any given speed there were differences in the calculated heat removal rates between tests, they changed relative positions with speeds and no general trend was observed thus indicating no appreciable change in the lubrication quality resulting from the decreased flow rate. The test bearing was not removed between Test 8 and Test 9.

#### 6.2.9 Test No. 9, Reduced Through Bearing Cooling Air Flow Rate

The purpose of this test was to evaluate the feasibility of operating at 20,000 rpm with a reduced through bearing cooling air as suggested possible in the second extended period test (Test 7). The test was performed after Test 8 without a rig disassembly using the same lubricant (XRL850A plus 5% Kendall resin) and in the same manner. The through bearing cooling air was decreased from 0.83 scmm (29.5 scfm) to 0.44 scmm (15.4 scfm) for the initial checks. All other conditions were essentially the same with a mist oil flow rate of 786 cc/hr (48 cubic inches/hr). The shaft speed was increased slowly up to 20,000 rpm with data recorded at incremental speeds. At 20,000 rpm the through bearing cooling air flow rate was increased in two steps, first to 0.6 scmm (21.3 scfm) and then to 0.85 scmm (28.8 scfm). During these changes, the bearing outer ring temperature decreased from 505°K (450°F) to 491°K (425°F) and then to 477°K (400°F) showing the cooling effect of the increased air flow. The fact that it was possible to operate with through bearing cooling air reduced to approximately the same value as was established in the post Test 7 check (0.44 versus 0.34 scmm - 15.4 versus 12 scfm) essentially verified that a lower air flow rate than the intended .86 scmm was supplied in Test 7. The test data are presented in Table XII. Graphs of the test bearing outer ring temperatures and heat transfer rates at the various test speeds are presented in Figures 25 and 26 with those obtained in Test 8, Run 1.



TABLE-IX

Test No. - 8, Run 1 (Reduced Mist Oil Flow Rate),  
Lubricant - 850A+5% Kendall Resin, Bearing S/N - 18

Shaft Speed (rpm)	Brg. O.R. Temp. (°K - °F)	Brg. I.R. Temp. (°K - °F)	Mist Oil Flow Rate (cm <sup>3</sup> /hr.-in 3/hr)	Through Brg. Cooling Air (Scmm-Scfm)	Cooling Air In/Exhaust Temp. (°K - °F)
10	411-280	389-240	803-49	0.85-29.9	383/389 . 230/240
12	424-304	401-260	803-49	0.84-29.7	366/396 200/255
14	439-330	411-280	803-49	0.83-29.3	358/405 185/270
16	452-355	422-300	803-49	0.84-29.7	352/416 175/290
18	472-390	433-320	803-49	0.84-29.8	358/430 185/315
20	483-410	433-320	803-49	0.83-29.5	372/439 210/330

Shaft Speed (rpm)	Housing Cooling Air-Flow Rate (Scmm-Scfm)	In/Exhaust Temp. (°K - °F)	Mist Air Flow Rate (Scmm-Scfm)	In/Exhaust Temp. (°K - °F)	Total Air Flow Rate (Scmm-Scfm)
10	0.38-13.3	294/383-70/230	0.35-12.4	336/389 145/240	1.57-55.6
12	0.38-13.3	294/383-70/230	0.36-12.6	333/396 141/225	1.57-55.6
14	0.38-13.3	289/380-60/225	0.37-13.0	334/405 142/270	1.57-55.6
16	0.39-13.9	291/380-65/225	0.36-12.6	332/416 139/290	1.59-56.2
18	0.39-13.9	291/380-65/225	0.35-12.5	331/430 137/315	1.59-56.2
20	0.39-13.9	289/380-60/225	0.36-12.8	327/439 130/330	1.59-56.2

## HEAT TRANSFER RATE

Shaft Speed (rpm)	TBCA (Watts-Btu/hr)	HCA (Watts-Btu/hr)	Mist (Watts-Btu/hr)	Total (Watts-Btu/hr)
10	227-775	673-2300	373-1274	1273-4349
12	516-1763	673-2300	455-1556	1645-5619
14	788-2690	694-2370	525-1794	2007-6854
16	1079-3687	688-2350	603-2059	2370-8095
18	1225-4184	703-2400	704-2405	2632-8989
20	1119-3821	725-2475	807-2755	2584-8826

TABLE - X

Test No. - 8, Run 2 (Reduced Mist Oil Flow Rate)  
Lubricant - XRL850A+5% Kendall Resin Bearing S/N - 18

Shaft Speed (rpm)	Brg. O.R. Temp. (°K-°F)	Brg. I.R. Temp. (°K-°F)	Mist Oil Flow Rate (cm3/hr-in3/hr)	Through Brg. Flow Rate (Scmm-Scfm)	Cool Air In/Exhaust Temp. (°K - °F)
10	405-270	389-240	442-27	0.83-29.4	356/383-182/230
12	419-295	394-250	442-27	0.83-29.4	356/391-182/245
14	439-330	405-270	442-27	0.83-29.3	352/402-175/265
16	450-350	416-290	442-27	0.83-29.4	358/413-185/284
18	472-390	427-310	442-27	0.83-29.5	366/422-200/300
20	500-440	450-350	442-27	0.84-29.7	498/450-225/350

Shaft Speed (rpm)	Housing Cooling Air-Flow Rate (Scmm-scfm)	In/Exhaust Temp. (°K - °F)	Mist Air Flow Rate (Scmm-scfm)	In/Exhaust Temp. (°K - °F)	Total Air Flow Rate (Scmm-scfm)
10	0.41-14.4	291/379-65/222	0.37-12.9	332/383-138/230	1.60-56.7
12	0.39-13.9	289/378-60/220	0.37-12.9	330/391-135/245	1.59-56.2
14	0.39-13.7	289/378-60/220	0.37-13.0	330/402-135/265	1.58-56.0
16	0.39-13.9	289/378-60/220	0.37-12.9	332/413-138/284	1.59-56.2
18	0.39-13.9	289/375-60/215	0.36-12.8	330/422-135/300	1.59-56.2
20	0.39-14.8	289/375-60/215	0.35-12.5	330/450-135/350	1.61-57.0

## HEAT TRANSFER RATE

Shaft Speed (rpm)	TBCA (Watts-Btu/hr)	HCA (Watts-Btu/hr)	Mist (Watts - Btu/hr)	Total (Watts-Btu/hr)
10	446-1524	712-2430	374-1278	1532-5232
12	586-2000	705-2407	447-1523	1736-5930
14	834-2847	695-2373	533-1822	2062-7042
16	934-3189	705-2407	594-2029	2233-7625
18	932-3184	683-2332	666-2274	2281-7790
20	1174-4008	770-2629	852-2910	2796-9547

TABLE - XI  
 Test No. -8, Run 3 (Reduced Mist Oil Flow Rate)  
 Lubricant - XRL850A+5% Kendall Resin Bearing S/N - 18

Shaft Speed (rpm)	Brg. O.R. Temp. (°K-°F)	Brg. I.R. Temp. (°K-°F)	Mist Oil Flow Rate (cm <sup>3</sup> /hr-in <sup>3</sup> /hr)	Through Brg. Flow Rate (Scmm-Scfm)	Cooling Air In/Exhaust Temp. (°K-°F)
10,000	410-280	400-260	221-13.5	0.84 29.8	380/386-225/235
12,000	427-310	410-280	221-13.5	0.84 29.8	380/400-225/260
14,000	446-342	416-290	221-13.5	0.84 29.8	379/408-222/275
16,000	455-360	423-300	221-13.5	0.84 29.7	369/416-205/290
18,000	463-375	427-310	221-13.5	0.84 29.7	372/422-210/305
20,000	483-410	416-290	221-13.5	0.83 29.4	355/439-180/330

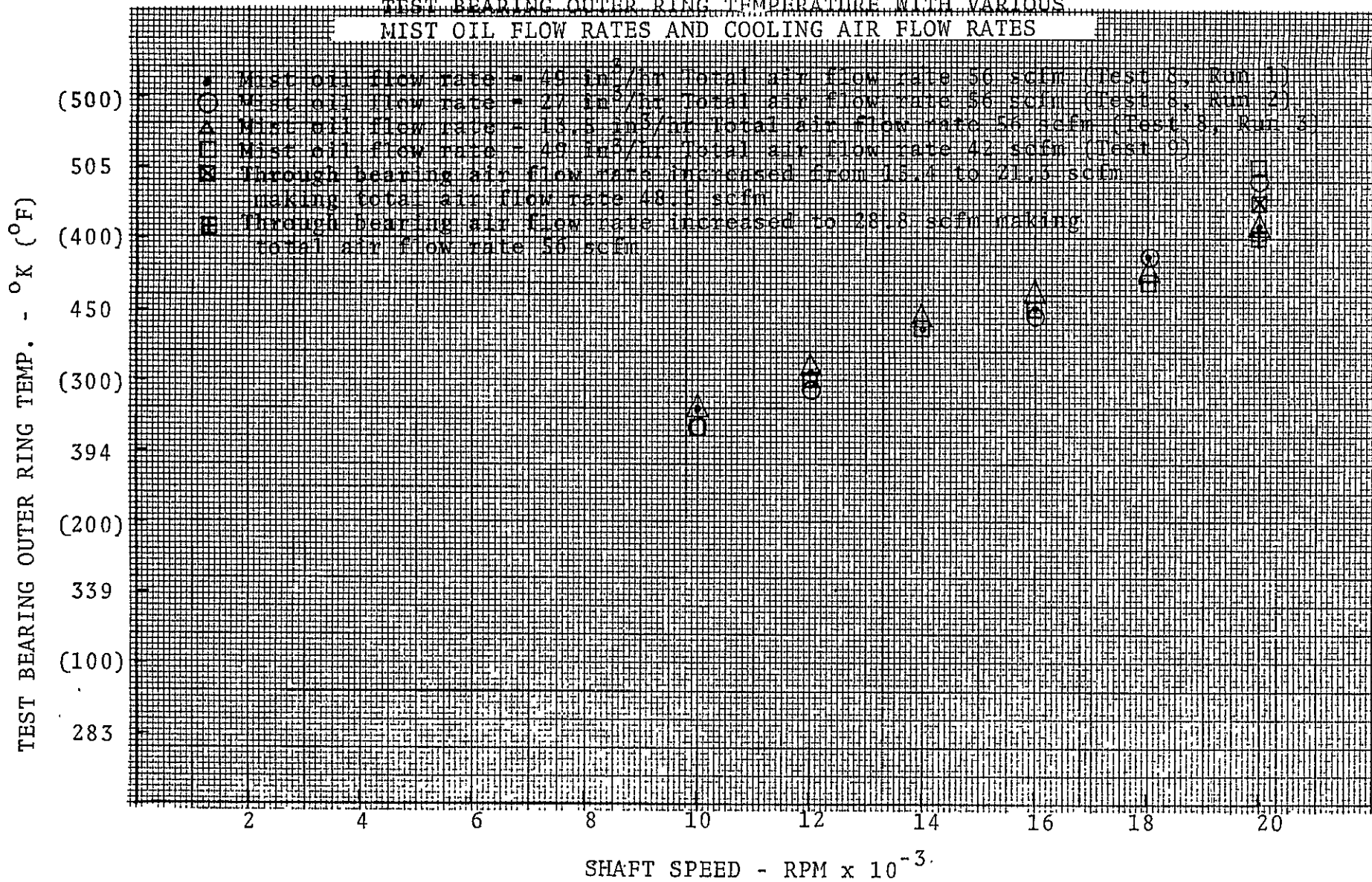
Shaft Speed (rpm)	Housing Cooling Air-Flow Rate (Scmm-scfm)	In/Exhaust Temp. (°K - °F)	Mist Air Flow Rate (Scmm-scfm)	In/Exhaust Temp. (°K - °F)	Total Air Flow Rate (Scmm-scfm)
10,000	0.43-15.2	294/377-70/220	0.35-12.5	313/386-140/235	1.63-57.5
12,000	0.43-15.2	294/279-70/222	0.35-12.5	313/400-140/260	1.63-57.5
14,000	0.43-15.2	294/380-70/225	0.35-12.5	313/408-140/275	1.63-57.5
16,000	0.43-15.2	294/380-70/225	0.36-12.7	313/416-140/290	1.63-57.5
18,000	0.43-15.2	294/380-70/225	0.36-12.6	312/422-138/305	1.63-57.5
20,000	0.43-15.2	294/377-70/220	0.37-12.9	329/439-133/330	1.63-57.5

## HEAT TRANSFER RATE

Shaft Speed (rpm)	TBCA (Watts-Btu/hr)	HCA (Watts-Btu/hr)	Mist (Watts - Btu/hr)	Total (Watts-Btu/hr)
10,000	94-321	720-2459	377-1286	1190-4066
12,000	329-1125	708-2419	476-1625	1514-5169
14,000	499-1703	744-2540	535-1828	1778-6071
16,000	797-2721	744-2540	600-2049	2140-7310
18,000	893-3048	744-2540	665-2270	2301-7858
20,000	1395-4763	720-2459	804-2745	2919-9967

FIGURE 25

# TEST BEARING OUTER RING TEMPERATURE WITH VARIOUS MIST OIL FLOW RATES AND COOLING AIR FLOW RATES

RESEARCH LABORATORY **SKF** INDUSTRIES, INC.

18

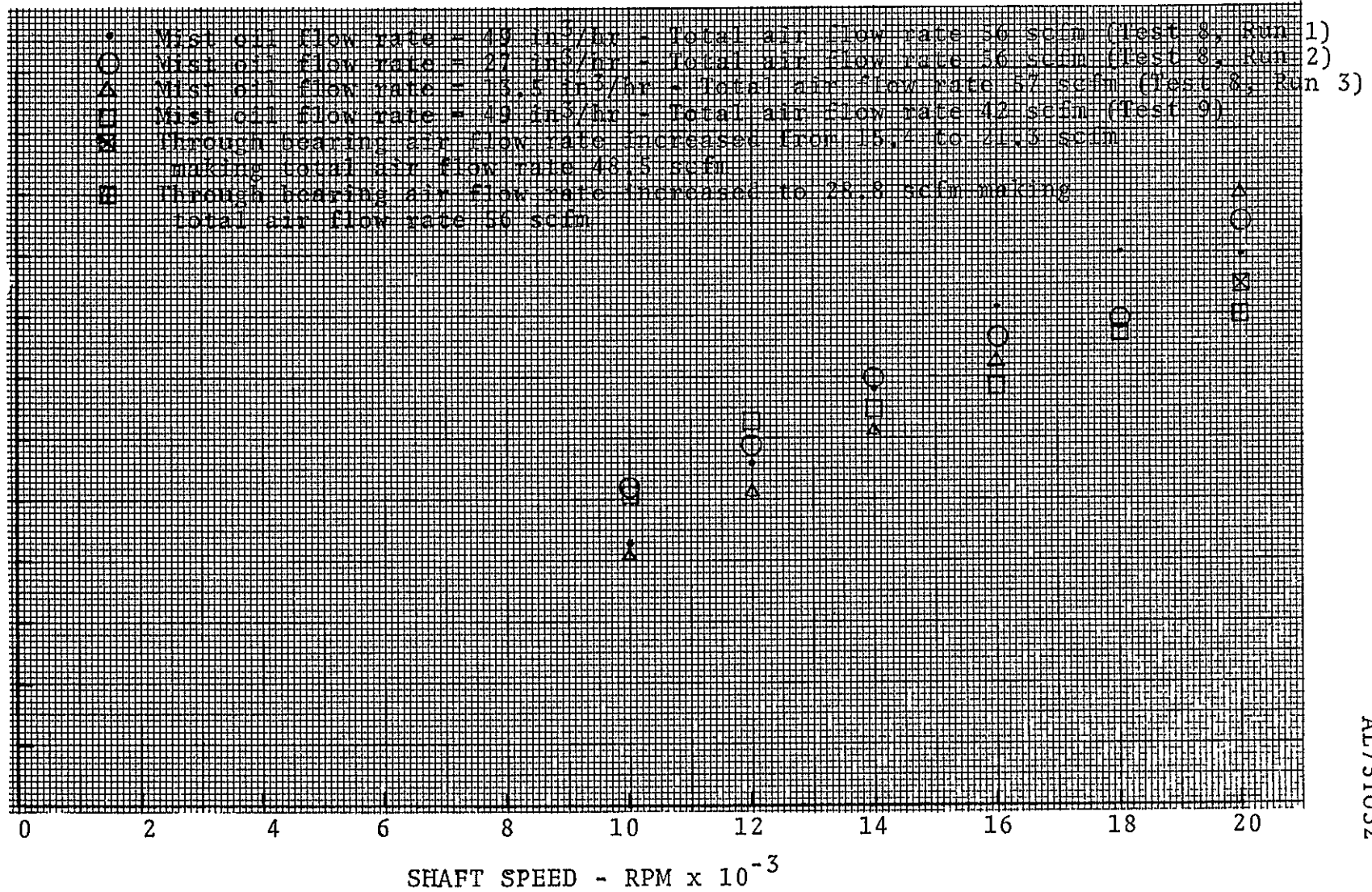
REPRODUCIBILITY OF THE  
ORIGINAL PAGE IS POOR

AL75T032

82

HEAT TRANSFERRED RATE - KW (Btu/Hr x  $10^{-3}$ )(12)  
3.22  
(10)  
2.64  
(8)  
2.05  
(6)  
1.46  
(4)  
0.89  
(2)  
0.29

FIGURE 26

HEAT TRANSFERRED TO MIST AND COOLING AIR WITH CHANGES IN THROUGH  
BEARING COOLING AIR AND MIST OIL FLOW RATE

AL75T032

TABLE XII  
Test No. - 9 (Decreased Cooling Air),  
Lubricant - XRL 850A+5% Kendall Resin Bearing S/N-18

Shaft Speed (rpm)	Brg. O.R. Temp. (°K-°F)	Brg. I.R. Temp. (°K-°F)	Mist Oil Flow Rate (cm <sup>3</sup> /hr.-in <sup>3</sup> /hr)	Through Brg. Flow Rate (Scmm-scfm)	Cooling Air In/Exhaust Temp. (°K-°F)
10,000	405-270	393-245	786-48	0.45-15.9	373/380-212/225
12,000	422-300	502-265	786-48	0.44-15.5	358/394-185/250
14,000	439-330	413-285	786-48	0.45-15.9	372/405-210/270
16,000	447-345	419-295	786-48	0.45-15.9	383/414-230/285
18,000	461-370	424-305	786-48	0.44-15.7	364/423-195/302
20,000	505-450	455-360	786-48	0.44-15.4	350/447-170/345
20,000	491-425	450-350	786-48	0.60-21.3	371/447-208/345
20,000	477-400	444-340	786-48	0.82-28.8	379/440-222/332
Shaft Speed (rpm)	Housing Cooling Air-Flow Rate (scmm-scfm)	In/Exhaust Temp. (°K-°F).	Mist Air Flow Rate (scmm-scfm)	In/Exhaust Temp. (°K-°F)	Total Air Flow Rate (scmm-scfm)
10,000	0.39-13.9	289/383 60/230	0.35-12.4	333/380 140/225	1.19 42.2
12,000	0.39-13.9	289/383 60/230	0.36-12.8	333/394 140/250	1.19 41.9
14,000	0.39-13.9	292/383 65/230	0.35-12.4	333/405 140/270	1.19 42.2
16,000	0.41-14.4	292/383 65/230	0.35-12.4	331/414 136/285	1.21 42.6
18,000	0.41 14.4	292/383 65/230	0.36-12.7	331/423 136/302	1.21 42.7
20,000	0.41-14.4	292/379 65/225	0.37-12.9	329/447 133/345	1.21 42.7
20,000	0.42-14.8	292/379 65/225	0.35-12.5	328/447 131/345	1.21 48.6
20,000	0.42-14.8	292/378 65/222	0.36-12.6	329/440 133/332	1.59 56.2
HEAT TRANSFER RATE					
Shaft Speed (rpm)	TBCA (Watts-Btu/hr)	HCA (Watts-Btu/hr)	Mist (Watts-Btu/hr)	Total (Watts-Btu/hr)	
10,000	60-205	747-2550	326-1114	1133-3869	
12,000	319-1090	747-2550	442-1510	1508-5150	
14,000	302-1030	725-2475	512-1750	1539-5255	
16,000	275-939	748-2554	586-2000	1608-5493	
18,000	530-1810	748-2554	665-2270	1943-6634	
20,000	864-2951	725-2477	864-2951	2454-8379	
20,000	847-2891	745-2544	847-2891	2438-8326	
20,000	791-2703	731-2496	792-2703	2314-7902	



A visual inspection of the test bearing following Tests 8 and 9 indicated that adequate lubrication was present and no over heating or thermal imbalance condition had occurred. No ball tracking had occurred in the bottom of either race and finish lines were still present in the ball tracks. The cage appeared similar to the pretest condition, see Figure 27. There was one accumulation of micropits in a 1/8 inch diameter spot at the edge of the ball track on the outer ring, essentially out of the most heavily traveled area. The exact cause of the micropits could not be determined. They did not appear to be the result of fatigue or lubrication distress, but rather seem to have been caused by some impact or shock load.

The results of Test 9 were encouraging from the stand point that even lower air flows than previously determined appeared to be adequate to cool the test bearing.

#### 6.2.10 Test No. 10, Standard Bearing

Two test runs were performed using a standard bearing S/N 22 (cage bore and inner ring not modified) with XRL850A plus 5% Kendall resin to determine if any difference in performance could be observed which would indicate the advantage (better distribution of the mist oil) provided by the modified bearing. The test was performed in the same manner with the same applied thrust load as all previous step-speed tests.

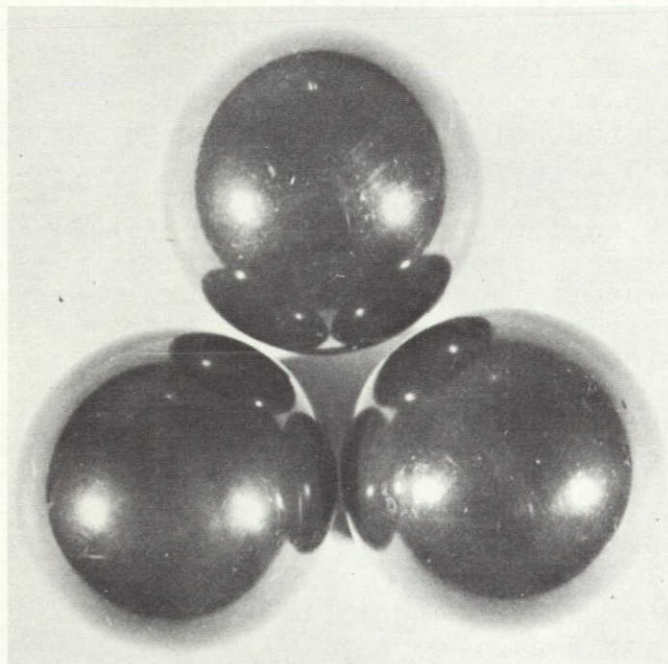
During the first run, it was noted that the bearing housing cooling air flow rate was appreciably greater for the same applied pressure and same inlet air temperature. This condition indicated a leak in the flow path around the housing; therefore, the test was terminated at 10,000 rpm since this condition could result in non-uniform cooling of the outer ring. Following disassembly it was established that a major leak was present between the air retaining ring and bearing housing at the air inlet location.

To remedy this problem, the O.D. of the housing was re-machined to obtain better roundness and a new retaining ring manufactured and assembled. The machining of the O.D. of the housing decreased the air flow path depth by approximately 25%.

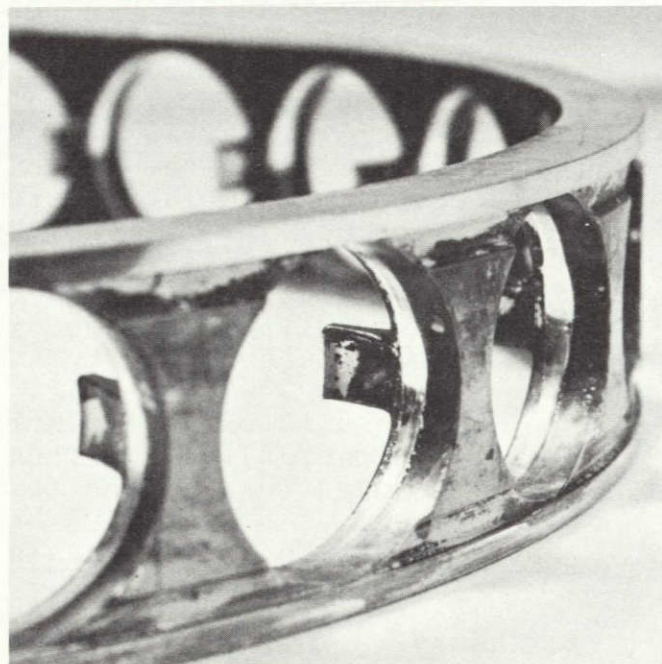
The second run was performed with the modified housing cooling air flow path. Although it was observed early in the test that only approximately one half the cooling air could be passed through the housing cooling air flow path, the decision was made to continue the test. This decision was based on the



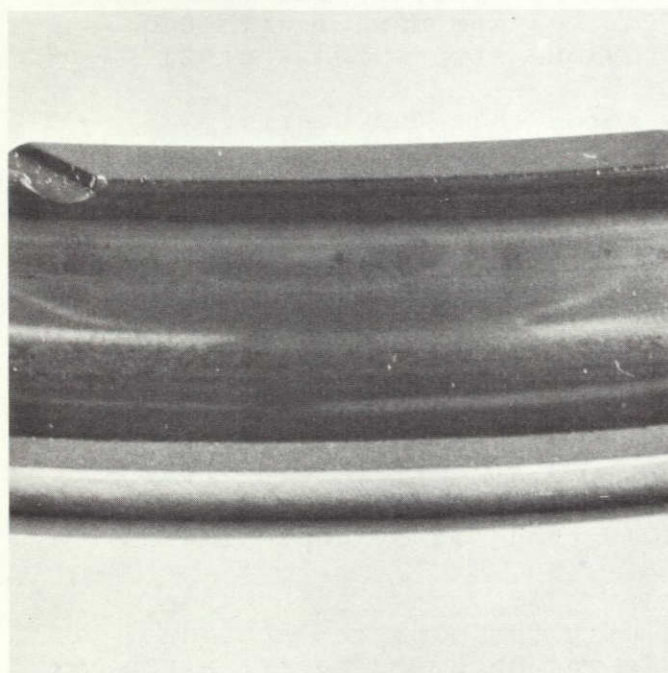
FIGURE 27  
TEST BEARING COMPONENTS AFTER TEST NO. 8 AND 9  
Step-Speed Mist System Test  
Low Viscosity Synthetic Paraffinic Hydrocarbon  
Fluid Plus 5% Heavy Paraffinic Resin  
Test 8 - Reduced Oil Flow Rate, Minimum Rate 221 cc/hr  
Test 9 - Reduced Air Flow Rate, Minimum Rate 1.2 scmm  
Bearing S/N 18



BALLS



CAGES



INNER RING LOADED HALF



OUTER RING



assumption that the air flow was constant around the complete flow path and the decreased air flow would result in a slightly high outer ring temperature which would not be detrimental to the bearing performance.

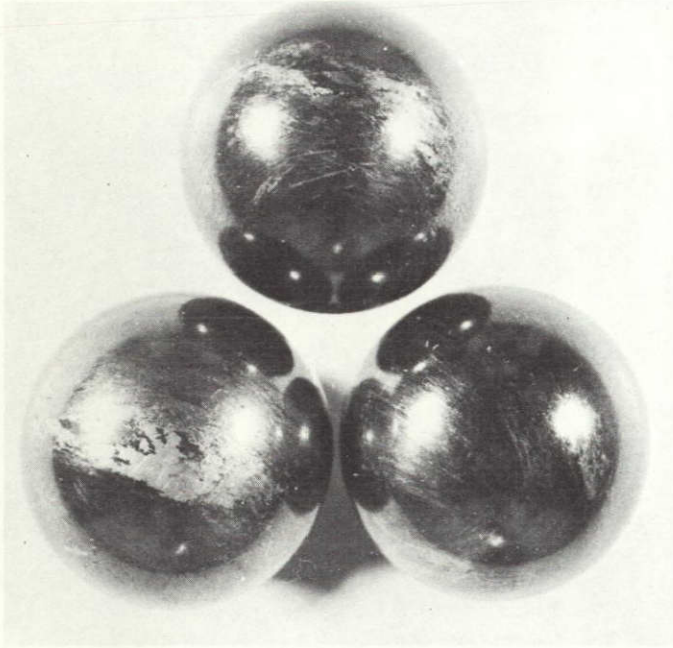
Applying essentially the same mist air and through bearing cooling air flow rates and the same mist oil flow rate as applied in Test 8, Run 1, the shaft was accelerated to 10,000 rpm and then increased in 2,000 rpm increments. It was noted during the recording of the stabilized temperatures that the outer ring was operating at approximately 30°F hotter than in Test 8, Run 1. This increase was not considered to be excessive. After operating at a shaft speed of 20,000 rpm for approximately 10 minutes the outer ring temperature increased rapidly from 511°K to 590°K (470°F to 600°F) in approximately 1 minute indicating a test bearing failure. The rig was turned off terminating the test. Post test inspection revealed that the failure resulted from extensive wear between the downstream cage rail and outer ring land. The races and ball were in relatively good condition. There were however, some wear material from the cage in the races and on some balls, see Figure 28.

The recorded test data and calculated heat transfer rates are presented in Table XIII and shown graphically in Figures 29 and 30 in conjunction with Test 8 values to permit direct comparison with a modified bearing run.

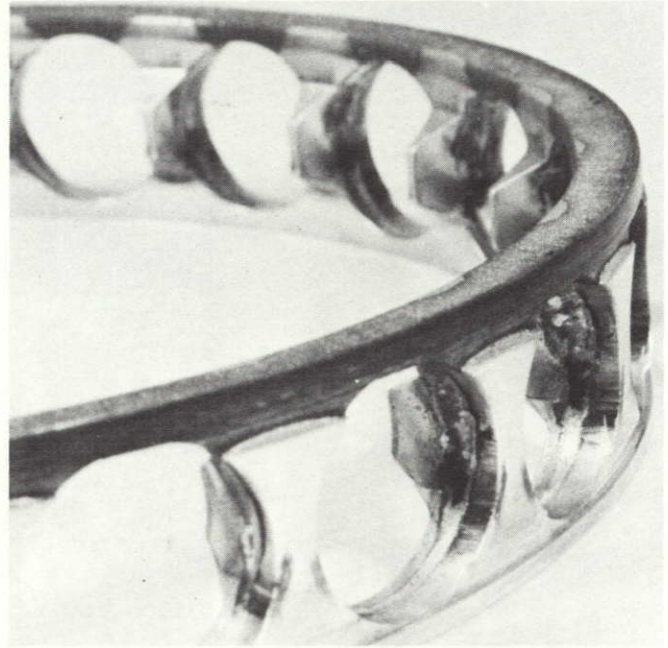
The outer ring temperature recorded during Test 10 average approximately 19°K (35°F) higher than those in Test 8. This condition is contributed to the decrease in the bearing housing cooling air flow rate and possible increased friction between the cage and land. It is also noted that the heat transfer rate to the cooling and mist air is not uniform with speed changes. Although this condition has been observed in prior tests, it was somewhat more drastic during this test which indicated erratic changes in the heat generation. This condition in combination with the excessive wear and failure at 20,000 rpm indicates that the lubrication and cooling of the cage-land contact surfaces on the downstream side which had been considered marginal (possibly the initial cause of failures in prior tests) was worse with the standard bearing.



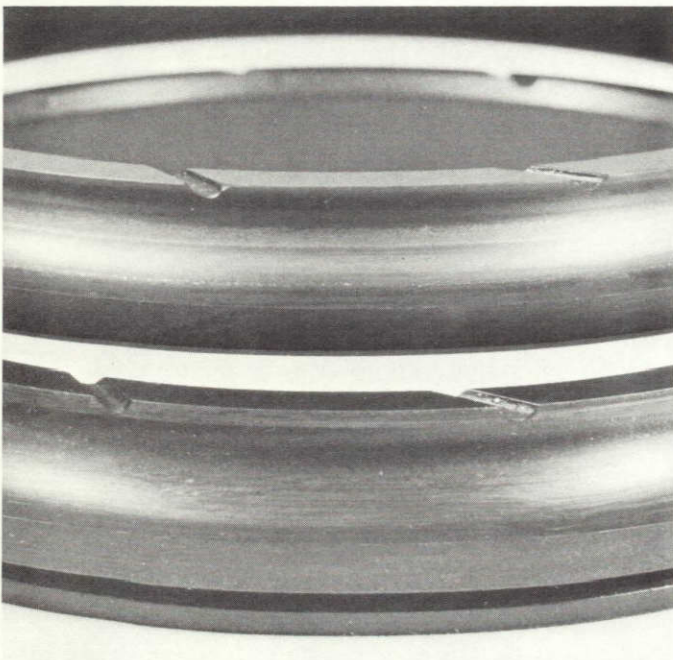
FIGURE 28  
 TEST BEARING COMPONENTS AFTER TEST NO. 10  
 Step-Speed Mist System Test-Standard Bearing  
 Low Viscosity Synthetic Paraffinic Hydrocarbon  
 Fluid Plus 5% Heavy Paraffinic Resin  
 Failure Occurred at 20,000 RPM-Bearing S/N 22



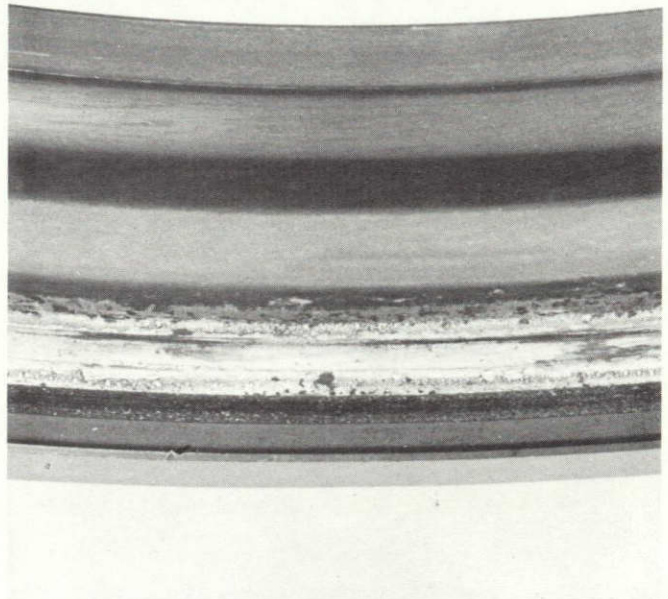
BALLS



CAGE



INNER RING, BOTH HALVES



OUTER RING

TABLE XIII  
Test No. - 10 (Std. Brg)

Lubricant - XRL850A+5% Kendall Resin Bearing S/N -22

Shaft Speed (rpm)	Brg. O.R. Temp. (°K-°F)	Brg. I.R. Temp. (°K-°F)	Mist Oil Flow Rate (cm3/hr-in3/hr)	Through Brg. Flow Rate (scmm-scfm)	Cooling Air In/Exhaust Temp. (°K-°F)
10,000	427-310	412-282	803-49	0.89-31.3	360/400-188/260
12,000	444-340	422-300	803-49	0.89-31.5	380/415-225/288
14,000	456-362	----	803-49	0.88-31.1	345/421-162/298
16,000	477-400	----	803-49	0.89-31.5	381/439-227/331
18,000	494-430	----	803-49	0.88-31.2	355/450-180/350
20,000	516-470	----	803-49	0.88-31.2	366/461-200/370

Shaft Speed (rpm)	Housing Cooling Air-Flow Rate (scmm-scfm)	In/Exhaust Temp. (°K - °F)	Mist Air Flow Rate (scmm-scfm)	In/Exhaust Temp. (°K - °F)	Total Air Flow Rate (scmm-scfm)
10,000	0.21-7.4	290/412-62/282	0.37-12.9	334/300-141/260	1.46-51.6
12,000	0.21-7.4	290/427-62/310	0.36-12.7	333/415-140/288	1.45-51.2
14,000	0.21-7.4	290/435-62/323	0.37-13.1	333/421-140/298	1.46-51.6
16,000	0.21-7.4	290/459-62/361	0.36-12.7	335/439-143/331	1.46-51.6
18,000	0.21-7.4	290/466-62/380	0.37-13.0	334/450-140/350	1.46-51.6
20,000	0.21-7.4	290/477-62/400	0.37-12.0	335/461-143/370	1.46-51.6

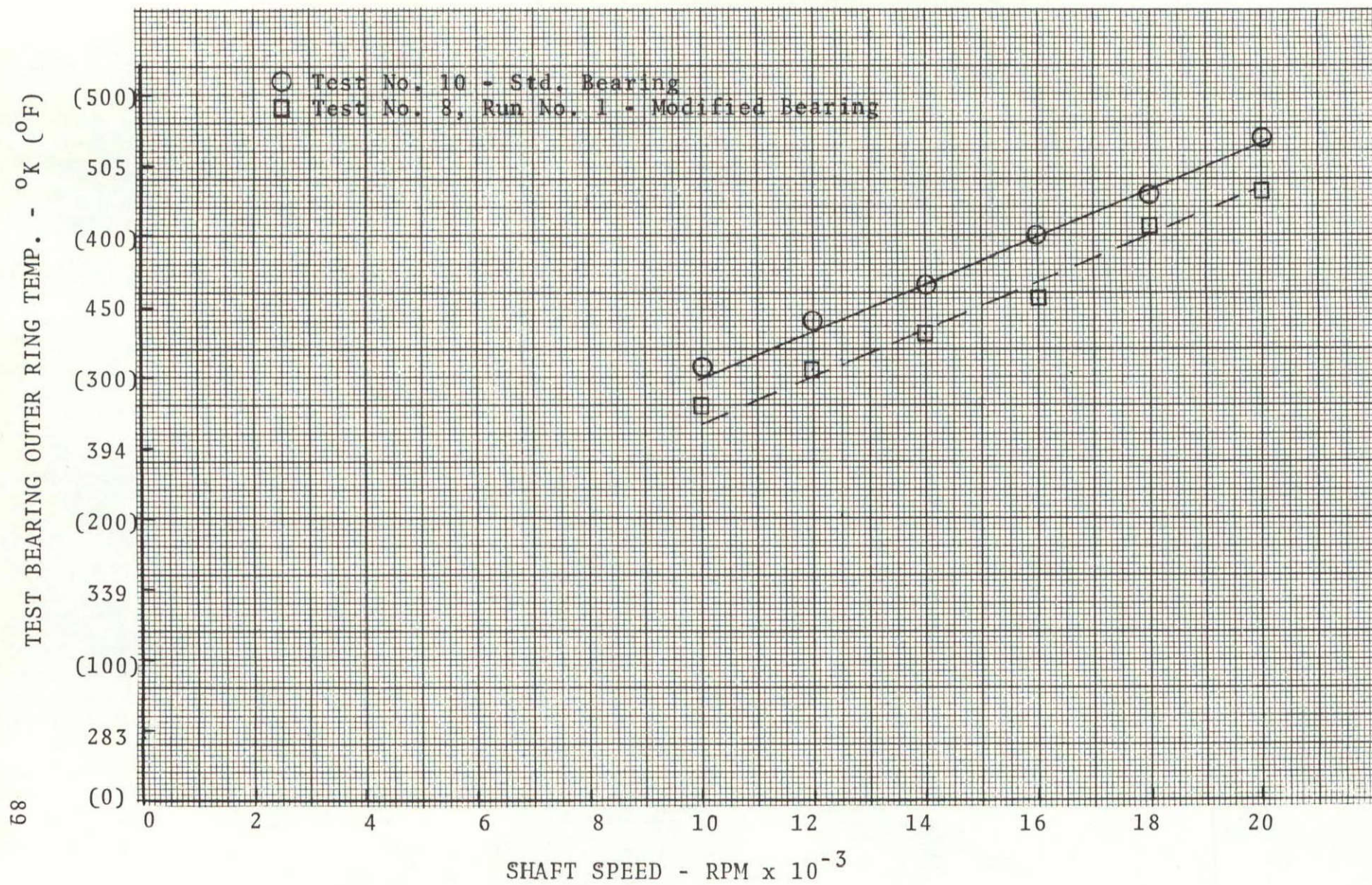
#### Heat Transfer Rate

Shaft Speed (rpm)	TBCA (Watts-Btu/hr)	HCA (Watts-Btu/hr)	Mist (Watts-Btu/hr)	Total (Watts-Btu/hr)
10,000	712-2433	513-1752	486-1659	1711-5844
12,000	628-2144	579-1976	608-2074	1814-6194
14,000	1328-4536	609-2080	680-2323	2618-8939
16,000	1036-3539	698-2382	753-2572	2487-8493
18,000	1672-5712	742-2535	856-2923	3271-11,170
20,000	1672-5712	785-2680	925-3160	3383-11,552



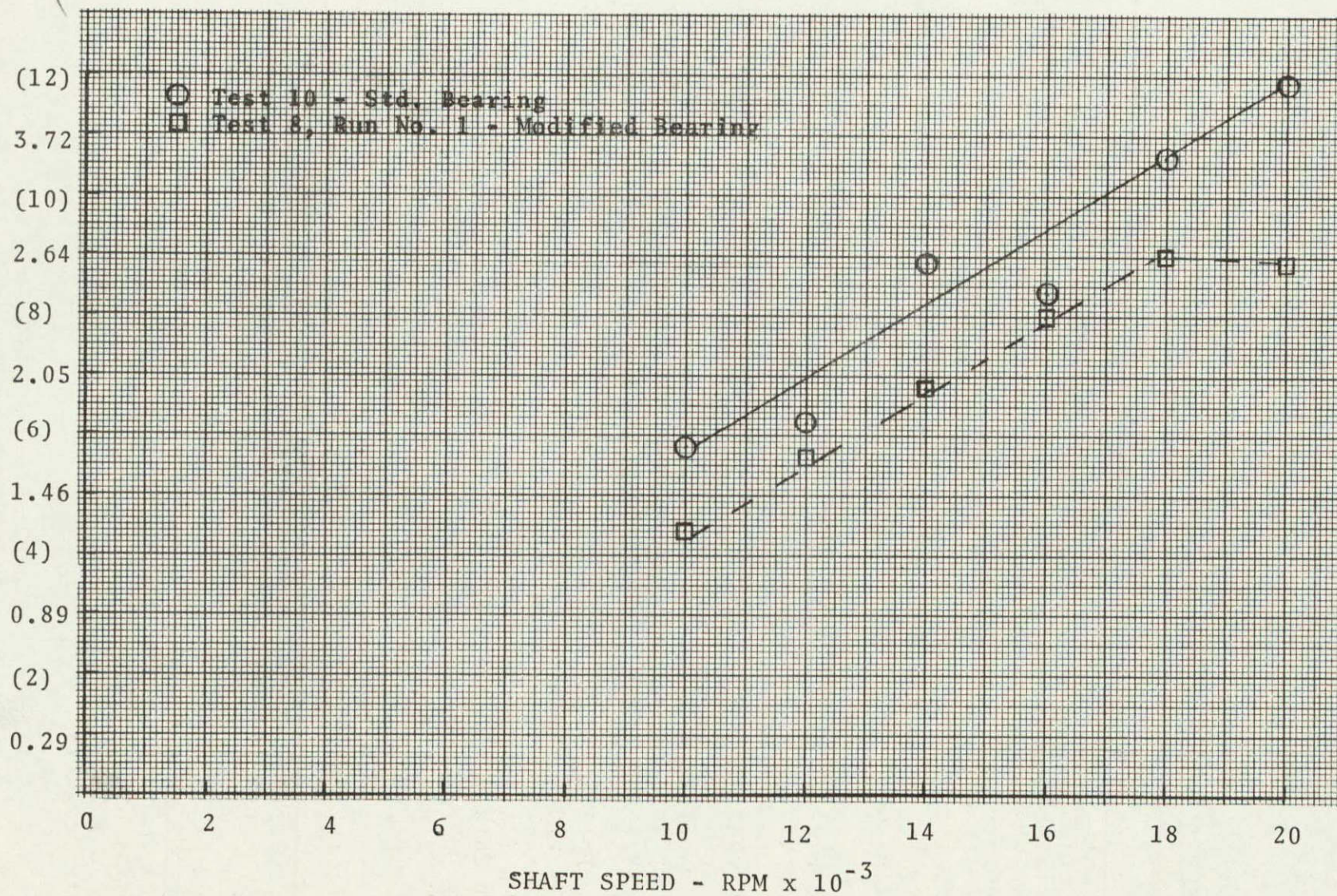
FIGURE 29

## TEST BEARING OUTER RING TEMPERATURE



AL75T032



HEAT TRANSFER RATE - KW ( $\text{Btu/hr} \times 10^{-3}$ )



### 6.2.11 Test No. 11, Increased Cooling Air Temperature

In prior tests the through-bearing cooling air and housing cooling air were supplied at temperatures of approximately 361°K (190°F) and 294°K (70°F) respectively with the mist air at 330°K (145°F). During this test both the through bearing and housing cooling air were supplied at a temperature of 422°K (300°F) to better simulate the compressor bleed air temperatures available in aircraft gas turbine engines. The mist air was supplied at the normal temperature of approximately 330°K (145°F) and the test performed similar to prior step-speed tests with an applied thrust load of 14,589 newtons. Test bearing S/N 15 used previously in Test 2 was used.

At a speed of 18,000 rpm the bearing outer-ring temperature had reached 533°K (500°F); therefore, the through-bearing cooling air was increased from 0.82 scmm (29 scfm) to 1.41 scmm (50 scfm). This increase produced a bearing outer-ring temperature drop of 5.5°K (10°F). The through-bearing cooling air flow was selected rather than the housing cooling air because it could effectively cool all elements of the bearing and thus result in less chance of developing a thermal imbalance condition within the bearing.

Following the increase in through-bearing cooling air the shaft speed was increased to 20,000 rpm and operated for approximately 20 minutes with the outer-ring temperature at 544°K (520°F) before manually terminating the test. The test data is presented in Table XIV. Test data showing the test bearing outer-ring temperatures and the bearing heat generation rates at the various speeds are presented in graph form in Figures 31 and 32 with baseline data obtained in Test 8, Run 1.

The two graphical presentations show that the bearing outer-ring temperature was approximately 55°K (100°F) higher than when the cooler cooling air was supplied and the bearing heat generation rate was approximately the same as that established during the baseline run. The 55°K increase in the bearing temperature approximated the average cooling air temperature increase of 64°K. The bearing temperature increase is considered to be quite reasonable since a consistent  $\Delta t$  between the bearing and cooling air was maintained in comparison with Test 8, Run 1 to remove approximately the same quantity of bearing generated heat.

The bearing inspection revealed that the ball tracks in the races were uniform and appeared similar to the pretest



TABLE XIV

Test No. - 11 (Increased Cooling Air Temperature)  
 Lubricant - XRL850A+5% Kendall Resin Bearing S/N - 15

Shaft Speed (rpm)	Brg. O.R. Temp. (°K-°F)	Brg. I.R. Temp. (°K-°F)	Mist Oil Flow Rate (cm <sup>3</sup> /hr-in <sup>3</sup> /hr)	Through Brg. Flow Rate (scmm-scfm)	Cooling Air In/Exhaust Temp. (°K-°F)
10,000	461-370	444-340	819-50	0.83-29.3	438/433-328/320
12,000	477-400	---	819-50	0.82-28.8	422/444-300/240
14,000	494-430	---	819-50	0.82-29.1	426/450 308/350
16,000	511-460	---	819-50	0.82-29.0	419/467-295/381
18,000	533-500	---	819-50	0.80-28.4	419/482-295/408
18,000	527-490	---	819-50	1.41-49.9	424/475-303/395
20,000	---	---	819-50	1.56-55.2	573/483-300/409
20,000	271-520	---	819-50	1.59-56.2	426/481-308/406

Shaft Speed (rpm)	Housing Cooling Air-Flow Rate (scmm-scfm)	In/Exhaust Temp. (°K - °F)	Mist Air Flow Rate (scmm-scfm)	In/Exhaust Temp. (°K - °F)	Total Air Flow Rate (scmm-scfm)
10,000	0.34-12.1	435/439-324/330	0.37-13.0	340/433-153/320	1.54-54.4
12,000	0.34-12.1	429/450-315/350	0.38-13.5	335/444-143/340	1.54-54.4
14,000	0.34-12.1	424/457-305/365	0.37-13.2	332/450-138/350	1.54-54.4
16,000	0.34-12.1	430/478-316/402	0.38-13.3	333/467-139/381	1.54-54.4
18,000	0.34-12.1	416/493-290/428	0.39-13.9	337/482-147/408	1.54-54.4
18,000	0.32-11.4	415/484-289/412	0.37-13.1	340/475-153/395	2.13-74.4
20,000	0.32-11.4	427/493-310/428	0.38-13.3	339/483-150/409	2.26-79.9
20,000	0.32-11.4	427/495-310/432	0.38-13.3	339/481-150/406	2.29-80.9

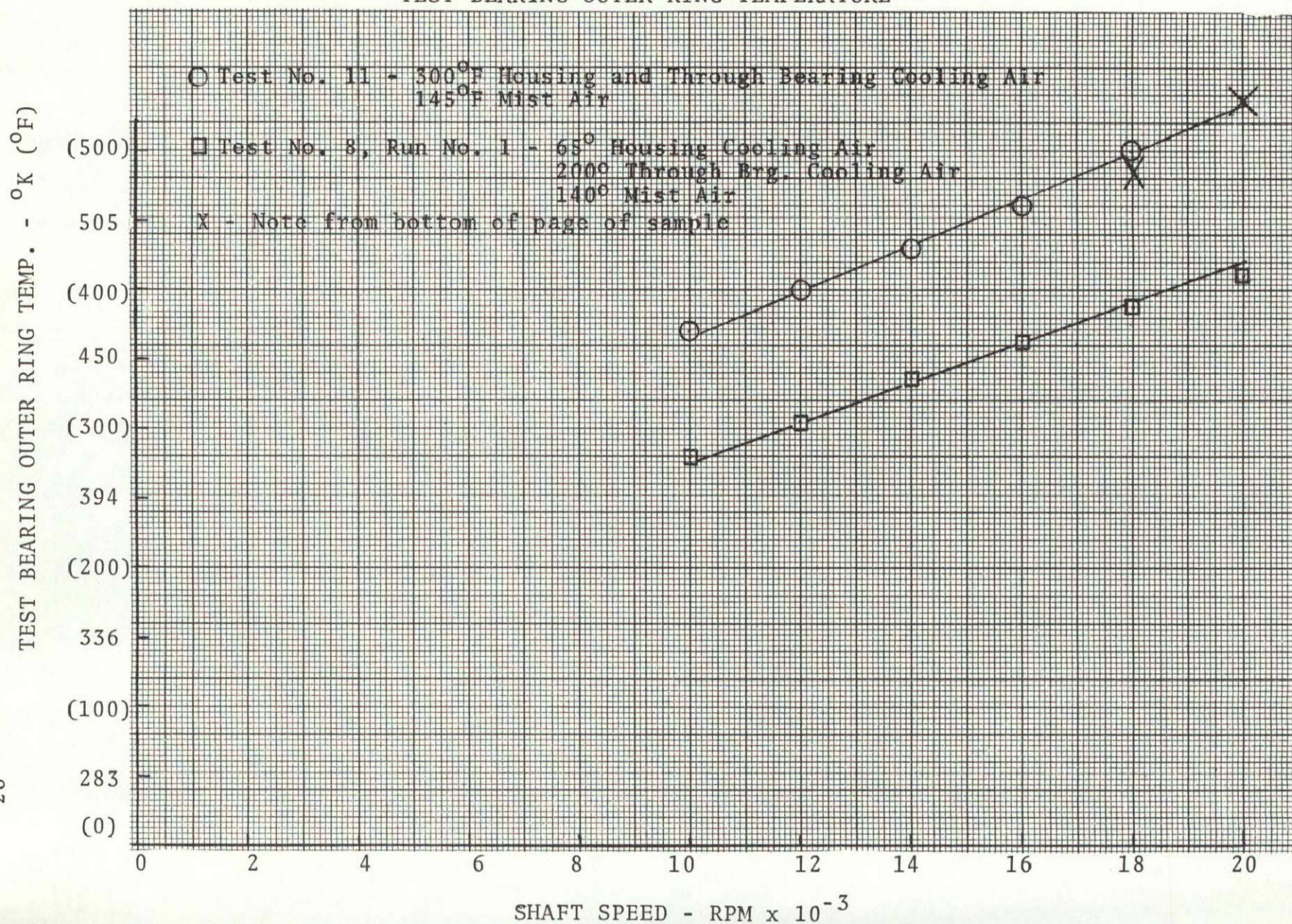
## Heat Transfer Rate

Shaft Speed (rpm)	TBCA (Watts-Btu/hr)	HCA (Watts-Btu/hr)	Mist (Watts-Btu/hr)	Total (Watts-Btu/hr)
10,000	(-74)-(-253)	17-78	687-2346	635-2171
12,000	364-1244	133-454	841-2872	1338-4570
14,000	386-1319	228-778	885-3022	1499-5119
16,000	789-2693	326-1114	1021-3486	2136-7293
18,000	1015-3466	524-1788	1156-3948	2695-9202
18,000	1458-4979	447-1527	1004-3427	2908-9933
20,000	1899-6487	425-1453	1089-3720	3414-11660
20,000	1742-5950	440-1502	1077-3677	3288-11229



FIGURE 31

## TEST BEARING OUTER RING TEMPERATURE

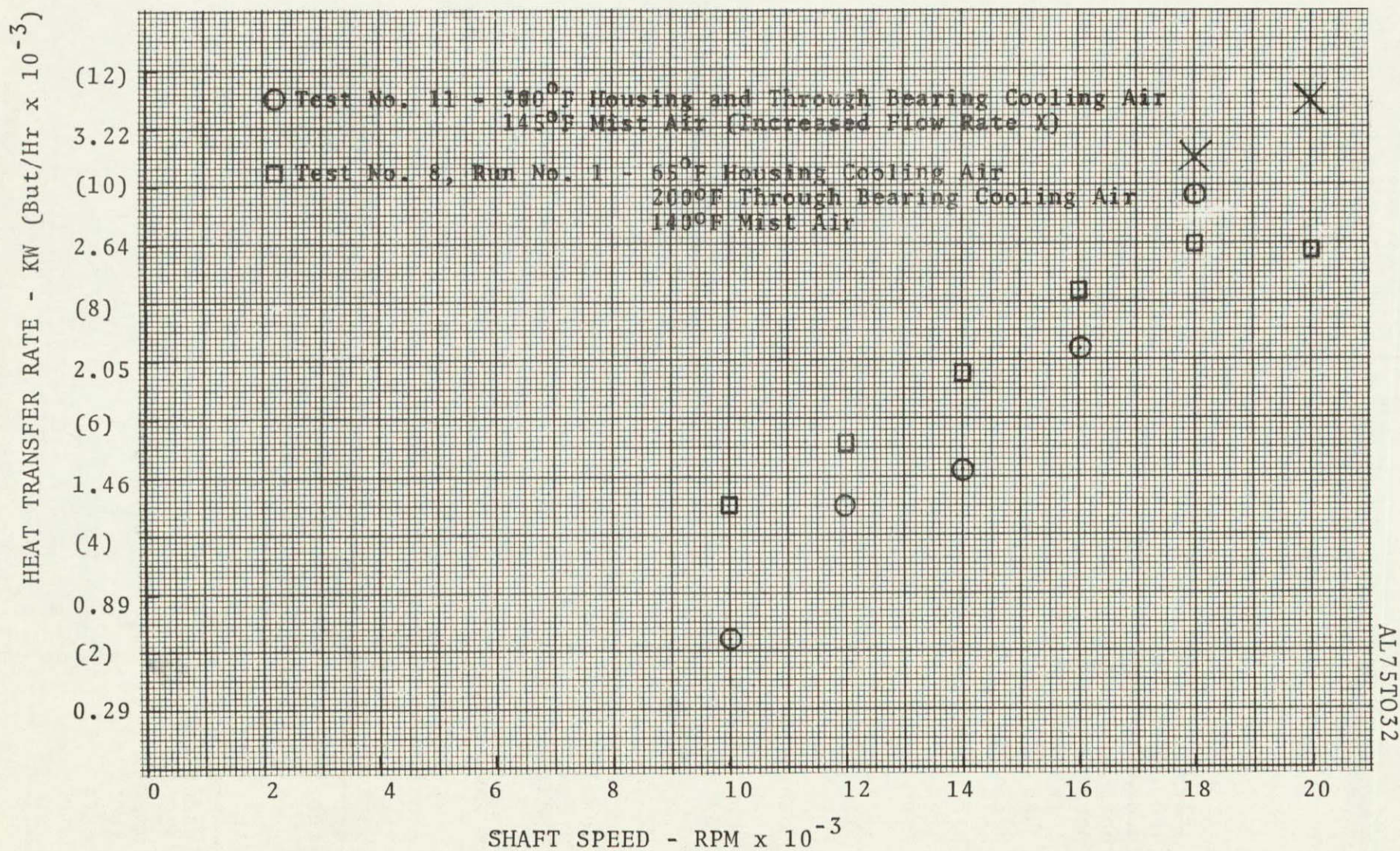


AL75T032



FIGURE 32

## HEAT TRANSFER RATE FROM TEST BEARING





condition with no indication of surface distress. Only a slight removal of the black oxide on the balls had occurred and the tracking marks present before the test were still present, see Figure 33. Polishing of the silver plating on both the upstream and downstream cage rails and the cage pockets had occurred. At no location was the silver plate worn through. The downstream rail was more heavily polished than the upstream rail with one section of approximately 120 degrees fully polished while the remaining arc was polished only at the cross bars where greater centrifugal growth takes place at the high velocities. At the most heavily polished area a thin layer of brown residue, appearing to be varnish from oil decomposition, was present.

In general the bearing was in good condition with no oil decomposition deposits present in the rig or on the bearing except as noted above. However, the polishing of the downstream cage rail indicated that the contact between the cage and land was not receiving adequate lubrication and a possible bearing failure may have resulted from this condition had the test period been extended.

The test results indicated that the increased cooling air temperature had no effects on the bearing operation except to increase the operating temperature. Therefore, it is considered feasible to mist lubricate and air cool a high speed gas turbine engine main shaft bearing when only high temperature air (up to 300°F) is available.

#### 6.2.12 Test No. 12, Under Race Mist Lubrication

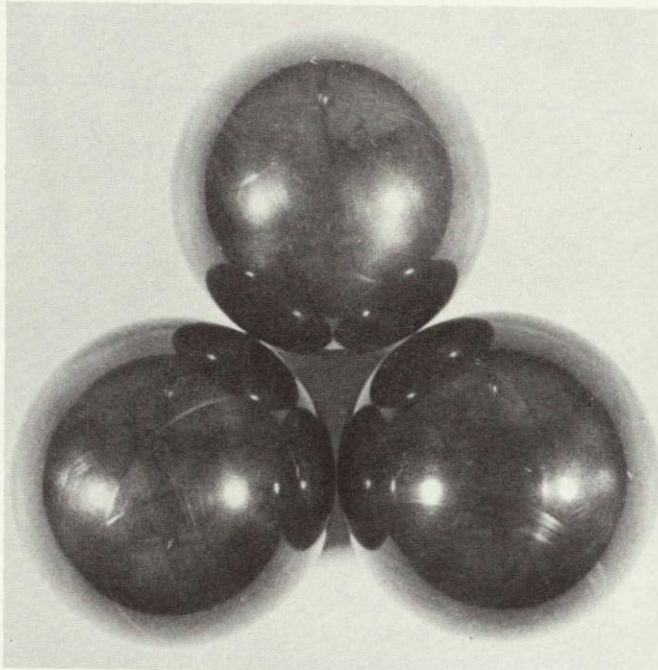
The purpose of this test was to determine the feasibility of supplying the mist delivered oil through the inner race of the test bearing. Through or under race lubricant supply in recirculating systems is extensively used by one of the major aircraft engine manufacturers and has proved to be very successful.

In preparation for this test, the rig was modified to supply the mist through eight reclassifying nozzles against a groove on the inside of the hollow rotating shaft and located directly under the test bearing. Twelve holes approximately 2.54 mm (.100 in.) in diameter were machined in the shaft, bearing mounting sleeve, and inner ring of the bearing. The nozzles located on the end of a stationary tube were inserted into the shaft and positioned to direct the mist radially and at a 45° angle to a tangent of the shaft bore in the direction of shaft

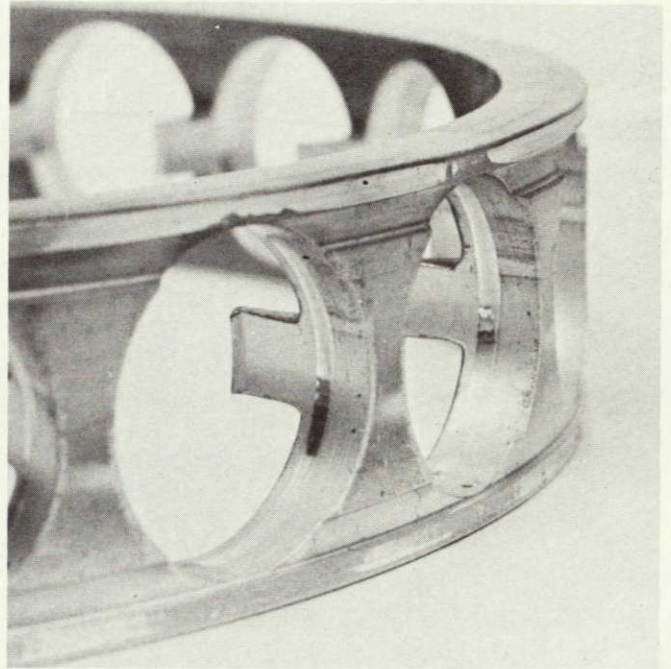


FIGURE 33

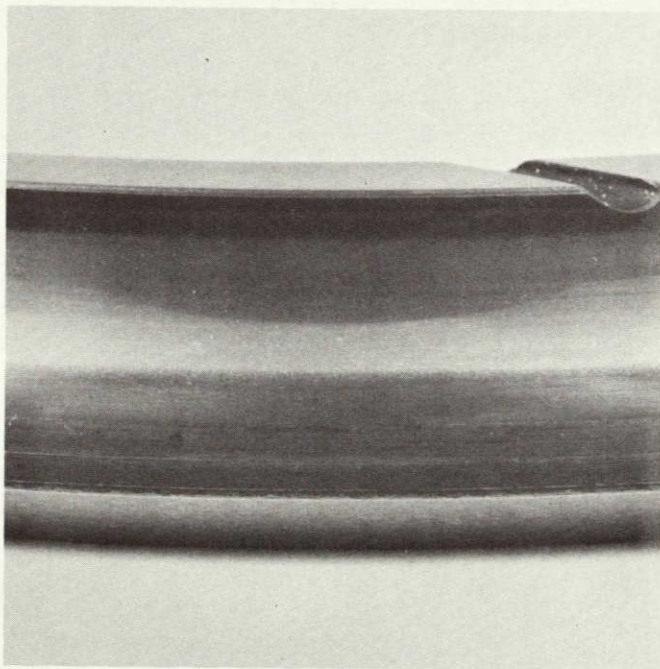
TEST BEARING COMPONENTS AFTER TEST NO. 11  
Step-Speed Mist Test - Increased Cooling Air Temperature  
Low Viscosity Synthetic Paraffinic Hydrocarbon  
Fluid Plus 5% Heavy Paraffinic Resin



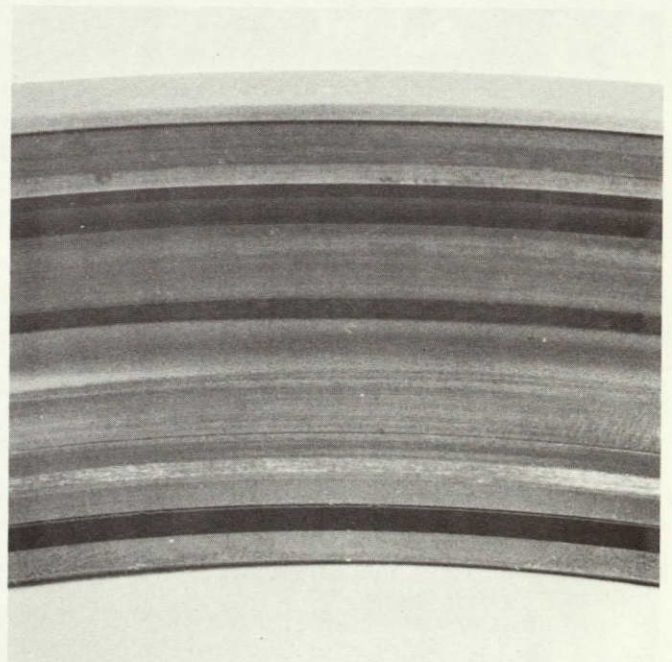
BALLS



CAGE



INNER RING LOADED HALF



OUTER RING



rotation. A layout drawing of the nozzle head and mounted bearing is presented in Figure 7.

It was anticipated that the oil carried in the mist would plate out in the shaft groove and be forced into the bearing by the centrifugal force generated by the rotating shaft. Prior to starting the shaft the mist was forced into the rig for 10 minutes to insure that the bearing was well wetted since the centrifugal force driving the oil would be at a minimum when rotation was initiated.

Due to the low density of the air carrying the mist, only a small portion was expected to be transferred through the holes into the bearing. For this reason, the through bearing cooling air was increased by an amount (approximately 0.36 scmm, 13 scfm) equal to the normal flow of mist air which during prior tests was passed through the bearing where it aided in cooling.

The test was performed similar to prior tests with a thrust load of 14,589 newtons applied to the test bearing S/N 15 used previously in Tests 2 and 11 and a mist oil supply rate of 819 cc/hr (50 in<sup>3</sup>/hr). The shaft was accelerated to 10,000 rpm and then in 2,000 rpm increments to higher speeds. The mist air, through-bearing cooling air, and housing cooling air was supplied at temperatures of approximately 350°K (170°F), 366°K (200°F) and 293°K (68°F), respectively.

The test bearing appeared to operate in a completely normal manner up to a speed of 20,000 rpm with no problems evident. After increasing the speed to 22,000 rpm and before temperatures had stabilized, the outer-ring temperature suddenly increased from 516°K (470°F) to approximately 644°K (700°F) before the rig could be shut off.

The test data are presented in Table XV. Graphical presentation of the test bearing outer ring temperatures and calculated heat transfer rates at the various operating speeds are presented in Figures 34 and 35 respectively along with that recorded in the baseline test (Test 8, Run 1). In calculating the heat generation rate it was assumed that no heat was removed by the mist air. No attempt was made to measure the exhaust mist air temperature since the mass of the mist air passing through either of two possible paths could not be determined.



TABLE XV

Test No. - 12

Lubricant - XRL850A+5% Kendall Resin Bearing S/N - 15

Shaft Speed (rpm)	Brg. O. R. Temp. (°K-°F)	Brg. I.R. Temp. (°K-°F)	Mist Oil Flow Rate (cm <sup>3</sup> /hr-in <sup>3</sup> /hr)	Through Brg. Flow Rate (smcc-scfm)	Cooling Air In/Exhaust Temp. (°K-°F)
10,000	422-300	366-200	819-50	1.16-40.9	377/396-220/255
12,000	439-330	377-220	819-50	1.16-40.9	372/411-210/280
14,000	450-350	383-230	819-50	1.17-41.3	380/424-225/303
16,000	461-370	389-240	819-50	1.16-40.8	363/428-185/312
18,000	483-410	400-260	819-50	1.17-41.3	375/442-215/337
20,000	505-450	408-275	819-50	1.17-41.4	369/463-205/373

Shaft Speed (rpm)	Housing Cooling Air - Flow Rate (scmm-scfm)	In/Exhaust Temp. (°K-°F)	Mist Air Flow Rate scmm-scfm	In/Exhaust Temp. (°K-°F)	Total Air Flow Rate (scmm-scfm)
10,000	0.33-11.8	289/391-60/245	0.38-13.6*	Temperature not measured since flow through different flow paths not known	1.49-52.7**
12,000	0.33-11.5	289/406-60/272	0.38-13.6		1.48-52.4
14,000	0.32-11.2	290/416-65/290	0.37-13.2		1.48-52.5
16,000	0.36-12.8	293/426-68/307	0.39-13.7		1.52-53.6
18,000	0.35-12.5	293/439-68/330	0.37-13.2		1.52-53.8
20,000	0.34-12.1	293/461-68/370	0.37-13.1		1.51-53.5

## Heat Transfer Rate

Shaft Speed (rpm)	TBCA (Watts-Btu/hr)	HCA (Watts-Btu/hr)	Mist (Watts-Btu/hr)	Total (Watts-Btu/hr)
10,000	1545	2278	Heat Transferred to mist air not established since flow rate into bearing and that through shaft could not be determined	3823***
12,000	3091	2636		5727
14,000	3437	2731		6158
16,000	5607	3304		8911
18,000	5446	3540		8985
20,000	7499	3950		11,449

\* - Mist air carried oil to shaft I.D. where a portion passed radially through shaft and a portion passed axially out of shaft.

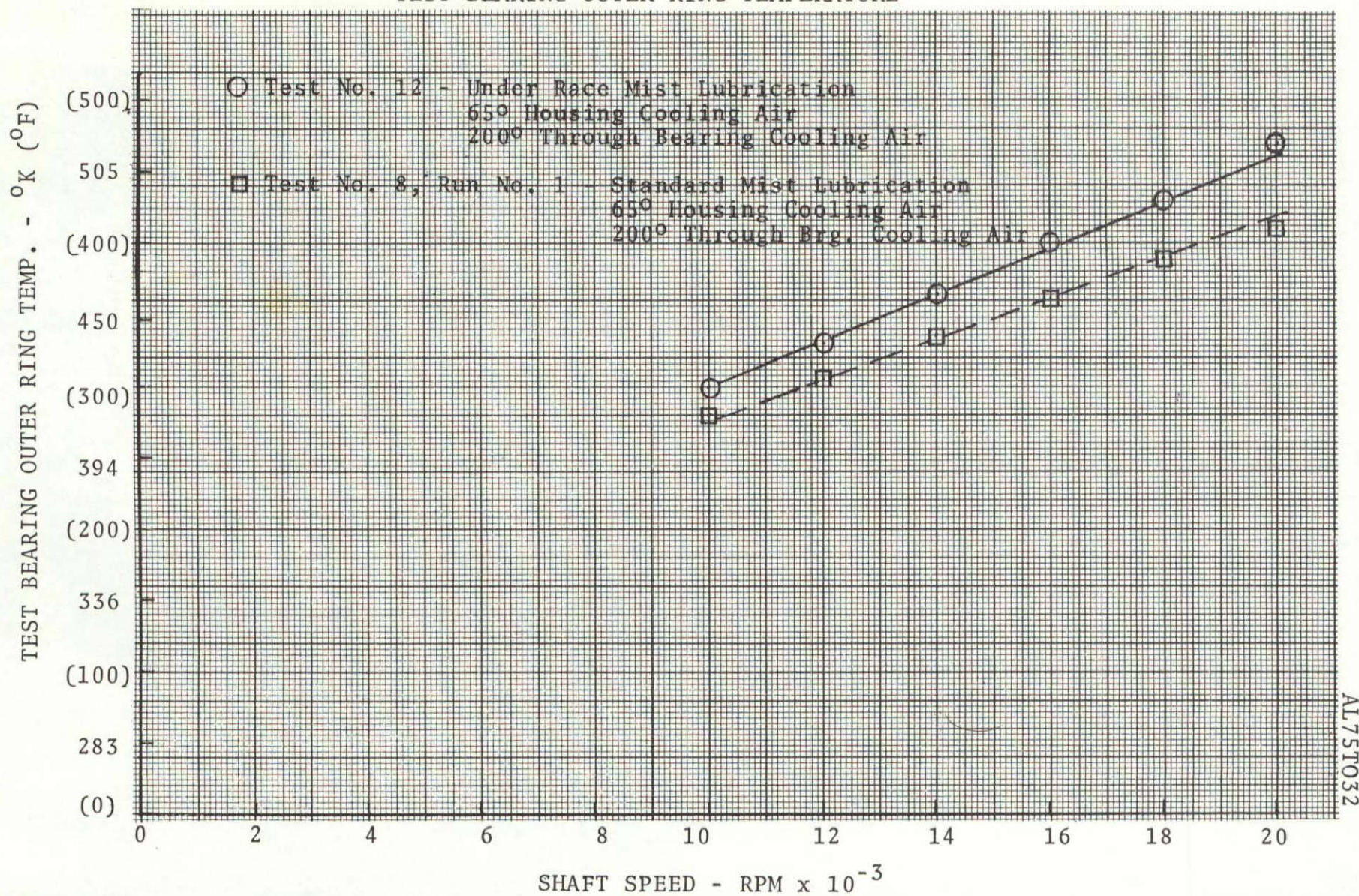
\*\* - Cooling air flow only. Does not include mist air flow

\*\*\* - Heat transferred to cooling air only.



FIGURE 34

## TEST BEARING OUTER RING TEMPERATURE



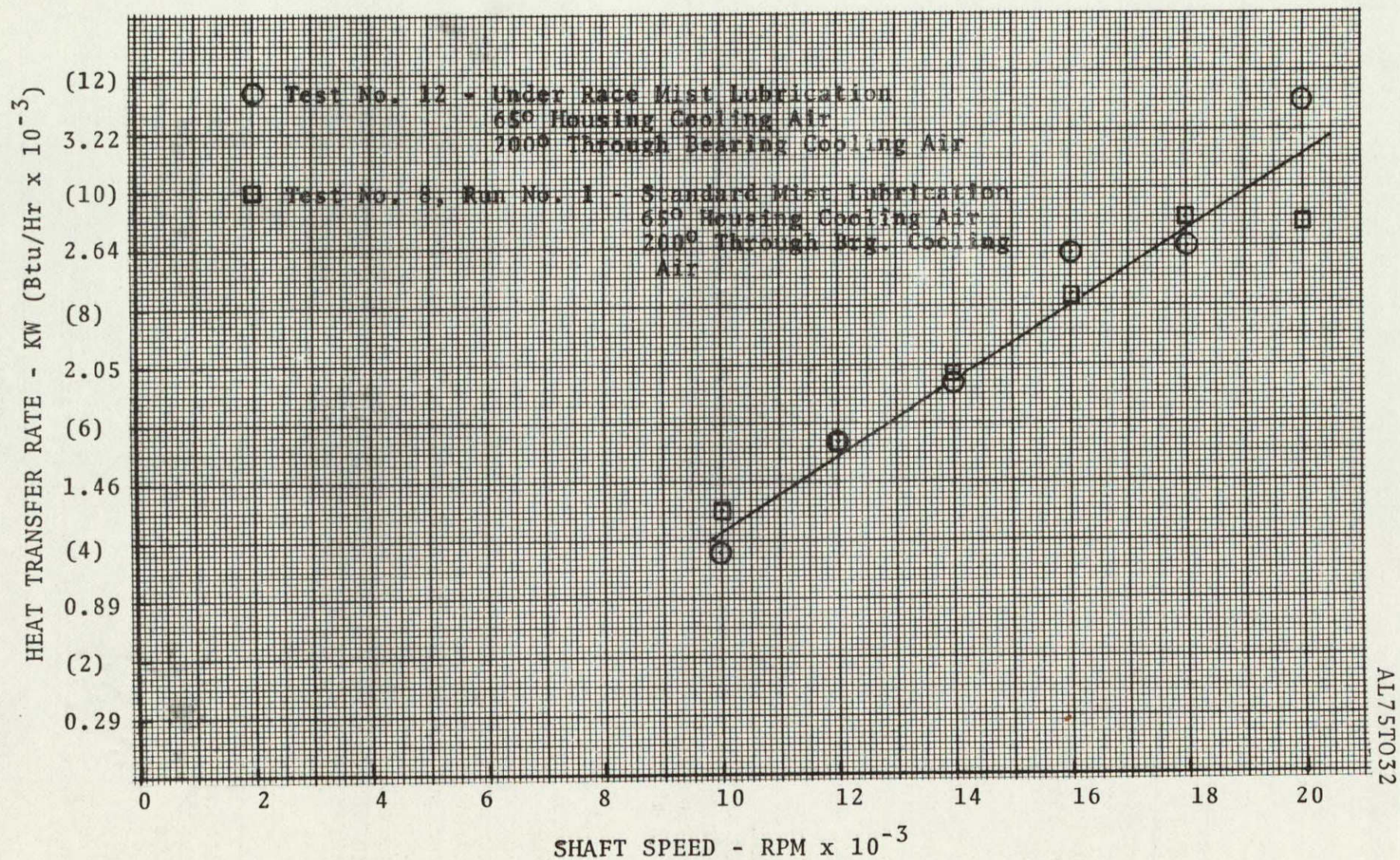
AL75T032



1001

FIGURE 35

## HEAT TRANSFER RATE TO MIST AND COOLING AIR



AL75T032



The graph shows that the bearing heat generation rate was similar to that occurring in Test 8, Run 1. Therefore, the assumption that little heat was removed by the mist air seems reasonable. The bearing outer-ring temperature ran approximately  $11^{\circ}\text{K}$  ( $20^{\circ}\text{F}$ ) warmer than in Test 8. This is assumed to have resulted from the average air temperature passing through the bearing being warmer. Through bearing cooling at  $366^{\circ}\text{K}$  ( $200^{\circ}\text{F}$ ) replaced the mist air normally at  $233^{\circ}\text{K}$  ( $140^{\circ}\text{F}$ ).

Inspection of the test bearing revealed that a thermal imbalance failure had occurred resulting in gross smearing of the races and balls, see Figure 36. Further evaluation indicated that the failure was probably initiated by excessive friction between the downstream cage rail and the outer ring cage riding land. This was concluded due to the heavy wear and smearing at this location and the wear pattern in the ball pockets. The ball pockets showed heavy wear on the leading face and a build up of race material on the trailing face. This condition indicates that the balls were trying to drive the cage which was resisting rotation due to the high friction between the cage rail and land. There was only slight polishing of the silver plating on the upstream cage rail where the mist is directly supplied.

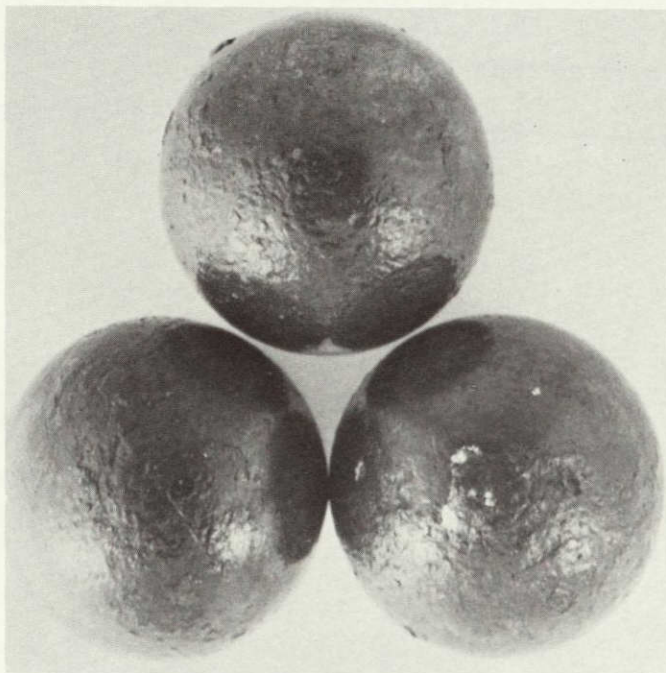
Although a bearing failure occurred at 22,000 rpm, the under race method of supplying the mist oil appeared to be essentially as effective as the through bearing method when an oil flow rate of 817 cc/hr is supplied. There are however, undesirable characteristics with the under race method which would dictate preference of the through bearing approach if either method could be applied. These include: 1) increased quantity of cooling gas required since the mist air is not as effective in cooling as when directed through the bearing, 2) greater possibility for losing oil and 3) possibility of oil passages in shaft plugging with oil decomposition products during an extended period of operation.

#### 6.2.13 Test No. 13, Tangential Cooling Air

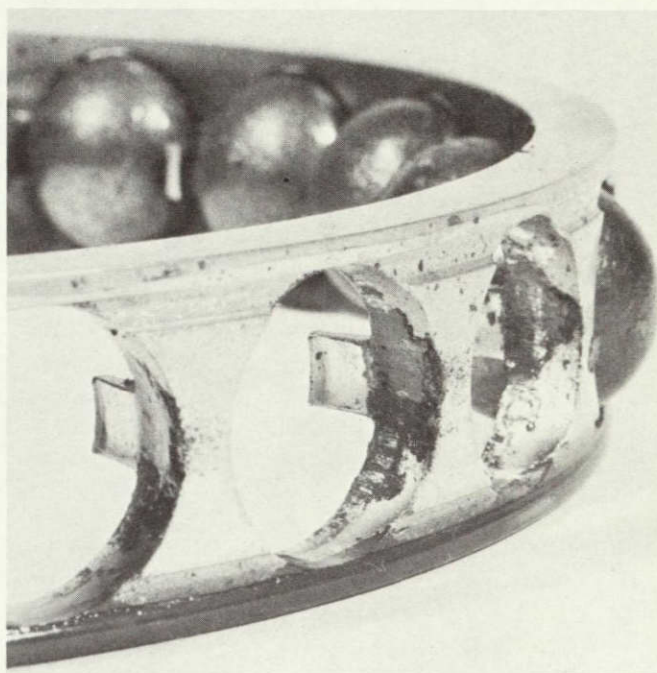
The purpose of this test was to determine if more efficient cooling could be obtained by directing the through bearing cooling air at an angle less perpendicular to the bearing face than in the initially conceived approach where the through bearing cooling air was directed in line with the bearing axis. The idea was to prevent stagnation of the cooling air due to direct impingement on the bearing face and thus minimize the amount of recovered heat which results from converting the



FIGURE 36  
 TEST BEARING COMPONENTS AFTER TEST NO. 12  
 Step-Speed Under Race Mist Lubrication Test  
 Low Viscosity Synthetic Paraffinic Hydrocarbon  
 Fluid Plus 5% Heavy Paraffinic Resin  
 Failure Occurred at 22,000 RPM-Bearing S/N 15



BALLS



CAGE



INNER RING BOTH HALVES



OUTER RING



kinetic energy gained by the air passing through the supply nozzles back into thermal energy. This would thus produce a greater heat transfer potential ( $\Delta t$ ) between the air and bearing. This in turn would reduce the bearing temperature for the same air flow rate or require less air to maintain the same bearing temperature.

Prior to the test the standard cooling air nozzles were plugged and ten additional nozzles assembled in the manifold. The nozzle exit posts were positioned 60 degrees with respect to the bearing axis and 16 degrees with respect to a tangent to the nozzle circle to permit the cooling air to pass half way through the bearing before intersecting the mist flow stream, see Figure 37.

The rig was assembled with a new test bearing, S/N 27, and the test performed in the same manner as the baseline test (Test 8, Run 1) but with approximately 0.17 scmm (6 scfm) less mist and through bearing cooling air (13 percent), which was approximately 11°K (20°F) warmer at the rig entrance. The housing cooling air supply rate was also approximately 0.05 scmm (25 scfm) or 15 percent less and 8°K (15°F) warmer. The bearing performed in a normal manner up to a speed of 20,000 rpm where a bearing failure occurred before temperature stabilization. The test data are presented in Table XVI.

The graph in Figure 38 shows that approximately the same quantity of bearing generated heat was transferred to the mist and cooling air for both 90 degree and 30 degree impingement at the various test speeds. Figure 39 shows that the outer ring temperature was also approximately the same, an average of 4°K (7.2°F) higher for the 30 degree impingement. Considering the differences in the mist and cooling air flow rates and temperatures the test results indicate that some advantage resulted from changing the initial direction of the through bearing cooling air. However, the difference noted is well within the margin of variability which could be expected from test to test.

Inspection of the test bearing showed that the failure was similar to that in Test 12 as shown in Fig. 40. A thermal imbalance failure had occurred. The failure appeared to have been initiated by excessive friction between the cage downstream rail and outer ring land. This indicated that poor lubrication existed in this area which had been noted in several earlier tests.



FIGURE 37

MIST AND COOLING AIR MANIFOLD WITH MODIFIED AIR NOZZLES

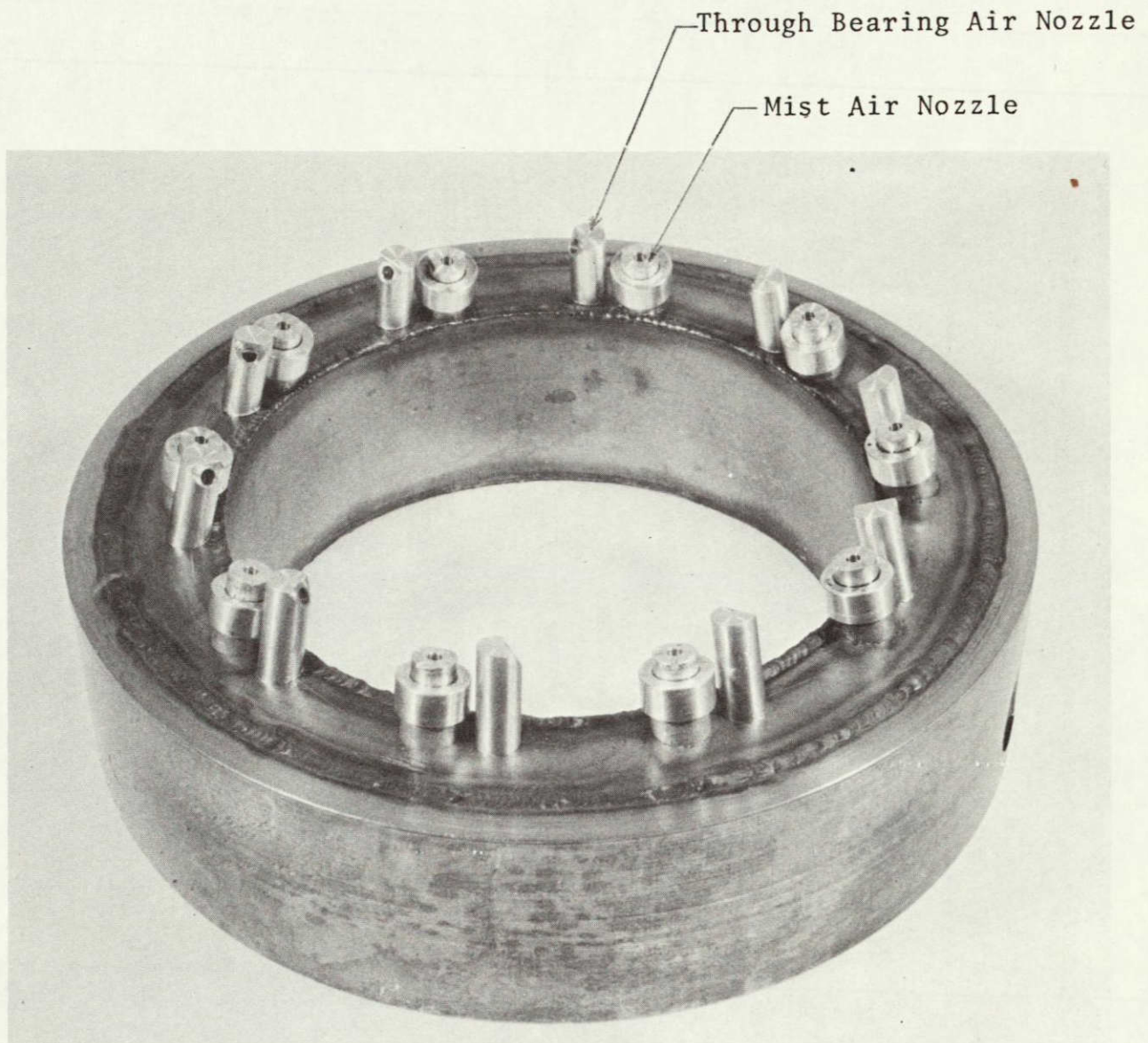


TABLE XVI  
Test No. - 13 (Tangential Cooling Air)  
Lubricant - XRL850A+5% Kendall Resin Bearing S/N - 27

Shaft Speed (rpm)	Brg. O.R. Temp. (°K-°F)	Brg. I.R. Temp. (°K-°F)	Mist Oil Flow Rate (cm3/hr-in3/hr)	Through Brg. Flow Rate (scmm-scfm)	Cooling Air In/Exhaust Temp. (°K-°F)
10,000	416-290	---	803-49	0.69-24.3	395/405-252/270
12,000	430-315	Slip-Ring Failure	803-49	0.70-24.9	382/419-228/295
14,000	444-340	---	803-49	0.69-24.3	372/430-211/315
16,000	458-365	---	803-49	0.65-23.0	372/441-210/335
18,000	474-395	---	803-49	0.67-24.0	376/452-218/355

Shaft Speed (rpm)	Housing Cooling Air - Flow Rate (scmm-scfm)	In/Exhaust Temp. (°K-°F)	Mist Air Flow Rate (scmm-scfm)	In/Exhaust Temp. (°K-°F)	Total Air Flow Rate (scmm-scfm)
10,000	0.33-11.7	299/391-78/245	0.35-12.5	343/405-158/270	1.37-48.4
12,000	0.32-11.4	300/405-81/270	0.33-11.8	343/419-158/295	1.36-48.1
14,000	0.31-11.0	301/420-82/297	0.35-12.5	341/430-155/315	1/35-47.7
16,000	0.31-11.0	301/430-82/315	0.39-13.7	341/441-153/335	1.35-47.7
18,000	0.31-11.0	301/444-82/340	0.36-12.8	339/452-150/355	1.35-47.7

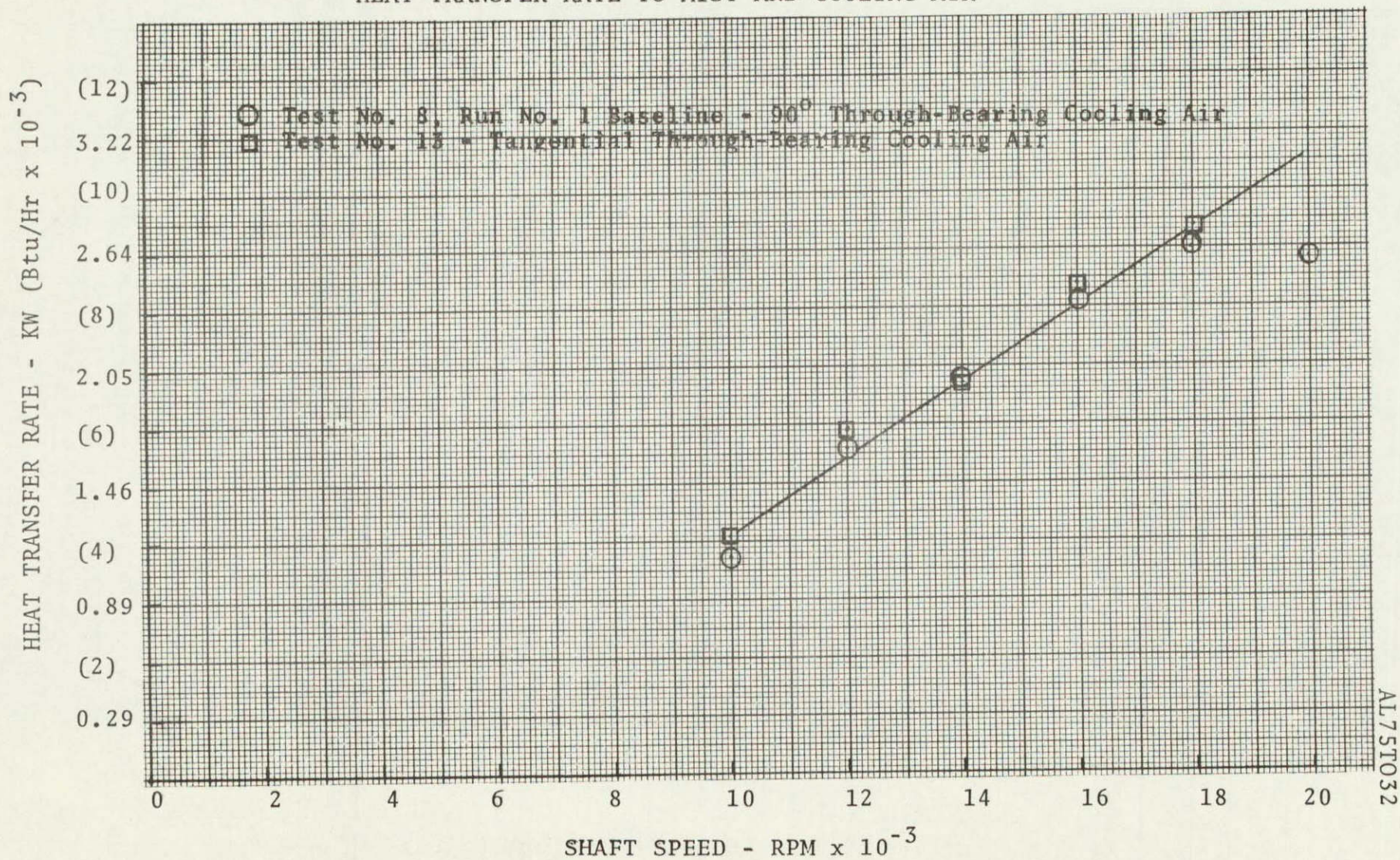
Heat Transfer Rate

Shaft Speed (rpm)	TBCA (Watts-Btu/hr)	HCA (Watts-Btu/hr)	Mist (Watts-Btu/hr)	Total (Watts-Btu/hr)
10,000	138-471	617-2108	439-1498	1194-4077
12,000	535-1828	679-2319	511-1746	1726-5893
14,000	798-2727	721-2461	630-2150	2149-7338
16,000	909-3105	781-2667	790-2698	2480-8470
18,000	1038-3544	865-2954	832-2841	2735-9339



FIGURE 38

## HEAT TRANSFER RATE TO MIST AND COOLING AIR

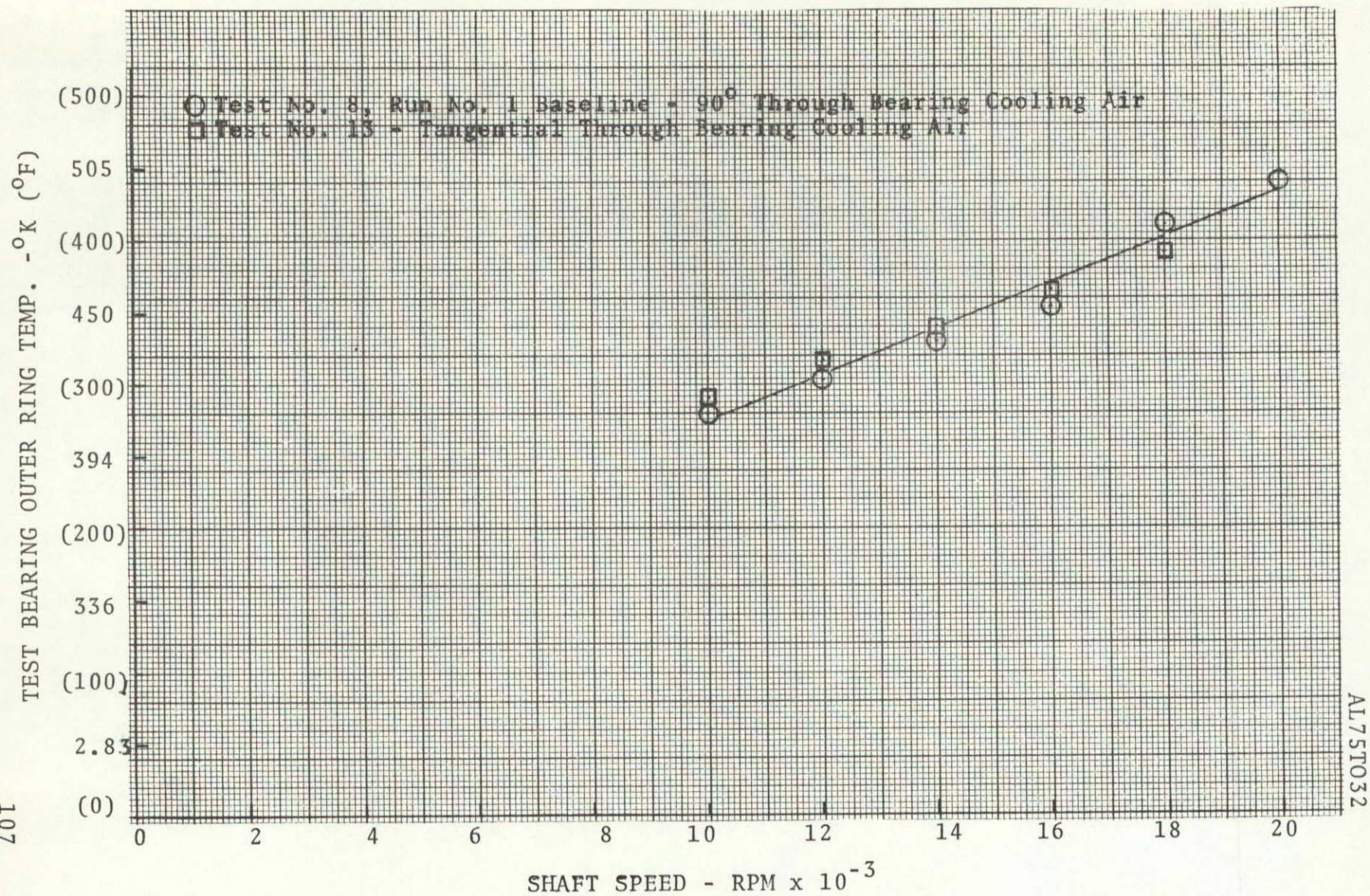


AL75T032



FIGURE 39

## TEST BEARING OUTER RING TEMPERATURE

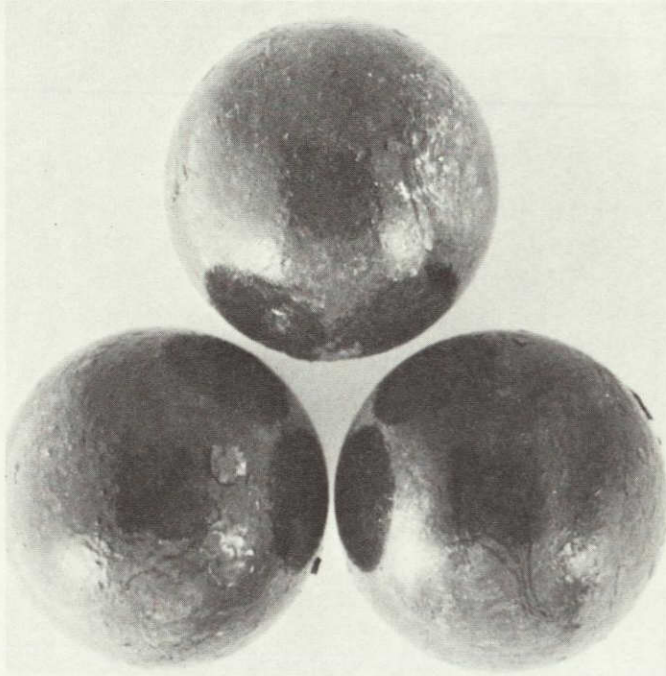


AL75T032

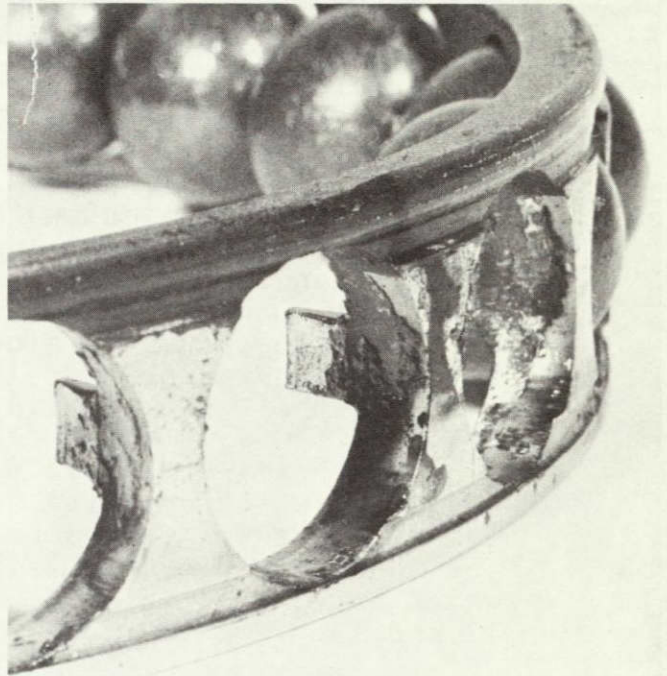
REPRODUCIBILITY OF THE  
ORIGINAL PAGE IS POOR



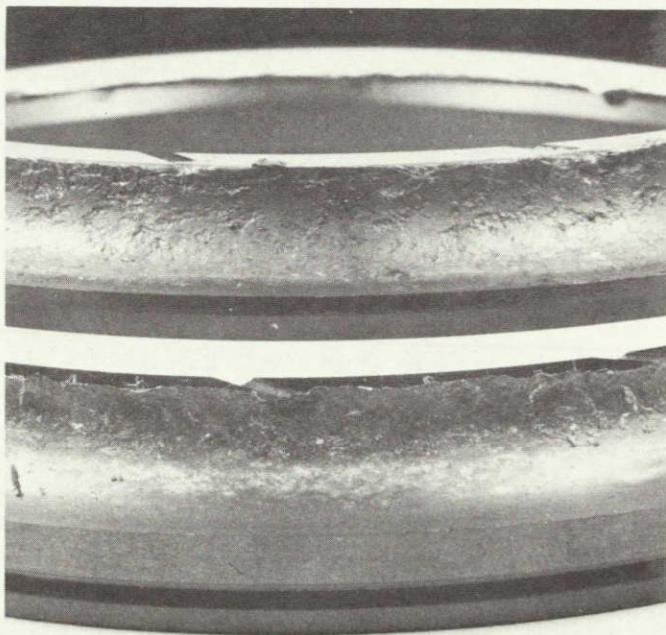
FIGURE 40  
 TEST BEARING COMPONENTS AFTER TEST NO. 13  
 Step-Speed Mist Test-Tangential Cooling Air  
 Low Viscosity Synthetic Paraffinic Hydrocarbon  
 Fluid Plus 5% Heavy Paraffinic Resin  
 Failure Occurred at 20,000 RPM-Bearing S/N 27



BALLS



CAGE



INNER RING, BOTH HALVES



OUTER RING



#### 6.2.14 Test No. 14, Extended Period Test

This test was the third attempt to obtain fifty hours of operation at 20,000 rpm. The rig was reverted to its initial configuration and a new test bearing S/N 27 assembled into the rig. The test was performed in the same manner as prior extended period tests. The test bearing failed during the first run at a speed of 18,000 rpm before the desired operating speed was obtained. The failure was detected by an outer ring temperature increase from 505°K (450°F) to 672°K (750°F) in approximately 15 seconds.

The bearing failure resulted from a thermal imbalance condition which appeared to have been initiated by excessive friction between the downstream rail and outer ring land. The condition of the bearing was essentially identical to those which had failed in prior extended period tests and Tests 10, 12 and 13.

#### 6.3 General Discussion of Results

The results of the test program showed the feasibility of using oil mist lubrication and cooling air as a method to lubricate and cool high speed, high temperature aircraft engine bearings. Many hours of operation were obtained at speeds of  $2.5 \times 10^6$  DN and for a short period as high as  $3.0 \times 10^6$  DN,

Examination of the failed bearings and analysis of the cause indicated that all failures were essentially identical and varied only in the degree of damage. All failures, with the exception of bearing S/N 22 in Test 10, ultimately occurred because of a thermal imbalance condition between the inner and outer rings. However, an analysis of the failure progression indicates that the initial cause in all failures and ultimate cause in bearing S/N 22 was inadequate lubrication of the contacts between the downstream cage rail and outer ring land. This conclusion is based on the gross wear at this location, as much as 0.58 mm (0.023 inches) of material removed from the cage O.D. and 0.56 mm (0.038 inches) removed from land (Test 12, Bearing S/N 15), and the wear and smearing pattern in the ball pockets. The ball pockets showed heavy wear in the leading face and a buildup of race material on the trailing face. This condition indicates that the balls were driving the cage



which was resisting rotation due to the high friction at the cage-land interface. There was only slight or normal polishing of the silver plating on the upstream cage rail in the failed bearings. This slight polishing is similar to that observed on unfailed bearing cages.

The cage-land interface is the most vulnerable to this type of problem with the oil mist and cooling air system employed. With the outer land riding cage design, the clearance between the cage and outer ring land of the test bearing was 0.38 mm (0.015 inches) compared to a clearance at the inner ring of 2.1 mm (0.083 inches). This difference in gap size combined with intentionally directing the mist air at the inner ring gap minimizes the oil directly applied to the cage-land interfaces. It was anticipated, during the design of the system, that the centrifugal pumping of the bearing inner ring and cage would force oil into this location.

The wear being only on the downstream rail and land is considered to have occurred as the result of restricted outer ring thermal growth at this location and a greater thermal growth of the cage rail. The outer ring was restricted by the relatively heavy cross section ring assembled on the bearing housing at this location to form the circumferential cooling air flow path. The housing cooling air, in addition to removing heat from the outer ring, limits the temperature increase of the air retaining ring which minimizes thermal growth and thus restricts the thermal growth of the bearing outer ring. The greater growth of the downstream cage rail results from the mist and through bearing air temperature increasing as the air passes axially through the bearing; thus, a higher cage rail temperature on the downstream side.

Possible solutions to this problem include the elimination of the bearing housing cooling, increase of the cage-land gap on the downstream side to offset the differential thermal growth and allow the cage to ride on both lands, direct oil mist into the gap, provide small holes radially through the cage rail to permit oil to flow to the interface, or some combination of the individual solutions.

It became apparent during the early dynamic tests that the combined mist and cooling air flow rate established during the system study, Task I (5.66 scmm at 24,000 rpm and 3.9 scmm at 20,000 rpm) were in excess of what was required. In the major portion of the test a total air flow rate of 1.4 scmm (50 scfm) was supplied. Therefore, the mist and through bearing cooling air velocities exiting the application nozzles

were appreciable lower than the design value. No apparent problems resulted from this condition as was made more obvious in Test 9 where a test run was performed without a bearing failure with only 1.2 scmm (42.7 scfm) air supplied.

The lower air flow rate requirements were basically the result of a lower bearing heat generation rate than anticipated with mist lubrication. The heat transfer film coefficients used in the analysis to determine the air requirement and based on the values 322 to 362 W/m<sup>2</sup>°K (57 to 64 Btu/hr ft<sup>2</sup>°F) established during the Mobil work (3) were consistent with those determined from the test data. The following heat transfer film coefficients were calculated from Test 8, Run 1 and Test 13:

Test No.	Shaft Speed (rpm)	Film Coefficient (W/m <sup>2</sup> °K - Btu/hr ft <sup>2</sup> °F)
8	10,000	226-40
8	12,000	254-45
8	14,000	271-48
8	16,000	300-53
8	18,000	300-53
8	20,000	277-49
13	10,000	294-52
13	12,000	418-74
13	14,000	430-76
13	16,000	441-78
13	18,000	390-69

The calculations were based on the mean temperature difference of the air and bearing outer ring, a bearing exposed surface area of 0.095 square meters (1.02 square feet) which included all surfaces except the bore and outer ring O.D., and the heat transfer rates measured.

An appreciable difference exists between the heat transfer rates calculated in Test 1 (XRL850A fluid) and those calculated in the remaining tests in which other fluids were used. This difference is not considered to have resulted from higher traction forces with the XRL850A fluid but the result of air leakage through other than intended flow paths at the high flow rate used in Test 1. Since the amount of leakage was not established, the total air flow was used in calculating the heat transfer rates.

A general trend was noted throughout the test series that higher mist and through bearing cooling air flow rates resulted in greater calculated heat transfer rates. This trend indicated that all the mist and through bearing cooling air was not passing through the bearing. A check of this possibility showed the air was escaping from the test bearing chamber through the labyrinth seal and exhausting through the recirculating oil drain. It was also believed that air was escaping through the Teflon seal between the bearing rig housings although this possibility could not be checked. As a result of the air leakage, the heat transfer rates calculated are considered to be slightly conservative on the high side in all tests where relative low flow rates were applied and appreciably in error in Test 1 where a high air flow rate was supplied.

The bearing drag torque reading proved to be very erratic and unreliable during the mist lubrication tests due to the thermal loading (differential temperature between the load plug and rig housing) of the load plug support bearings and resistance to rotation resulting from the necessary cooling air line attached to the load plug. Thus to evaluate the total energy dissipated in the tested bearings, normally established from the drag torque and shaft speed data, a thermal analysis was performed to obtain the quantity of heat conducted and radiated from the bearing. The total energy dissipated is the sum of the heat transfer rate to the mist and cooling air and the heat transfer rate conducted and radiated from the bearing.

For purposes of the analysis it was assumed that heat was conducted from the bearing outer ring through the housing and into the load plug, radiated from the bearing housing and from the shaft. No heat was considered to be conducted through the shaft since one end made no mechanical connection to an external heat sink and the other end passed through the rig bearing which operated at essentially the same temperature as the test bearing inner ring. It was also assumed that no heat was removed by convection from the shaft since the exhausting air was generally warmer than the bore of the inner ring.

The heat conducted from the outer ring was established by calculating the thermal resistance of the housing flange which connects to the load plug. The following standard thick wall cylinder thermal resistant equation was used for the calculation:

$$R = \frac{\ln D_o/D_i}{2 \pi k L}$$

where  $D_o$  = outside diameter of flange  
 $D_i$  = inside diameter of flange  
 $k$  = thermal conductivity  
 $L$  = width of flange  
 $\ln$  = log to base  $e$

The theoretical resistance obtained was 0.874 °K/watt (0.461 hr°F/Btu). Using this resistance value and the measured temperature difference between the bearing outer ring and the flange O.D. the following equation was used to determine the heat conduction rate through the housing:

$$q_1 = \frac{t_1 - t_2}{R}$$

To establish the heat radiated from the bearing housing and shaft the following standard radiation equation was used.

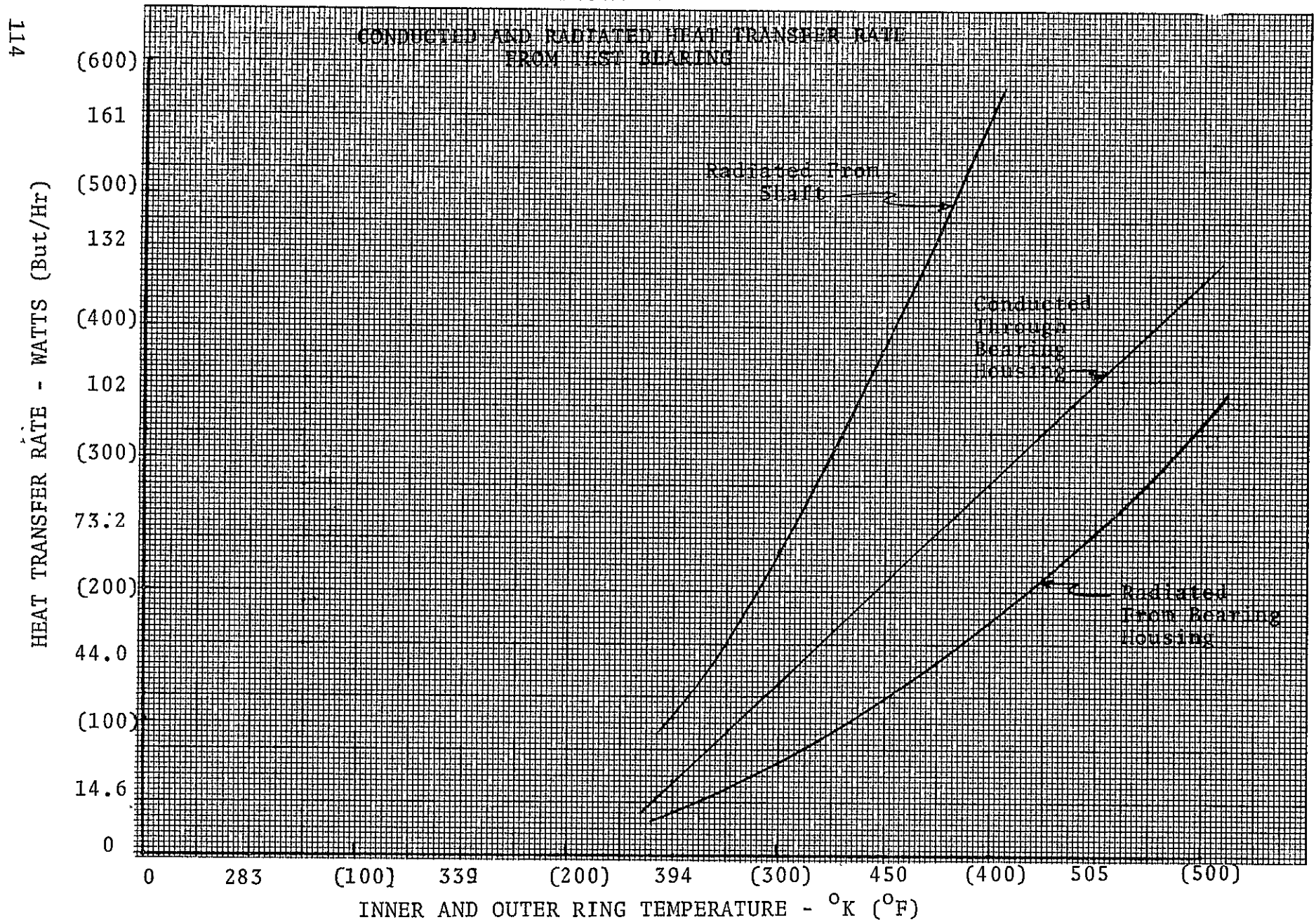
$$q = \sigma F_e F_a A (T_1^4 - T_2^4)$$

where  $\sigma$  = the Stefan-Boltzmann constant of  $0.173 \times 10^{-8}$   
 $F_e$  = a function of the emissivity  
 $F_a$  = a configuration factor  
 $A$  = radiating surface area  
 $T$  = absolute temperature in °R of the radiating surfaces

The flange and shaft were considered to be completely enclosed bodies; small compared with the enclosing body (rig housing). Thus,  $F_e$  equals the emissivity of the flange and shaft and  $F_a = 1$ . As a conservative approach (that which will give the greatest radiated heat rate) the rig housing was assumed to be 366°K (200°F) at all operating speeds, the bearing housing flange at the same temperature as the bearing outer ring, and the shaft at the same temperature as the bearing inner ring. The bearing housing flange surface area was calculated to be 0.045 square meters (0.48 square feet) and the shaft surface area 0.144 square meters (1.55 square feet).

In order to make the calculated conducted and radiated heat transfer rate applicable to all mist tests performed, transfer rates were established for several different outer ring and inner ring temperatures. These values are presented in graph form in Figure 41. By noting the temperature of the inner and outer ring at the various shaft speeds in any test the transfer rates can be directly obtained from the graph.

FIGURE 41



AL75T032

Using the recorded data from Test 8, Run 1 which is representative of a standard step-speed test, the heat transferred from the bearing by conduction and radiation was determined. Table XVII presents the established values in addition to the heat transferred to the mist and cooling air. It is noted from the table that the radiated and conducted heat rate is less than 8% of that transferred to the mist and cooling air. Thus the heat transferred to the air is a reasonable representation of the bearing generated heat.

Comparing the heat transferred to the mist and cooling air in Test 4 to that transferred to the recirculating oil in Test 6 in which the same lubricant (XRM205F) was used points out the major difference in the bearing generated heat rates (power loss) existing between the two lubrication techniques. A graph of the heat transfer rates at various DN values is presented in Figure 42. Also shown in the graph are the bearing heat generation rates measured by Pratt and Whitney Aircraft on a mainshaft bearing lubricated with 71 newtons/min (16 lbs/min) recirculating oil and a thrust load of 13,344 newtons (3000 lbs.) applied. Mist lubrication significantly reduces the heat generation rate, especially at the higher speeds, as a result of decreased oil churning. The reduction in bearing generated heat with a mist lubrication system is not only significant from the standpoint that it allows the heat to be removed by a relative low air flow but it also represents an energy savings for each bearing lubricated.

TABLE XVII

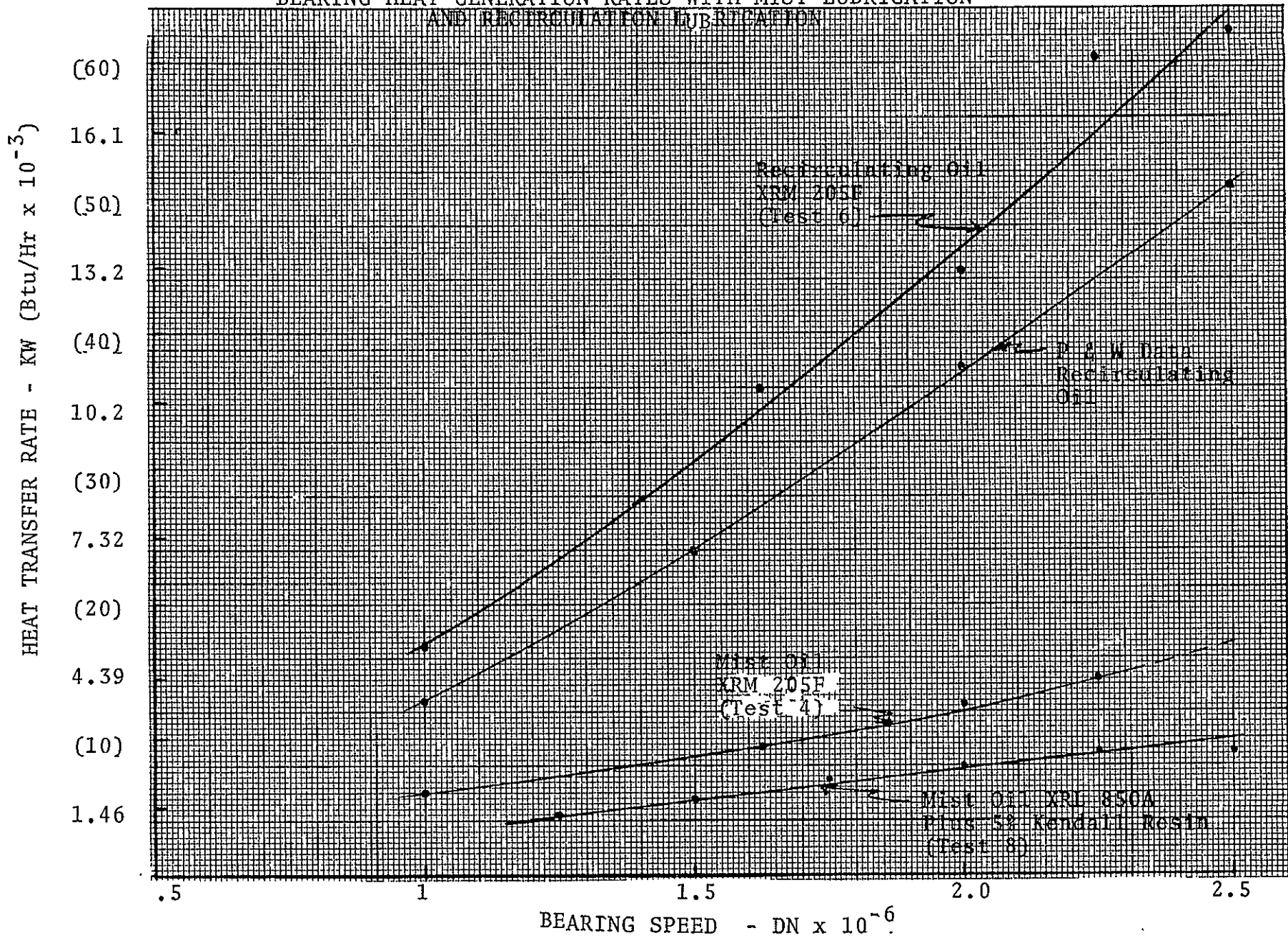
TEST BEARING HEAT GENERATION DATA  
(Test 8, Run1)

Shaft Speed (rpm)	Outer Ring Temp. (°K-°F)	Inner Ring Temp. (°K-°F)	Heat Conducted Brg. Housing (Watts-Btu/hr)	Heat Rad. Brg. Housing (Watts-Btu/hr)
10,000	412-280	389-240	24-82	14-48
12,000	424-304	400-260	40-137	21-72
14,000	439-330	411-280	52-176	28-96
16,000	449-355	422-300	62-212	35-120
18,000	472-390	433-320	77-264	47-162
20,000	483-410	433-320	84-286	55-188

Shaft Speed (rpm)	Heat Rad. Shaft (Watts-Btu/hr)	Total Heat Rad. and Cond. (Watts-Btu/hr)	Heat Trans. To Cooling Air (Watts-Btu/hr)	Bearing Heat Generation (Watts-Btu/hr)
10,000	14-48	64-218	1273-4349	1337-4567
12,000	21-72	96-333	1645-5619	1743-5952
14,000	28-96	130-444	2007-6854	2137-7298
16,000	35-120	165-562	2370-8095	2535-8657
18,000	74-162	207-706	2632-8989	2839-9695
20,000	55-188	221-754	2584-8826	2805-9580

FIGURE 42

BEARING HEAT GENERATION RATES WITH MIST LUBRICATION  
AND RECIRCULATION LUBRICATION



AL75T032



## 7.0 CONCLUSIONS

1. The feasibility of lubricating and cooling a high speed, high temperature aircraft engine bearing with a once-through oil mist and cooling air system was demonstrated at speeds to  $2.5 \times 10^6$  DN for periods of time up to 35 hours in one test run and for 29 hours in another run.

2. An oil mist and air cooling system in conjunction with minor bearing modification was designed which demonstrated reliable performance in lubricating and cooling a 125 mm bore angular contact bearing to speeds of 18,000 rpm ( $2.25 \times 10^6$  DN). Bearing failure, all of which occurred at speeds higher than 18,000 rpm, resulted from insufficient lubrication of the down stream cage land interface. This condition is attributed to the mist lubrication and cooling air system and bearing configuration employed and not the basic lubrication technique.

3. Successful bearing performance was demonstrated in short-term tests at a speed of 20,000 rpm ( $2.5 \times 10^6$  DN) with a mist oil flow rate as low as 221 cubic centimeters per hour (less than 0.5 pints per hour) with a total mist and cooling air flow rate of 1.63 scmm (57.5 scfm). This value is compared to 7570 cubic centimeters per minute (2 gallons per minute) normally used in a recirculating oil system to lubricate and cool a similar size bearing operating under the same load and speed conditions.

4. Bearing heat generation rates of one third to one-fourth that produced in a recirculating oil lubricated bearing were measured in a mist oil lubricated bearing. The low bearing heat generation rate results from minimized oil churning and makes air cooling feasible.

5. Increasing the mist and cooling air temperature results in an essentially equal increase in the bearing operating temperature when the bearing is operated under similar conditions. This observation indicates that no major change occurs in the heat transfer film coefficient over the range of bearing and air temperatures investigated. The heat transfer film coefficient values calculated from test data varied from 300 to 390 W/m<sup>2</sup>°K (53 to 69 Btu/hr ft<sup>2</sup>°F) at a bearing operating speed of 18,000 rpm. These values are consistent with values (322 to 362 W/m<sup>2</sup>°K) obtained by Mobil Research and Development Corporation for mist impinging on a rotating hot disk.

6. No major improvement was detected in the cooling capacity of the through bearing cooling air due to decreasing the angle of impingement with respect to the bearing face.

7. The underrace method of supplying the mist oil appeared essentially as effective as the through bearing method in lubricating the bearing. However, it is considered less desirable from the standpoint of effective cooling by the mist air.

8. It was not possible to rank the four lubrication fluids with respect to their applicability to mist lubrication. No major difference could be detected with respect to decomposition products adhering to the test bearing or adjacent components. Their lubricating ability was not adequately evaluated due to the limited test durations and the unique application. However, the more viscous synthetic paraffinic hydrocarbon fluid is considered less desirable from the standpoint of its higher viscosity which is considered to have produced a higher bearing heat generation rate and a reduced mist oil flow at higher air flow rates. Also, the lowest bearing heat generation rate was obtained with the less viscous synthetic paraffinic hydrocarbon plus 5% by weight of a heavy paraffinic resin.

8.0 RECOMMENDATIONS

This program has established the feasibility of using mist lubrication and air cooling for high temperature, high speed aircraft engine bearings. The program also showed that more development work is required in the area of mist deployment to eliminate the sporadic failures due to inadequate lubrication of the downstream cage-land interface. It is recommended that future work be directed at eliminating this condition by evaluation testing various mist application approaches along with minor bearing geometry changes that could enhance the flow of lubricant to the desired location. Extended period tests should then be performed using the most promising solution to establish reliability.

Vortex coolers should be demonstrated as a method of decreasing simulated compressor bleed off air temperature to reduce the quantity of cooling air required or the bearing temperature for a given air flow rate.

Evaluation testing should be performed with a simplified cooling air system using through bearing cooling air only.

A simplified mist system consisting of oil dripping directly into the through bearing cooling air stream should be demonstrated as a method of eliminating the need for a mist generator.

9.0 LIST OF REFERENCES

1. Rhoads, W. L. and Sibley, L. B., "Supersonic Transport Lubrication System Investigation", Phase I Final Report on NASA Contract NAS3-6267, S K F Report AL67TO60, NASA Report CR-54662 (1967).
2. Shim, J. and Leonardi, S. J., "Microfog Lubrication Application System for Advanced Turbine Engine Components", Final Report on NASA Contract NAS3-9400, NASA Report CR-72489 (1968).
3. Shim, J. and Leonardi, S. L., "Microfog Lubrication Application System for Advanced Turbine Engine Components - Phase II", Final Report on NASA Contract NAS3-13207, NASA Report CR-120843 (1971).
4. Petrucco, R. J. and Leonardi, S. L., "Microfog Lubricant Application System for Advanced Turbine Engine Components - Phase III", Final Report on NASA Contract NAS3-16729, NASA Report NASA CR-121271 (1973).
5. Jones, D. A., "High Temperature Lubricant Screening and System Studies", Final Report on NASA Contract NAS3-14320, S K F Report AL73TO24, NASA Report CR-121188 (1973).
6. Chiu, Y. P., "Analysis and Prediction of Lubricant Film Starvation in Rolling Contact Systems", ASLE Trans. 17, No. 1, pp. 22-35 (January, 1974).

## APPENDIX I

ESTIMATED BEARING COOLING AIR FLOW  
RATE REQUIREMENT

Based on prior test data and theoretical calculations it was established that a 125 mm bore angular contact ball bearing would generate heat at a rate of 44,000 Btu/hr when operating at 24,000 rpm ( $3 \times 10^6$  DN) and lubricated with oil mist with a thrust load of 3280 lbs. applied. Using this value of bearing heat generation rate the estimate of the cooling air required to remove the heat was performed in the following manner.

From test data obtained in mist lubrication testing reported in Reference 1 and considering the bearing as a heat exchanger where the bearing temperature is uniform on all surfaces the surface coefficient can be established using the equation

$$H = \frac{q}{A \Delta t_m}$$

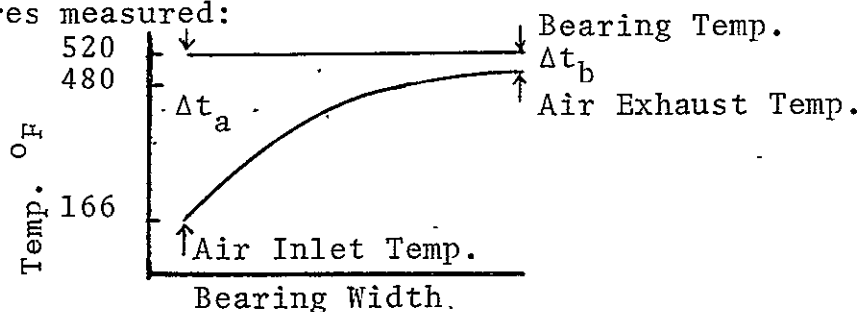
where  $H$  = the surface heat transfer coefficient in Btu/hr-ft<sup>2</sup>-°F

$q$  = heat transfer rate in Btu/hr

$A$  = surface area in ft<sup>2</sup>

$\Delta t_m$  = mean temperature difference between the bearing and air as the air passes axially through the bearing

For the particular case evaluated the bearing heat generation rate of 15,222 Btu/hr was established and the following temperatures measured:



The exposed surfaces of the 125 mm bore bearing (SKF 459981-G1) is 1.02 ft<sup>2</sup>. The exposed surface includes all surfaces except the inner ring bore and the outer ring O.D. surfaces.

The mean temperature difference in a heat exchanger is obtained from the following equation from which  $\Delta t_m$  of 144°F was calculated.

$$\Delta t_m = \frac{\Delta t_a - \Delta t_b}{\ln \frac{\Delta t_a}{\Delta t_m}} = \frac{354 - 40}{\ln \frac{354}{40}} = 144^\circ\text{F}$$

$$\text{then } H = \frac{15,222}{(1.02)(144)} = 103 \text{ Btu/hr-ft}^2\text{-}^\circ\text{F}$$

The efficiency of the bearing as a heat exchanger based on the ratio of the actual temperature rise of the air to the possible temperature rise of the air is 89 percent.

$$n = \frac{\text{Actual Temp. Rise}}{\text{Possible Temp. Rise}} \times 100 = \frac{314}{354} \times 100 = 89\%$$

Both of these values are considerably higher than published values of convective heat transfer coefficients and heat exchanger efficiencies. Surface heat transfer coefficients of mist oil impinging on a heated rotating disk were measured by Mobil Research and Development Corporation and reported in Reference 3. The values ranged from 57 to 64 Btu/hr-ft<sup>2</sup>-°F. Since these values are in better agreement with other published data on convective heat transfer values a bearing heat exchanger efficiency of 66 percent was selected for estimating the bearing cooling air requirement.

The bearing cooling air flow rate (Q) is then computed using the following formula:

$$Q = q / (C_p \Delta t)$$

where

- q = bearing heat generation rate at 24,000 rpm - 44,000 Btu/hr
- Δ = air density at 70°F - 0.075 lb/ft<sup>3</sup>
- C<sub>p</sub> = specific heat of air at constant pressure - 0.24 Btu/lb°F
- Δ t<sup>p</sup> = air inlet and outlet temperature-difference

AL75T032

For the expected air inlet temperature of 200°F and bearing temperature of 500°F,  $\Delta t$  equals 200°F when the bearing efficiency as a heat exchanger is 66 percent.

Then

$$Q = \frac{44,000}{(0.075)(0.24)(200)} = 12,222 \text{ ft}^3/\text{hr} = 200 \text{ scfm}$$



## APPENDIX II

## MIST AND COOLING AIR NOZZLE DESIGN

In determining the design of the mist nozzles the desired velocity of the mist impinging on the bearing components or passing through the bearing must be considered. In the analysis presented below it was considered desirable for the mist to have a velocity which would permit it to transverse a distance equal to a ball diameter in the time interval afforded by the distance between ball passes. This insures that mist is available for the leading surface of the balls to collide with as they pass by each nozzle. It can be argued that only half this velocity is necessary due to the shape of the rolling element; however, the retarding forces of the air currents generated by the bearing are not known and the higher velocity may be desirable. There will also be a natural deceleration of the mist particles once they leave the nozzle. In addition, higher mist velocities will produce a greater wetting of the surface on which the mist impinges. Therefore, the higher velocity seems desirable.

The maximum or design speed of the shaft is 24,000 rpm. At this speed the linear orbital velocity of the balls is 263 ft/sec. This velocity is based on the bearing pitch diameter of 6.280 in. and a cage to inner ring velocity ratio of 0.4 which is a reasonable approximation for most ball bearing designs. The ball diameter is 0.822 in. and the gap between balls is approximately 0.2 in. Therefore, the mist velocity should be  $(0.875/.2) 263$  or 1082 ft/sec.

With the air entering the nozzle at 200°F and zero velocity, and making the assumption that the flow through the nozzle is isentropic the flow rate at the nozzle exit can be calculated in the following manner:

First determine the temperature drop of the mist as it passes through the nozzle using the isentropic flow rate equation.

$$V_2 = \sqrt{2gC_p(778)(T_0 - T_2)}$$

where  $V_2$  = velocity of mist exiting nozzle  
 $C_p$  = specific heat at constant pressure  
 $T_0$  = stagnation temperature of gas entering nozzle  
 $T_2$  = temperature of gas exiting nozzle  
 $g$  = acceleration constant

Rearranging and solving

$$\Delta t = \frac{V_2^2}{2gC_p(778)} = \frac{1082}{2(32.2)(.24)(778)} = 97^\circ\text{R}$$

Then the exit temperature  $T_2 = T_0 - \Delta t = 660 - 97 = 563^\circ\text{R}$

The nozzle exit pressure is determined by calculating the pressure drop across the bearing. To perform this analysis the turbulent flow equation between parallel surfaces is used. This equation is used based on the assumption that the major restriction exists between the cage rails and the ring land. To calculate the pressure drop the equation is used in the following form:

$$P_1^2 - P_2^2 = \frac{0.133M^{7/4}RT\mu^{1/4}L}{g l^{7/4}h^3}$$

where  $P_1$  = pressure upstream of bearing or at nozzle exit -  $\text{lb}/\text{ft}^2$   
 $P_2$  = pressure downstream of bearing -  $\text{lb}/\text{ft}^2$   
 $M$  = combined mass flow rate of mist and cooling air -  $\text{lb}_m/\text{sec}$   
 $g$  = gravitational constant -  $\frac{\text{lb}_m\text{ft}}{\text{lb}_f\text{sec}^2}$

$R$  = gas constant  $\frac{\text{lb}_f \text{ft}}{\text{lb}_m \text{ } ^\circ\text{R}}$

$T$  = absolute temperature of air -  $^\circ\text{R}$

$u$  = dynamic viscosity of gas -  $\frac{\text{lb}_f \text{ sec}}{\text{ft}}$

$L$  = flow length - ft

$l$  = circumferential length of gap - ft

$h$  = gap height - ft

Substituting values into this equation results in a pressure drop of less than  $.001 \text{ lb}/\text{in}^2$  and therefore could be neglected in establishing the density change in the gas at the nozzle exit.

Based on a 45 scfm mist flow rate (w), the flow rate at the nozzle exit is:

$$w_2 = \frac{wT_2}{T_{\text{std}}} = 45 \frac{562}{530} = 47.8 \text{ ft}^3/\text{min}$$

Using the flow rate equation

$$w_2 = V_2 A$$

where A = nozzle exit area

and rearranging to solve for A the combined (10) nozzle exit areas equal

$$A = \frac{47.8 (144)}{1080 \times 60} = 0.0160 \text{ in}^2$$

and the diameter of each nozzle equals

$$d = \sqrt{\frac{0.0162(4)}{4}} = 0.116 \text{ in.}$$

To maintain a nozzle inlet to outlet ratio of 4 to 1 with a screen located in the inlet which is 37% open space an inlet diameter of 0.38 in. is required.

Since the total through bearing cooling air flow rate is essentially the same as the mist air (45 scfm), a straight tube concentric and external to the mist nozzle having the same cross sectional area was selected. The O.D. of the mist nozzle was set at 0.375 in. The I.D. of the air nozzle was calculated to be 0.43 in.

CAUTION - REMOVE PROTECTOR SHEET BEFORE TYPING  
"TO BE STORED IN A COOL DRY LOCATION"

<b>MATERIAL INSPECTION AND RECEIVING REPORT</b>		1 PROC INSTRUMENT IDEN(CONTRACT)  <div style="text-align: center; font-size: 1.2em;">NAS3-16826</div>		(ORDER) NO  6 INVOICE NO  DATE		7 PAGE <div style="text-align: center;">1</div> OF	
						8 ACCEPTANCE POINT  <div style="text-align: center; font-size: 1.2em;">D</div>	
2 SHIPMENT NO <div style="font-size: 1.2em;">SKFO00372</div>		3 DATE SHIPPED <div style="font-size: 1.2em;">18JUNE76</div>		4 B/L  TCN		5 DISCOUNT TERMS  <div style="text-align: center; font-size: 1.2em;">G</div>	
PRIME CONTRACTOR CODE <div style="font-size: 1.2em;">SKF Industries, Inc. 1100 First Avenue King of Prussia, Pa. 19406</div>				10 ADMINISTERED BY CODE <div style="font-size: 1.2em;">Lewis Research Center Aeronautics Procurement Sec. MS 77-3 21000 Brookpark Road Cleveland, Ohio 44135</div>			
11 SHIPPED FROM If other than 91 CODE  <div style="text-align: center; font-size: 1.2em;">See Block 9</div>				FOB 0		12 PAYMENT WILL BE MADE BY CODE <div style="font-size: 1.2em;">Financial Division NASA Lewis Research Center 21000 Brookpark Road Cleveland, Ohio 44135</div>	
13 SHIPPED TO CODE <div style="font-size: 1.2em;">NASA Lewis Research Center 21000 Brookpark Road Cleveland, Ohio 44135</div>				14 MARKED FOR CODE <div style="font-size: 1.2em;">Receiving (L. W. Schopen, MS 500-206)</div>			

15	ITEM NO	16 STOCK/PART NO <small>(Indicate number of shipping containers - type of container - container number)</small>	DESCRIPTION	17 QUANTITY SHIP/REC'D	18 UNIT	19 UNIT PRICE	20 AMOUNT
	1		Final Report on Microfog Lubrication for Aircraft Engine Bearings NASA Contract NAS3-16826	153			

21 PROCUREMENT QUALITY ASSURANCE				22 RECEIVER'S USE	
<b>A ORIGIN</b>  <input type="checkbox"/> PQA <input type="checkbox"/> ACCEPTANCE of listed items has been made by me or under my supervision and they conform to contract, except as noted herein or on supporting documents  <div style="display: flex; justify-content: space-between;"> <div>DATE  TYPED NAME AND OFFICE</div> <div>SIGNATURE OF AUTH GOVT REP</div> </div>		<b>B DESTINATION</b>  <input type="checkbox"/> PQA <input type="checkbox"/> ACCEPTANCE of listed items has been made by me or under my supervision and they conform to contract, except as noted herein or on supporting documents  <div style="display: flex; justify-content: space-between;"> <div>DATE  TYPED NAME AND TITLE</div> <div>SIGNATURE OF AUTH GOVT REP</div> </div>		Quantities shown in column 17 were received in apparent good condition except as noted  <div style="display: flex; justify-content: space-between;"> <div>DATE  TYPED NAME AND OFFICE</div> <div>SIGNATURE OF AUTH GOVT REP</div> </div>	

23 CONTRACTOR USE ONLY

SHIPPING  
CONTAINER  
TALLY

1 2 3 4 5 6 7 8 9 10 11 12 13 14 15 16 17 18 19 20 21 22 23 24 25 26 27 28 29 30 31 32 33 34 35 36 37 38 39 40 41 42 43 44 45 46 47 48 49 50

MATERIEL INSPECTION AND RECEIVING REPORT (CONTINUATION SHEET)		9. PRIME CONTRACT OR P.O. NUMBER NAS3-16826		15. PROC. DIR. OR REQUISITION NO.		3. SHEET NO. 2		4. NO. OF SHEETS 9	
		16. SHIPMENT ORDER NO. SKFO0037Z		17. SHIPMENT NO. ON CONTRACT a. PARTIAL b. FINAL					
CONTRACT NUMBER	REQUISITION LINE ITEM	STOCK AND/OR PART NO. AND DESCRIPTION OF ARTICLES (Indicate No of Ship Container -- Type of Ship, Container -Ship, Container No.)		UNIT OF MEAS.	QUANTITY SHIPPED				
	25.	26.		27.	28.	29.	30.	31.	
NASA Lewis Research Center 21000 Brookpark Road Cleveland, Ohio 44135 Attention: Contract Section A, MS 500-206 Technology Utilization Office, MS 3-19 Library, MS 60-3 Report Control Office, MS 5-5 N. T. Musial, MS 500-113 A. Ginsburg, MS 5-3 J. H. Weeks, MS 5-3 W. R. Loomis, MS 23-2 H. E. Sliney, MS 23-2 W. J. Anderson, MS 23-2 E. V. Zaretsky, MS 6-1 G. J. Weden, MS 5-3 L. D. Wedeven, MS 23-2 E. E. Bailey, MS 77-5					1  1 2 1 1 1 1 1 20 1 1 1 1 1 1				
NASA Headquarters Washington, D. C. 20546 Attention: Mr. N. F. Rekos (RLC) Mr. J. Maltz (RWM)					1 1				
NASA Langley Research Center Langley Station Hampton, VA 23365 Attention: Richard E. Kuhn, MS 403					1				
NASA Scientific & Technical Information Facility P. O. Box 8757 Balt/Wash International Airport Maryland 21240 Attn: Accessioning Dept.					40				
Air Force Aero Propulsion Laboratory Wright Patterson AFB, Ohio 45433 Attn: Howard Jones, APFL/SFL J. L. Morris, APFL G. A. Beane IV, APFL K. L. Berkey, APFL					1 1 1 1				
Air Force Materials Laboratory Wright-Patterson AFB, OH 45433 Attention: Major L. Fehrenbacher, AFML/MBT C. Snyder, AFML/MBT G. Morris, AFML/MBT					1 1 1				

51 52 53 54 55 56 57 58 59 60 61 62 63 64 65 66 67 68 69 70 71 72 73 74 75 76 77 78 79 80 81 82 83 84 85 86 87 88 89 90 91 92 93 94 95 96 97 98 99 100



SHIPPING  
CONTAINER  
TALLY

1 2 3 4 5 6 7 8 9 10 11 12 13 14 15 16 17 18 19 20 21 22 23 24 25 26 27 28 29 30 31 32 33 34 35 36 37 38 39 40 41 42 43 44 45 46 47 48 49 50

MATERIEL INSPECTION AND RECEIVING REPORT (CONTINUATION SHEET)		9. PRIME CONTRACT OR P.O. NUMBER NAS3-16826		15. PROC. DIR. OR REQUISITION NO.		3. SHEET NO. 3		4. NO. OF SHEETS 9	
		16. SHIPMENT ORDER NO. SKF00037Z		17. SHIPMENT NO. ON CONTRACT a. PARTIAL      b. FINAL					
CONTRACT ITEM NUMBER	REQUISITION LINE ITEM	STOCK AND/OR PART NO. AND DESCRIPTION OF ARTICLES (Indicate No. of Ship, Container - Type of Ship, Container - Ship, Container No.)		UNIT OF MEAS.	QUANTITY SHIPPED				
	25.	26.		27.	28.	29.	30.	31.	
Air Force Systems Engineering Group Wright-Patterson AFB, OH 45433 Attention: S. Prete, ENJPH					1				
Eustis Directorate (SAVDL-EU-PP) U.S. Army Air Mobility R & D Lab. Fort Eustis, VA 23604 Attention: John W. White A. Royal R. Mulliken					1 1 1				
Department of the Navy Washington, D. C. 20013 Attention: Bureau of Naval Weapons, A. B. Nehman, RAAE-3 C. C. Singleterry, RAPP-44  Bureau of Ships Harry King, 634A					1 1				
Department of the Navy Bureau of Navy Aeronautics Room 3840, Munitions Bldg. Washington, D. C. Attention: Ben Mette					1				
U.S. Naval Air Development Center Aeronautical Materials Department Warminster, PA 18974 Attention: M. J. Devine Al Conti, 30212					1 1				
Office of Naval Research Code 411 Arlington, VA 22217 Attention: Lt. R. Miller					1				
U.S. Army Mobility Equipment R&D Center Petroleum and Materials Department Ft. Belvoir, VA 22060 Attn: Mr. M. LePeva, STSFB-GL					1				
Commanding Officer U.S. Army BRL Aberdeen Proving Grounds, MD 21005 Attention: R. Bernier, AMXRD-BVL					1				

51 52 53 54 55 56 57 58 59 60 61 62 63 64 65 66 67 68 69 70 71 72 73 74 75 76 77 78 79 80 81 82 83 84 85 86 87 88 89 90 91 92 93 94 95 96 97 98 99 100

MATERIEL INSPECTION AND RECEIVING REPORT (CONTINUATION SHEET)		9. PRIME CONTRACT OR P.O. NUMBER NAS3-16826		15. PROC. DIR. OR REQUISITION NO.		3. SHEET NO. 4		4. NO. OF SHEETS 9	
		16. SHIPMENT ORDER NO. SKF00037Z		17. SHIPMENT NO. ON CONTRACT a. PARTIAL      b. FINAL					
CONTRACT NUMBER	REQUISITION LINE ITEM	STOCK AND/OR PART NO. AND DESCRIPTION OF ARTICLES <small>(Indicate No. of Ship Containers - Type of Ship, Container - Ship, Container No.)</small>		UNIT OF MEAS.	QUANTITY SHIPPED				
		26.		27.	28.	29.	30.	31.	
		Commander Naval Air Systems Command Department of the Navy Washington, D. C. 20360			1				
		FAA Headquarters 800 Independence Ave., SW Washington, D. C. 20553 Attention: F. B. Howard			1				
		AiResearch Manufacturing Corp. 402 S. 36th Street Phoenix, AZ 85034 Attention: F. Blake Wallace			1				
		Alcor, Inc. 2905 Bandera Rd. San Antonio, TX 78238 Attention: L. Hundere			1				
		Avco Corp. Lycoming Div. 550 Main Street Stratford, CT 06497 Attention: P. Lynwander			1				
		Battelle Memorial Institute Columbus Labs 505 King Ave. Columbus, OH 43201 Attention: C. M. Allen			1				
		Bell Helicopter Co. P. O. Box 482 Ft. Worth, TX 76101 Attention: N. Powell			1				
		Boeing Commercial Airplane Co. P. O. Box 3707 Seattle, WA 98124 Attention: W. G. Nelson A. W. Waterman			1 1				

SHIPPING  
CONTAINER  
TALLY

1 2 3 4 5 6 7 8 9 10 11 12 13 14 15 16 17 18 19 20 21 22 23 24 25 26 27 28 29 30 31 32 33 34 35 36 37 38 39 40 41 42 43 44 45 46 47 48 49 50

MATERIEL INSPECTION AND RECEIVING REPORT (CONTINUATION SHEET)		9. PRIME CONTRACT OR P.O. NUMBER NAS3-16826		15. PROC. DIR. OR REQUISITION NO.		3. SHEET 5		4. NO. OF SHEETS 9	
		16. SHIPMENT ORDER NO. SKF00037Z		17. SHIPMENT NO. ON CONTRACT a. PARTIAL b. FINAL					
CONTRACT NUMBER	REQUISITION LINE ITEM	STOCK AND/OR PART NO. AND DESCRIPTION OF ARTICLES (Indicate No of Ship Containers - Type of Ship, Container - Ship, Container No)		UNIT OF MEAS.	QUANTITY SHIPPED	QUANTITY RECEIVED	UNIT COST	TOTAL COST	
		26.		27.	28.	29.	30.	31.	
The Boeing Co., Vertol Division Advanced Drive Systems Tech. Dept. Boeing Center, P. O. Box 16858 Philadelphia, Pa. 19142 Attention: A. J. Lemanski					1				
Convair Aerospace Division Ft. Worth, TX Attn: H. C. Hoffman, Mail Zone 5860					1				
Curtiss-Wright Corporation Wright Aeronautical Division 333 W. First St. Dayton, OH 45400 Attn: S. Lombardo					1				
Eaton, Yale and Towne, Inc. Farval Division 3249 E. 80th St. Cleveland, OH 44104 Attn: E. J. Gesdorf					1				
Eaton, Yale and Towne, Inc. Research Center 26201 Northwestern Highway Southfield, MI 48075 Attn: H. M. Reigner					1				
Exxon Research & Engineering Co. P. O. Box 51 Linden, N. J. 07036 Attention: R. R. Bertrand R. F. Overhoff					1 1				
Fairchild Hiller Corp. Republic Aviation Div. Space Systems & Research Farmingdale, Long Island, NY 11735 Attention: C. Collis					1				
Franklin Institute Research Labs. 20th and Parkway Philadelphia, Pa. 19103 Attention: W. Shugart					1				

51 52 53 54 55 56 57 58 59 60 61 62 63 64 65 66 67 68 69 70 71 72 73 74 75 76 77 78 79 80 81 82 83 84 85 86 87 88 89 90 91 92 93 94 95 96 97 98 99 100

SHIPPING  
CONTAINER  
TALLY

1 2 3 4 5 6 7 8 9 10 11 12 13 14 15 16 17 18 19 20 21 22 23 24 25 26 27 28 29 30 31 32 33 34 35 36 37 38 39 40 41 42 43 44 45 46 47 48 49 50

MATERIEL INSPECTION AND RECEIVING REPORT (CONTINUATION SHEET)		9. PRIME CONTRACT OR P.O. NUMBER NAS3-16826		15. PROC. DIR. OR REQUISITION NO.		3. SHEET NO. 6	4. NO. OF SHEETS 9	
		16. SHIPMENT ORDER NO. SKF00037Z		17. SHIPMENT NO. ON CONTRACT a. PARTIAL      b. FINAL				
CONTRACT NUMBER	REQUISITION LINE ITEM	STOCK AND/OR PART NO. AND DESCRIPTION OF ARTICLES (Indicate No. of Ship Container - Type of Ship, Container - Ship, Container No.)		UNIT OF MEAS.	QUANTITY SHIPPED			QUANTITY RECEIVED
25.	25.	26.		27.	28.	29.	30.	31.
General Electric Company Gas Turbine Division Evendale, OH 45215 Attention: I. Sumey E. N. Bamberger					1 1			
General Electric Company 1000 Western Ave. Lynn, MA 01910 Attention: O. D. Taylor					1			
Grumman Aircraft Engineering Corp. Bethpage, NY 11714 Attention: M. Tarase					1			
Hercules Powder Co., Inc. 900 Market St. Wilmington, DE 19801 Attention: Dr. Homer Haggar					1			
Heyden Newport Chemical Corp. Heyden Chemical Division 290 River Drive Garfield, NJ 07026 Attn: D. X. Klein					1			
Hughes Aircraft Company International Airport Station P. O. Box 90515 Los Angeles, CA 90209					1			
Industrial Tectonics, Inc. Research & Development Div. 18301 Santa Fe Ave. Compton, CA 90024 Attention: Heinz Hanau					1			
Kendall Refining Co. Bradford, PA 16701 Attn: F. I. I. Lawrence L. D. Dromgold					1 1			
Lockheed Aircraft Corp. Lockheed Missile & Space Co. Material Science Laboratory 3251 Hanover St. Palo Alto, CA 94301 Attention: Francis J. Clauss					1			

51 52 53 54 55 56 57 58 59 60 61 62 63 64 65 66 67 68 69 70 71 72 73 74 75 76 77 78 79 80 81 82 83 84 85 86 87 88 89 90 91 92 93 94 95 96 97 98 99 100

SHIPPING  
CONTAINER  
TALLY

1 2 3 4 5 6 7 8 9 10 11 12 13 14 15 16 17 18 19 20 21 22 23 24 25 26 27 28 29 30 31 32 33 34 35 36 37 38 39 40 41 42 43 44 45 46 47 48 49 50

MATERIEL INSPECTION AND RECEIVING REPORT (CONTINUATION SHEET)		9. PRIME CONTRACT OR P.O. NUMBER NAS3-16826		15. PROC. DIR. OR REQUISITION NO.		3. SHEET NO. 7		4. NO. OF SHEETS 9	
		16. SHIPMENT ORDER NO. SKF00037Z		17. SHIPMENT NO. ON CONTRACT a. PARTIAL      b. FINAL					
CONTRACT ITEM NUMBER 25.	REQUISITION LINE ITEM 25.	STOCK AND/OR PART NO. AND DESCRIPTION OF ARTICLES (Indicate No of Ship Containers - Type of Ship Container - Ship Container No.) 26.		UNIT OF MEAS. 27.	QUANTITY SHIPPED 28.	QUANTITY RECEIVED 29.	UNIT COST 30.	TOTAL COST 31.	
Marlin-Rockwell Corp. Jamestown, NY 14701 Attention: Arthur S. Irwin					1				
McDonnell-Douglas Aircraft Co. 3000 Ocean Park Blvd. Santa Monica, CA 90406 Attention: Robert McCord					1				
Mechanical Technology, Inc. 968 Albany-Shaker Road Latham, NY 12110 Attention: Donald F. Wilcock					1				
Mobil Oil Co. Research Dept. Paulsboro, NJ 08066 Attention: S. J. Leonardi E. M. Johnson E. L. Armstrong					1 1 1				
Monsanto Research Corporation 800 North Lindbergh Blvd. St. Louis, MO 63166 Attn: J. Herber F. S. Clark					1 1				
C. A. Norgren Co. Englewood, CO 80110 Attention: D. G. Faust					1				
North American Rockwell Corp. Los Angeles Div., International Airport Los Angeles, CA 90209 Attn: Frank J. Williams					1				
Pennsylvania State University Dept. of Chemical Engineering University Park, PA 16802 Attn: Prof. E. E. Klaus					1				
Rocketdyne Division of Rockwell International 6633 Canoga Ave. Canoga Park, CA 91304 Attn: G. E. Williams Library					1 1				

51 52 53 54 55 56 57 58 59 60 61 62 63 64 65 66 67 68 69 70 71 72 73 74 75 76 77 78 79 80 81 82 83 84 85 86 87 88 89 90 91 92 93 94 95 96 97 98 99 100



SHIPPING  
CONTAINER  
TALLY

1 2 3 4 5 6 7 8 9 10 11 12 13 14 15 16 17 18 19 20 21 22 23 24 25 26 27 28 29 30 31 32 33 34 35 36 37 38 39 40 41 42 43 44 45 46 47 48 49 50

MATERIEL INSPECTION AND RECEIVING REPORT (CONTINUATION SHEET)		9. PRIME CONTRACT OR P.O. NUMBER NAS3-16826		15. PROC. DIR. OR REQUISITION NO.		3. SHEET NO. 8		4. NO. OF SHEETS 9	
		16. SHIPMENT ORDER NO. SKF00037Z		17. SHIPMENT NO. ON CONTRACT a. PARTIAL b. FINAL					
CONTRACT NUMBER	REQUISITION LINE ITEM	STOCK AND/OR PART NO. AND DESCRIPTION OF ARTICLES (Indicate No. of Ship, Containers - Type of Ship, Container - Ship, Container No.)		UNIT OF MEAS.	QUANTITY SHIPPED				
	25.	26.		27.	28.	29.	30.	31.	
Shell Oil Company Wood River Research Laboratory Advanced Products Group Wood River, IL 62095 Attn: J. J. Heithaus					1				
Southwest Research Institute P. O. Drawer 28510 San Antonio, TX 78284 Attention: P. M. Ku					1				
Sikorsky Aircraft Division United Aircraft Corp. Stratford, CT 06602 Attn: Carl Keller Frank McGrogan					1 1				
Stewart-Warner Corp. Alemite Division 1826 Diversey Parkway Chicago, IL 60614					1				
Sun Oil Company Applied Research Dept. P. O. Box 1135 Marcus Hook, PA 19061 Attention: Dr. J. L. Lauer					1				
Teledyne CAE 1330 Laskey Rd. Toledo, OH 43612 Attn: M. Dowdell, Librarian					1				
Texaco, Inc. P. O. Box 509 Beacon, NY 12508 Attention: Dr. G. B. Arnold					1				
The Timken Company 1835 Dueber Ave., SW Canton, OH 44706 Attention: C. H. West					1				

51 52 53 54 55 56 57 58 59 60 61 62 63 64 65 66 67 68 69 70 71 72 73 74 75 76 77 78 79 80 81 82 83 84 85 86 87 88 89 90 91 92 93 94 95 96 97 98 99 100

SHIPPING  
CONTAINER  
TALLY

1 2 3 4 5 6 7 8 9 10 11 12 13 14 15 16 17 18 19 20 21 22 23 24 25 26 27 28 29 30 31 32 33 34 35 36 37 38 39 40 41 42 43 44 45 46 47 48 49 50

MATERIEL INSPECTION AND RECEIVING REPORT (CONTINUATION SHEET)		9. PRIME CONTRACT OR P.O. NUMBER NAS3-16826		15. PROC. DIR. OR REQUISITION NO.		3. SHEET NO. 9		4. NO. OF SHEETS 9	
		16. SHIPMENT ORDER NO. SKFO0037Z		17. SHIPMENT NO. ON CONTRACT a. PARTIAL b. FINAL					
CONTRACT NUMBER	REQUISITION LINE ITEM	STOCK AND/OR PART NO. AND DESCRIPTION OF ARTICLES (Indicate No. of Ship Containers - Type of Ship, Container - Ship, Container No.)		UNIT OF MEAS.	QUANTITY SHIPPED				
	25.	26.		27.	28.	29.	30.	31.	
United Aircraft Corporation Pratt & Whitney Aircraft East Hartford, CT 06108 Attn: R. P. Shevchenko P. Brown A. R. Marsh					1 1 1				
United Aircraft Corporation Pratt & Whitney Aircraft Engineering Dept. West Palm Beach, FL 33402 Attn: R. E. Chowe					1				
Williams Research Corp. 2280 W. Maple Rd. Walled Lake, MI 48088 Attn: J. A. Royer Library					1 1				

51 52 53 54 55 56 57 58 59 60 61 62 63 64 65 66 67 68 69 70 71 72 73 74 75 76 77 78 79 80 81 82 83 84 85 86 87 88 89 90 91 92 93 94 95 96 97 98 99 100